THE REGULATION OF ION TRANSPORT IN THE MIDGUT OF THE LEPIDOPTERAN LARVA *MANDUCA SEXTA*.

JOHN-PAUL SUMNER B.Sc. (Hons).
Laboratory of Cell Biology,
Division of Molecular and Cellular Biology.

A thesis submitted to the Faculty of Science of the University of Glasgow for the degree of Doctor of Philosophy.

February 1995

Acknowledgements

I would like to thank my supervisor Dr Julian Dow for inviting me into his team, his continued encouragement and and his peerless sense of humour. Many thanks to Prof. Adam Curtis for providing the facilities required to complete this thesis and to all the staff and students at the Department of Cell Biology, University of Glasgow.

It's a pleasure to thank to Dr Fergus Earley for his enthusiasm and his optimism during times of despair. Many thanks to all the staff at Zeneca Agrochemicals, Jeallot's Hill Berks, especially Jim Goodchild for his companionship, hospitality and vintage home-vino.

Special thanks go to Prof. Helmut Wieczorek and the Wieczorek Family for extending their kindness and hospitality beyond the call of duty. I would like to thank all the staff and students at the Ludwig Maximilians Universitat in Munich who conspired to make my stay most enjoyable, especially Alexandra Lepier, Ralph Gräf, Bruni Förg-Bray and Ulla Klein.

I would like to thank all the technical staff who contributed to the realisation of this investigation. I am most grateful to Scott Arkinson for his encyclopaedic knowledge of the laboratory. I would also like to thank the chief technician Carlo Mucci and Andy Hart for much needed dark-room help.

Finally I would like to thank my family and friends whose precious support is appreciated hugely.

This work was supported by SERC CASE award in association with ICI Agrochemicals, Jealott's Hill, Berkshire

Table of Contents

List of Figures

CHAPTER 1.

Chapter 2.

Chapter 3.

Chapter 4.

Chapter 5.

Abbreviations

ADP	Adenosine diphosphate
ATP	Adenosine triphosphate
ATPase	Adenosine triphosphatase
BSA	Bovine serum albumin
Btk	Bacillus thuringiensis endotoxin
cAMP	Cyclic adenosine monophosphate
cGMP	Cyclic guanosine monophosphate
DCCD	N,N'-dicyclohexyl carbidiimide
DMSO	Dimethyl sulfoxide
DNA	Deoxyribonucleic acid
EDTA	Ethylenediamine tetraacetic acid
ER	Endoplasmic reticulum
GCAM	Goblet cell apical membrane
GTP	Guanosine triphosphate
kDa	KiloDaltons
KPi	Potassium phosphate
NEM	N-ethyl maleimide
PBS	Phosphate buffered saline
PD	Potential difference
pm	Plasma membrane
pmf	Proton motive force
RNA	Ribonucleic acid
SCC	Short circuit current
SET	Sucrose, EDTA, TRIS buffer
TEP	Transepithelial potential difference
TRIS	Tris (hydroxymethyl) aminomethane

Summary

Rapid growth during the larval stage of Lepidopteran insects is facilitated by vigorous transepithelial K^+ transport from blood to gut lumen across the midgut. Active transport of K^+ into the midgut lumen is required to energise amino acid uptake and is believed to contribute to the generation of the extremely high pH found in insect midgut. K^+ transport is facilitated by a V-ATPase and K^+/nH^+ antiporter on the apical plasma membrane of the midgut goblet cell. A transmembrane voltage is generated by V-ATPase driven proton transport, consequently potassium is secreted by exchange for protons *via* the antiporter.

This thesis confirms that the K^+ transport system is abolished during periods of non feeding prior to pupation and during larval/larval moults. The moult from fourth to fifth instar was studied in detail. Transepithelial voltage, indicating net active K^+ transport, was found to be approximately 100 mV during feeding periods but was found to fall to 0 mV during the moult. The transepithelial voltage was regenerated upon exit from the moult during ecdysis, just prior to resumption of feeding behaviour. The short circuit current was found to mirror these results. The pH of the midgut lumen was found to decline over the period of K^+ transport inactivation. Thus during a moult, when the midgut is void of food, the K^+ transport system is apparently not required and is consequently switched off. A transmembrane voltage is re-generated prior to the next gorge of food.

The identity of the regulatory component of the K^+ transport system was sought. The K^+ pump is composed of two main components: the V-ATPase and the antiporter. ATPase activity assays on partially purified goblet cell apical membranes (GCAM) demonstrated that the V-ATPase was inactivated during the moult. ATP dependent proton transport into GCAM derived vesicles was also inactivated during the moult. ATP independent (antiporter) activity was not inhibited in vesicles derived from GCAM during

the moult. The V-ATPase component thus appears to be the target of a control mechanism.

In an effort to elucidate the mechanism of inactivation of the V-ATPase the V-ATPase structure was investigated using SDS gel electrophoresis. GCAM membranes, extracted from moulting or feeding larvae, were run on SDS gels and the V-ATPase subunit components were compared. Loss of V-ATPase activity paralleled the disappearance of specific V-ATPase subunits. The subunits missing were those considered to compose the peripheral V_1 catalytic 'head' of the V-ATPase molecule. The integral membrane V_O subunits remained in the GCAM of moulting larvae. A mechanism, believed to be the first demonstration of which *in vivo*, of inactivation of a V-ATPase by dissociation of V_1 from V_O is discussed.

An attempt was made to reproduce the hormonal and intra cellular signals required for regulation of V-ATPase activity *in vitro*. cGMP was found to modestly activate transepithelial K^+ transport. NADPH diaphorase staining suggested that nitric oxide synthase was present in the midgut tissue. However, sodium nitroprusside (a spontaneous generator of nitric oxide) did not stimulate K^+ transport.

This thesis has identified that K^+ transport is regulated and that regulation occurs at the level of the V-ATPase. The V-ATPase is inactivated by the loss of the V_1 domain of the molecule. Transport may be manipulated in vitro by various secondary messengers.

CHAPTER 1
INTRODUCTION

Ion transport overview

In every cell known, a significant fraction of energy is expended maintaining the concentration gradients of ions across the plasma membrane and across the membranes of intracellular compartments. These activities are among the most fundamental in nature (Darnell, Lodish, & Baltimore, 1986). Active transport is the process whereby metabolic energy is used to move ions or molecules against an electrochemical gradient. An ATPase is an enzyme system coupling the free energy released in the hydrolysis of ATP and using it to move ions up an electrical or concentration gradient (Kyte, 1981).

In at least three types of active transport systems the hydrolysis of ATP is directly coupled to the transport of ions. One of these systems, the Na^+/K^+ ATPase, transports Na^+ out of a cell and K^+ in (Shull, Schwartz, & Lingrel, 1985). A second transports H^+ on the inner membrane of mitochondria and generates ATP in the process (Cross, 1981). A third system transports protons exclusively at the expense of ATP.

Ion gradients are used to drive many biological processes. The Na^+ gradient, generated by the Na^+/K^+ ATPase, is used in absorptive cells to transport glucose into the cell, against its concentration gradient, via a glucose-Na^+ symport. An amino acid transport system works in a similar manner. The Ca^{2+} gradient within the sarcoplasmic reticulum is used to release Ca^{2+} rapidly into the cytoplasm upon hormonal stimulation (MacLennan, Brandl, Korczak, & Green, 1985). In mitochondria and chloroplasts the proton gradient is used 'in reverse' to generate ATP via the proton ATPase (Hinkle & McCarty, 1978).

Much is now known about the structure and function of these transport systems and attention is now being turned to the regulation of these systems.

This study will use the caterpillar midgut epithelium as a model system for ATPase driven active transport. The function of the larval phase of the insect life cycle is rapid growth to a size whereby the animal is ready for the metamorphosis into the adult. The larva is therefore specialised in eating and the absorption of nutrients from the food. The absorption of nutrients is facilitated by a highly specialised ion transport system in the midgut of the animal. The focus of this investigation will be the regulation of this ion transport system, specifically during various stages in the growth of the larvae.

1.1 Hormonal Control of Growth and Moulting

Insect larval growth and development can be divided into two behavioural phases; the intermoult phase, when the animal is feeding and increasing in weight; and the moult phase, in which feeding is interrupted to allow the replacement of the exoskeleton. The insect of interest in this study is the larval phase of the sphingid moth *Manduca sexta*. This insect has an extremely rapid growth rate from 1 mg upon hatching to 10 g by pupation, an increase of x10,000 in about three weeks. The rigid exoskeleton or cuticle restricts growth, therefore must be shed periodically and replaced with a larger version. The replacement of the larval cuticle with another larval cuticle occurs during a larval/larval moult or L_n/L_{n+1}, where n refers to the instar. Shedding of the old cuticle is termed ecdysis. The caterpillar undergoes four larval/larval moults as it grows to a size ready to pupate. Towards the end of the L_5 (5th or final) larval instar the behaviour changes, whereby the larva stops eating and burrows into the ground, this is termed the wandering stage and is in preparation for the final moult to a pupa. During pupation the larva undergoes

metamorphosis into the adult moth, emergence of the moth from the chrysalis is called eclosion.
Each moult follows a precise sequence of physiological and behavioural activity which is directed by the hormonal mechanisms of the insect.

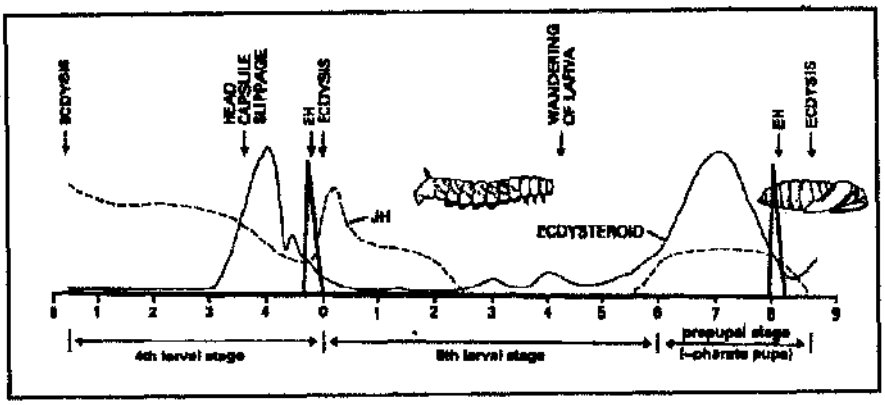

Figure 1.1. Diagrammatic representation of the hormonal events controlling development of *Manduca sexta* larvae. JH, juvenile hormone; EH, eclosion hormone. The numbers on the x-axis refer to number of days. Modified after (Bollenbacher, Smith, Goodman, & Gilbert, 1981; Gullan & Cranston, 1994; Riddiford, 1986; Truman, 1978)

In 1917 Kopec first identified the nervous system of insects as a source for endocrine agents when he reported that the brain regulated moulting and metamorphosis in gypsy moth larvae (Kopec, 1917). The focus of this study will be the events during the 4th to 5th instar, or final larval, moult. The endocrine events co-ordinating this moult have been painstakingly studied and a highly organised system has been discovered. The moult is organised by four major hormones; Prothoracotropic hormone (PTTH) or ecdysiotropin, which initiates the endocrine cascade; Juvenile hormone, which ensures a larval/larval moult; 20-hydroxyecdysone, which co-ordinates the progression of the moult, and eclosion hormone which triggers ecdysis (see **Figure 1.2**).

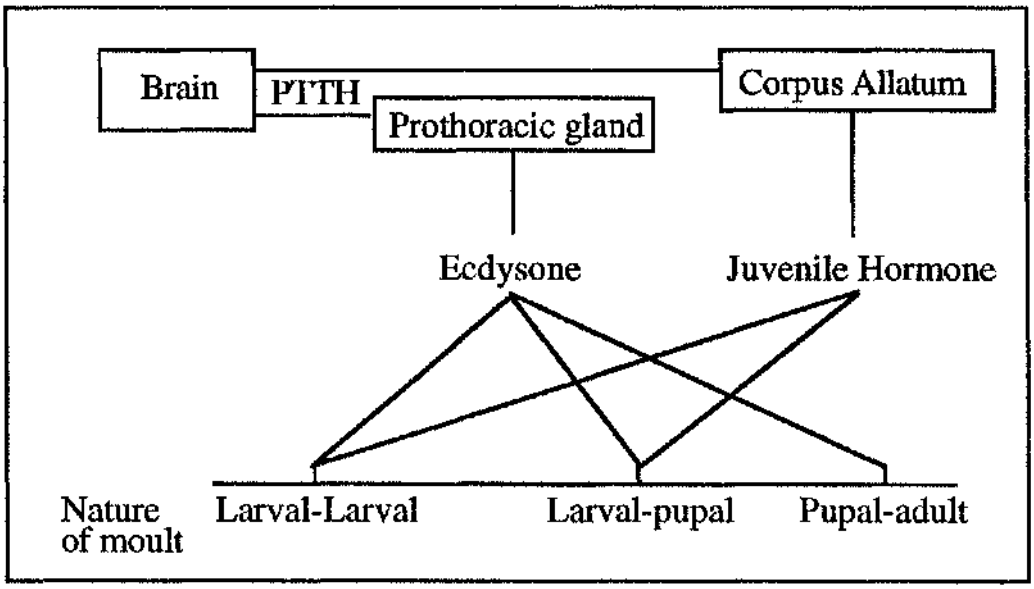

Figure 1.2. The Classical scheme of interactions between PTTH, ecdysone and juvenile hormone (after Steel & Davey, 1985)

1.1.1 Summary of endocrine events during larval/larval moult

i) Larva reaches developmental gate or cue which permits/stimulates competent PTTH release.
ii) PTTH induces a pulse of juvenile hormone and 20-hydroxyecdysone release into the haemolymph.
iii) 20-hydroxyecdysone co-ordinates the moult and cellular response.
iv)Ecdysone levels fall and cells become responsive to eclosion hormone.
v) Reduced ecdysone levels stimulate release of eclosion hormone.
vi) Eclosion hormone stimulates ecdysis, see **Figure 1.3.**

1.1.2 Release of PTTH initiates the moult

Towards the end of the fourth instar the moult is initiated by the release of PTTH from the brain. PTTH is only released during certain periods of the day termed gates. The opening of the gate is not dependent on photoperiod but is dependent on the larvae reaching a pre-defined morphological stage. The precise mechanism of PTTH release is unknown but is probably determined by a critical weight or rate of growth (Steel & Davey,

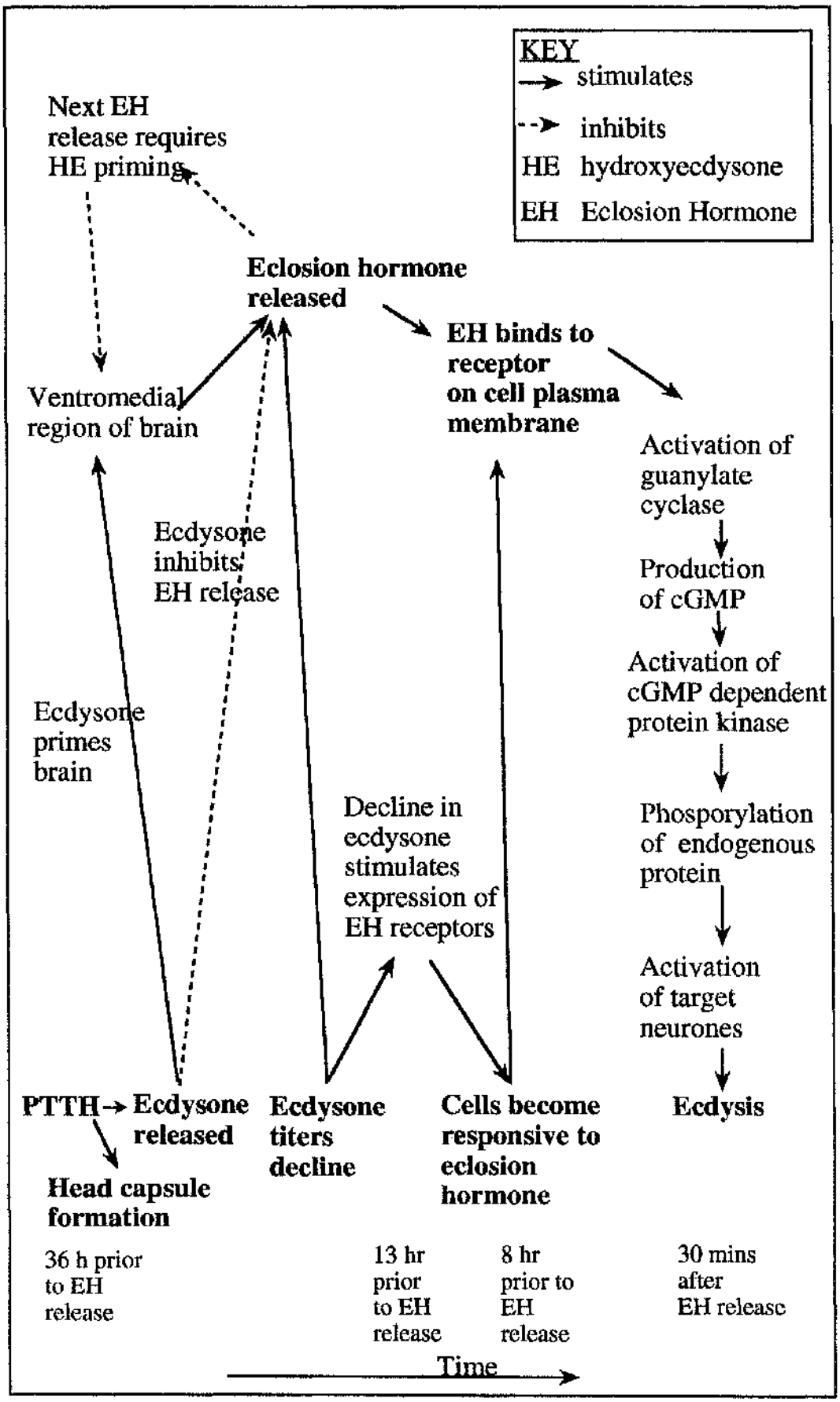

Figure 1.3. Hormonal interaction during larval/larval moul

1985).If the larva reaches or has reached the critical stage during an open gate then PTTH will be released and the cascade of hormonal activity that orchestrates the moult will be initiated.

PTTH acts on the prothoracic glands to stimulate the production, and release, of ecdysteroid (Bollenbacher, Agui, Granger, & Gilbert, 1979). The mechanism of PTTH-mediated stimulation follows a classical pathway, triggered initially by PTTH association with a specific plasma membrane receptor. Receptor mediated intracellular release of calcium stimulates a calcium/calmodulin sensitive adenylate cyclase. Consequently, cAMP synthesis is enhanced in turn, activating a cAMP-dependent protein kinase. Ensuing phosphorylation of a membrane-associated 34 kDa protein leads to ecdysone synthesis and release into the haemolymph (Gilbert, Combest, Smith, Meller, & Rowntree, 1988) (Smith, 1993). Subsequent regulation of ecdysteroid production is by the ecdysteroids themselves, or by juvenile hormone. Ecdysone is released into the haemolymph whereby it has access to target organs.

1.1.3 Ecdysone acts on the tissues to bring about the moult

20-hydroxyecdysone (20-HE) is the most widely distributed ecdysteroid used by insects to regulate the moult cycle and associated physiological events. Nearly every insect tissue has been suggested as a target for ecdysteroids, some of which are summarised in table 1. If juvenile hormone (JH) is present during a rise in ecdysteroid, then the stage is repeated with the same genes being expressed. If JH is absent at the time of ecdysteroid action, new genes can be expressed. During larval life JH is continuously present. During a larval/larval moult ecdysone acts upon the epidermis causing apolysis (detachment of the epidermis from the old cuticle), secretion of a new cuticle and numerous associated metabolic adjustments.

1.1.4 Mode of action of ecdysone

In 1974 Asburner *et al* (Ashburner, Chihara, Meltzer, & Richards, 1974) proposed the model of ecdysteroid action that is still used

today. By diffusion, 20-hydroxyecdysone can enter any cell. Target cells contain a cytoplasmic ecdysteroid receptor which retains the ecdysteroid in the cell. The steroid receptor complex is translocated to the nucleus where it interacts with target areas of DNA. This interaction of hormone/receptor complex and nuclear DNA induces the synthesis of specific mRNA(s), which, in turn, code for the protein(s) responsible for the phenotypic response of the cells to the hormone.

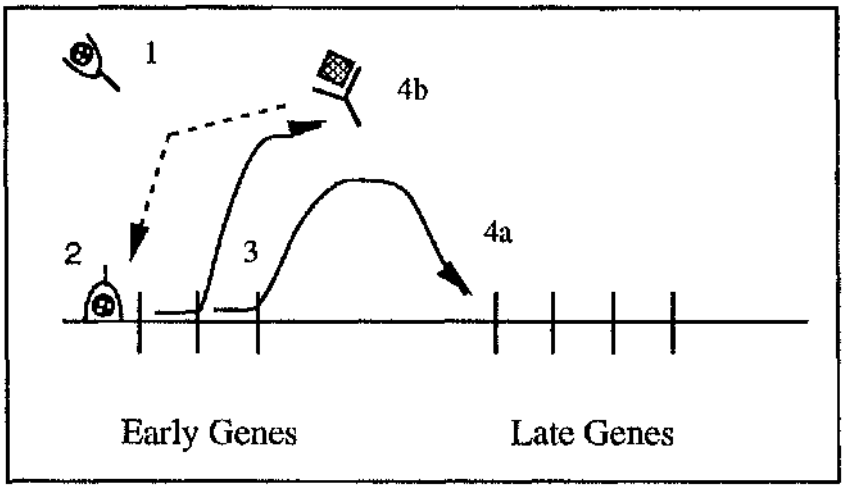

Figure 1.4. Mode of action of ecdysone. 1. Ecdysone binds to cytoplasmic receptor. 2. Ecdysone-receptor complex binds to DNA, promoting early genes. 3. Products of early genes expressed. 4a. Product of early genes stimulates late genes. 4b. Product of early genes, possibly during larval/larval moult product binds juvenile hormone, and displaces ecdysone-receptor complex, resulting in repression of late genes.

The increased transcription of ecdysone-responsive genetic loci occurs in a sequential manner. Chromosome puffing, due to the accumulation of RNA and protein, indicates genetic activity before, during and after ecdysone exposure. Cultured salivary glands show three classes of puff response to ecdysone (Ashburner 1974); intermoult puffs regress upon exposure to ecdysone, following this, early puffs are stimulated. Early puff stimulation is followed by the late puffs. The ecdysone/receptor complex has a positive effect on the early site causing induction of mRNA synthesis and protein synthesis. At the same time, the ER complex

acts to inhibit RNA synthesis at late puff sites. Only when a sufficient concentration of early proteins are synthesised is the ER complex displaced from the late site and RNA synthesis can occur. The early site protein also displaces the early site receptor complex from the early site, causing termination of early site transcription, for review see 0' Connor, 1985. In this manner ecdysone regulates sequential expression and repression of specific genes, (See **Figure 1.4**)

1.1.5 Eclosion hormone stimulates ecdysis

The ecdysone peak occurs at the entry into the moult 8 hours after head cap slippage; after which the ecdysteroid levels fall until, upon ecdysis, titres have reached near basal levels (Curtis, 1984). The decline in ecdysone titres appears to be the cue for melinisation of the new cuticle, and the release of eclosion hormone (Curtis 1984, Truman 1992). Eclosion hormone is a peptide hormone released from the proctodeal nerves at a Declining steroid titres trigger eclosion hormone responsiveness. The normal decline in ecdysteroid levels alters the threshold of the neurones and initiates the release of eclosion hormone (Truman 1994). Thus there is an in-built co-ordination system whereby steps will occur in the correct sequence. Eclosion hormone stimulates ecdysis by acting upon the nervous system, whereby the larvae will begin the behavioural patterns associated with ecdysis, resulting in the shedding of the old cuticle.

1.2 Ion Transport in Manduca

1.2.1 Structure of the midgut

The insect larval stage occurs to facilitate growth to a suitable weight to allow development into the adult and the digestive system dominates the body plan of the larvae. The Lepidopteran larval alimentary canal is divided structurally and functionally into 3 main regions; the foregut, midgut and hindgut. The short foregut is cuticle lined and does not have a role in absorption. The midgut is the most dominant region and is the principal site of secretion of digestive enzymes and the absorption of nutrients.

Some absorption occurs in the hindgut prior to excretion of the faeces.

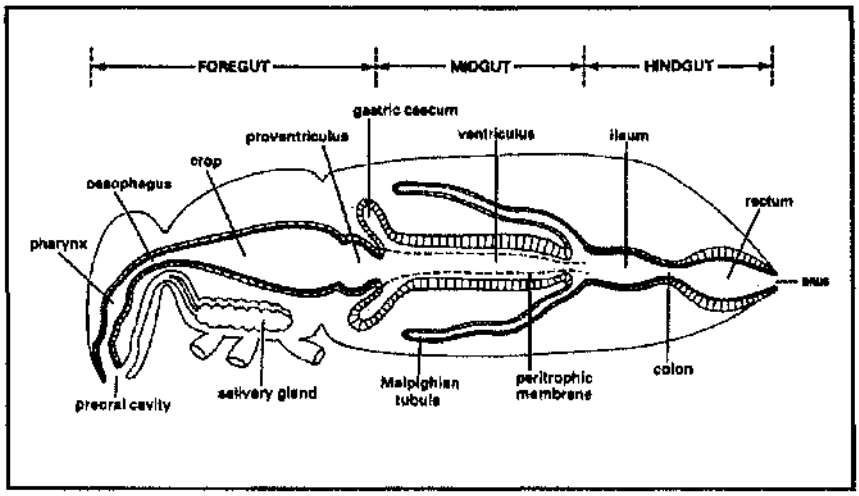

Figure 1.5. Morphology of *Manduca* larva after Dow 1982.

The midgut is a simple epithelium composed of a monolayer of cells sitting on a basement membrane (Anderson & Harvey, 1966). On the gut lumen side there is a thin, porous and protective film termed the peritrophic membrane (Adang, 1982; Adang & Spence, 1981; Wolfersberger, Spaeth, & Dow, 1986). Six longitudinal muscles, equidistant from one another, run along the length of the midgut. Extensive folding of the epithelium gives the tissue a ruffled appearance (Anderson & Harvey, 1966); this folding is generated by the tissue being gathered along the longitudinal muscles (Cioffi, 1979).

The midgut can be divided into anterior, middle and posterior regions based on the degree of epithelial folding, with the anterior and posterior regions being more highly folded than the mid-midgut region (Cioffi, 1979). There are also structural and morphological differences between regions, within the cell types that comprise the midgut.

1.2.2 Cell types in the midgut

The midgut epithelium is composed of two major cell types, the columnar and the goblet cells (Anderson & Harvey, 1966; Cioffi,

1979). The columnar cells are the most prevalent and surround individual goblet cells, outnumbering the goblet cells 2:1 (Hakim, Baldwin, & Bayer, 1988). The columnar cells have a thick apical brush border which provides an increased surface area for secretion/absorption and favours local ion concentration gradients. The columnar cell cytoplasm contains much rough endoplasmic reticulum, many mitochondria and a centrally placed nucleus. The basal membrane is convoluted and the lateral membranes are coupled to other cells by gap and smooth septate junctions (Baldwin & Hakim, 1981). The columnar cell morphology changes subtly between the anterior, mid and posterior regions of the midgut (Cioffi, 1979). In the anterior region, the apical microvilli structure is composed of a network of projections from which vesicles bud off, the function of these microvilli is likely to be primarily secretary. In the mid and posterior regions the microvilli become more pronounced, without vesicle production, and are believed to have a principally absorptive role (Cioffi, 1979).

The goblet cells, distinct from the mucus-secreting vertebrate intestinal cell of the same name, are unique to insect epithelia and have a highly specialised structure. The cell is dominated by a large (20 μm in diameter) cavity or "goblet" which constitutes much of the volume of the cell (Cioffi, 1979). **Fig 1.6.** The goblet membrane is lined internally with apical projections resembling microvilli and studded with 10 nm particles called portasomes, which act as a marker for this membrane. The goblet membrane is derived from an intracellular vesicle that fuses with the apical plasma membrane (Baldwin & Hakim, 1991; Turbeck, 1974) and (although the fine line between vesicular/plasma membrane is unclear) is termed the goblet cell apical membrane or "GCAM" (Cioffi, 1979). The site of fusion with the plasma membrane incorporates a complex interdigitation of membrane processes forming a "valve" which isolates the goblet cavity from the gut lumen (Dow & Peacock, 1989a; Flower & Filshie, 1976). The GCAM structure is not only physically but electrically isolated from the lumen (Dow & Peacock, 1989a). The goblet cell ultrastructure, analogous to the columnar cell's, is modified

between regions of the midgut. The goblet cells from anterior and mid-midgut regions are similar in structure, incorporating a basally located cavity and, unique to these goblet cells, mitochondrial insertion into the GCAM microvilli. The posterior goblet cells, by contrast, have an apically located cavity and mitochondria are not associated with the goblet microvilli. The apical valve is not highly developed in posterior goblets, compared with anterior/mid midgut cells (Cioffi, 1979). The portasomes, believed to be involved in ion transport, are located on the cytoplasmic face of the GCAM in all three areas.

The midgut epithelium also contains regenerative (Turbeck, 1974), or stem cells (Baldwin & Hakim, 1991) and possibly endocrine cells (Endo, 1981).

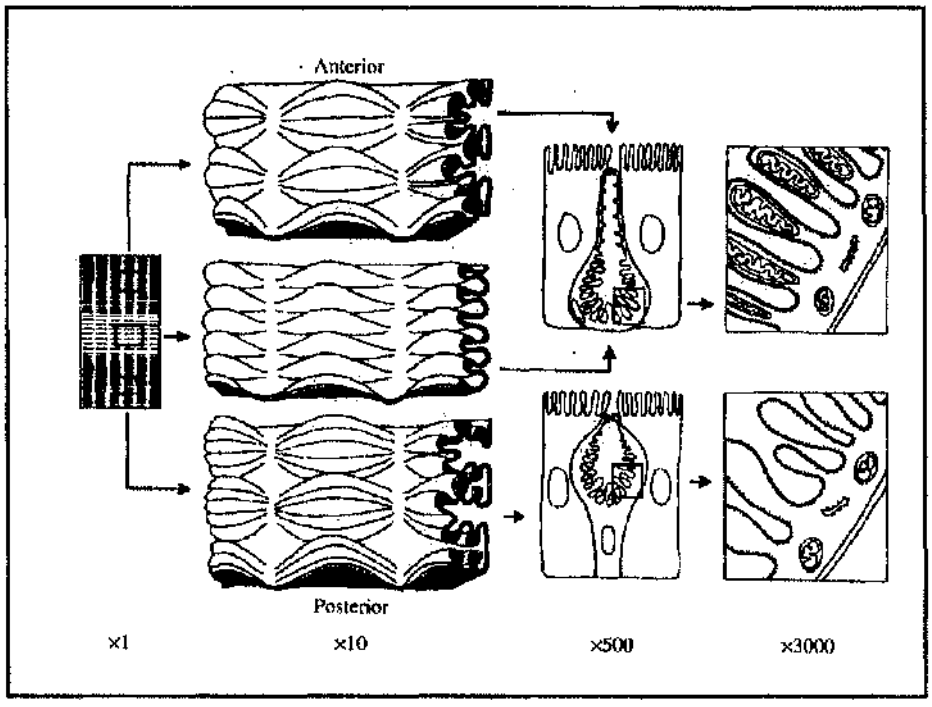

Figure 1.6. A diagrammatic representation of the *Manduca* midgut. Anterior, mid and posterior specialisation is visible. Note the degree of folding of the tissue, the position of the goblet cell cavity and the insertion of mitochondria into the GCAM microvilli. Approximate magnifications are shown. (after Cioffi, 1979 and Dow, 1992)

1.2.3 The midgut is a major site of ion transport

The midgut of Lepidopteran larvae is the site of an outstanding active potassium ion transport system that generates a transepithelial potential difference (TEP) of 80-150 mV, lumen positive (Harvey, 1967; Harvey, 1980; Harvey & Nedergaard, 1964) and a short circuit current of 0.5-1 mA/cm^2 (Dow, 1984a; Wood, 1978). In *Manduca*, despite the differences in morphology, all three regions of the isolated midgut display similar electrical signatures (Cioffi & Harvey, 1981). The transport system requires oxidative phosphorylation and is rapidly and reversibly inhibited by anoxia (Harvey, 1967) and metabolic inhibitors such as cyanide (Mandel, 1980) and azide (Dow, Boyes, Harvey, & Wolfersberger, 1985). Using radiolabelled K^+ it was demonstrated (Wood, 1978) that the short circuit current was conveyed entirely by potassium, which is transported from blood to gut lumen and is later re-absorbed in the hind gut. The high voltage is generated despite a very low resistance of 100 Ωcm^2 indicating extremely vigorous transport. In vitro the epithelium has been shown to transport other cations in the order of K=Rb>Na>Li>Cs (Harvey & Zehran, 1972; Wolfersberger, 1982).

1.2.4 Location of the K^+ pump

Since the presence of portasomes was restricted to the goblet cavity membrane, this membrane was postulated to be the site of the K^+ pump (Anderson & Harvey, 1966). Electrophysiological evidence demonstrates that, of the two potential steps measured when a microelectrode is advanced through a midgut epithelium, only the apical potential was affected by anoxia, suggesting active transport occurs across this membrane (Wood, 1969). In addition, ion sensitive microelectrode impalements indicate a high potassium concentration and positive potential across goblet cavities, but a negative potential from blood to cytoplasm (Chao, Moffett, & Koch, 1991; Dow & Peacock, 1989a; Moffett, Hudson, Moffett, & Ridgeway, 1982). These findings indicate that K^+ can move from blood to cytoplasm passively via a K^+ channel but must be transported actively across the goblet cavity. The *Manduca* midgut basal K^+ channel is blocked by barium (Moffett & Koch, 1988) and the K^+ channel inhibitor lidocane (Moffett & Koch, 1991),

however, the K^+ channel of midgut differs in the pharmacological and selectivity profiles from other known channels (Zeiske, 1992). Harvey's prediction that the goblet membrane as the site of active K^+ transport, was confirmed by X-ray microanalysis of potassium levels that showed potassium concentrations fall on the apical side of the cavity membrane upon anoxia (Dow, Gupta, Hall, & Harvey, 1984). The development of an ingenious technique to isolate fractions enriched with specific plasma membrane segments from both midgut cell types (Cioffi & Wolfersberger, 1983) demonstrated K^+ ATPase activity exclusively co-purifies with the portasome studded, goblet cell apical membrane (Wieczorek, Wolfersberger, Cioffi, & Harvey, 1986).

1.2.5 Proton transporting ATPases

There are three classes of proton transporting ATPases; the P-, F-, and V- ATPases. The groups are classed on their inhibitor sensitivities, structure, function, location and nucleic acid and amino acid sequences. The P-ATPases (or E_1-E_2 type) operate via a phosphoenzyme intermediate and are hence inhibited by the intermediate phosphate analogue vanadate, and are also inhibited by oubain. The Na^+/K^+ ATPase of animal plasma membrane is an example of the P-ATPases. So too is the Ca^{2+} ATPase of sarcoplasmic reticulum and the H^+/K^+ ATPase of the gastric mucosa. The P-ATPase is composed of a single catalytic subunit of 100 kDa, probably present as a dimer.

The F-ATPases (or F_0F_1 type) are inhibited by azide, oligomycin and DCCD. F-ATPases are located on the plasma membranes of eubacteria and on the inner membranes of mitochondria and chloroplasts. This enzyme generates an ATP-hydrolysis-driven proton gradient for use in ion transport processes. Under normal conditions it works 'in reverse' and synthesises ATP in response to an electron transfer generated proton gradient. The F-ATPases are made up of two parts; the F_1 catalytic domain and the F_0 transmembrane domain. The F_1 domain is made up of five different subunits (α, β, γ, δ and ε) with the catalytic site located on the β subunit. The mitochondrial transmembrane F_0 part is complex with as many as 12 different subunits. The F_0 part

includes the 8 kDa protein which binds DCCD and is a major component of the proton channel. The catalytic site and proton channel are coupled by conformational changes. The evidence suggests that the energy transformation is coupled to proton transport via a conformational change in the molecule.

The V-ATPases are similar to the F-ATPases in both sequence homologies between analogous subunits, and subunit composition (Nelson, Nelson, & Mandiyan, 1989). This suggests that they evolved from a common ancestor (Nelson & Nelson, 1989). Despite these similarities there exist sufficient differences to place the V-ATPases in a separate category. V-ATPases are insensitive to azide and vanadate, but are inhibited by nitrate, NEM and the specific V-ATPase inhibitor, bafilomycin (Nelson, 1991). The V-ATPases were first isolated from eukaryotic endomembranes, where they play a key role in acidification of intracellular compartments such as clathrin coated vesicles, endosomes, lysosomes and golgi apparatus (Nelson & Taiz, 1989). The proton gradient generated by the V-ATPases energises the accumulation of neurotransmitters by synaptic vesicles and salt balance in plant cell tonoplasts.

It is now known that V-ATPases actively transport protons across many plasma membranes including kidney cells, where the V-ATPase energises the acidification of urine (Brown, Hirsch, & Gluck, 1988; Gluck, Nelson, Lee, Wang, Guo, Fu, *et al.*, 1992). In osteoclasts the V-ATPase acidifies the extracellular fluid leading to bone reabsorbtion (Chatterjee, Chakraborty, Leit, Neff, Jamsakellokumpu, Fuchs, et al., 1992). The V-ATPase also energises secondary transport in macrophage (Grinstein, Nanda, Lukacs, & Rotstein, 1992) and insect epithelia (Klein, 1992).

1.2.6 K^+ transport is energised by a V-ATPase

Manduca midgut transepithelial K^+ transport energises the apical membrane and is not inhibited by ouabain. This indicates that the K^+ pump is powered by a mechanism other than that of the classical, ouabain-sensitive, basolateral, Na^+/K^+ ATPase common to invertebrate epithelia (Harvey, Cioffi, Dow, & Wolfersberger,

1983a; Jungreis & Vaughn, 1977). Purified goblet cell apical membranes (Cioffi & Wolfersberger, 1983) incorporate a K^+ stimulated, Mg^{2+} dependent ATPase (Wieczorek, et al., 1986). The ATPase activity is insensitive to the Na^+/K^+ ATPase (P-type ATPase) inhibitors oubain and vanadate, in addition, ATPase activity is insensitive to the mitochondrial (F-type ATPase) inhibitors azide and oligomycin. ATPase activity is, however, inhibited by N,N'-dicyclohexylcarbodiimide, nitrate and submicromolar concentrations of bafilomycin A_1 (Bowman, Altendorf, & Siebers, 1988b; Nelson, 1991; Wieczorek, Putzenlechner, Zeiske, & Klein, 1991). On the basis of the activity and inhibitor sensitivity profiles, the GCAM ATPase is a member of the Vacuolar-type, or V-ATPase, family of ion transporting ATPases (Klein, 1992; Klein, Löffelmann, & Wieczorek, 1991; Klein, Weerth, & Wieczorek, 1988; Klein & Zimmermann, 1991; Schweikl, Klein, Schindlebeck, & Wieczorek, 1989; Wieczorek, et al., 1991; Wieczorek, Weerth, Schindlebeck, & Klein, 1989).

1.3 The V-ATPase Proton Pump

1.3.1 The V-ATPase is a ubiquitous protein

The V-ATPase is a multimeric molecule composed of a mushroom shaped structure with a transmembrane "stalk" termed the V_O domain and a cytoplasmic "head" termed the V_1 domain (Puopolo & Forgac, 1990). The V_O domain is the proton pore, with the V_1 domain being the catalytic region. This structure is analogous to that of the F_1F_O-ATPases, and indeed, amino acid homologies between subunits of these molecules (Bowman, Bowman, Allen, & Wechser, 1988a; Bowman & Bowman, 1988) and similar subunit stoichiometries indicate that these molecules are related (Arai, 1988). The subunit structure within the class of V-ATPases is similar between V-ATPases isolated from various sources.

1.3.2 Structure of the **Manduca** *midgut V-ATPase*

Upon isolation from the GCAM membrane, the purified ATPase displays the same substrate and inhibitor sensitivity as the

membrane bound form. Western blots, after sodium dodecylsulphate polyacrylamide gel electrophoresis (SDS-PAGE), probed with immune serum directed to the purified ATPase show that the ATPase consists of at least nine subunits with relative molecular masses of 67 000, 56 000, 43 000, 40 000, 28 000, 20 000, 17 000, 16 000 and 14 000. This high number of subunits corresponds to the subunit profile found in other V-ATPases. The subunit arrangement forms a structure composed of a peripheral "head" group (V_1) and an integral group (V_0) including the proton channel. The V_1 cytosolic head is believed to be composed of the 67 kDa catalytic subunit, and the 56, 28 and 16 kDa subunits. The V_0 is composed of the 43, 40, 20 and 17 kDa proton pore. The 17 kDa proton pore is inhibited and labelled by N,N'-dicyclohexylcarbodiimide (DCCD) (Mandel, Moriyama, Hulmes, Pan, Nelson, & Nelson, 1988).

A common nomenclature is used for comparisons between analogous V-ATPase subunits isolated from different sources. Bands of approximately 67 and 56 kDa are termed the A and B subunits respectively. The A subunit is believed to be involved in ATP binding and hydrolysis and is present in a stoichiometry of six copies per holoenzyme (Arai, 1988). The A subunit isolated from *Manduca* midgut binds radiolabelled ATP (Ralph Gräf pers communication). The *Manduca* 67 kDa subunit has been cloned from a midgut cDNA library and the primary structure closely resembled that of other known V-ATPase A subunits (Gräf, Novak, Harvey, & Wieczorek, 1992). The B subunit, present in three copies per holoenzyme, also contains a putative ATPase binding site as deduced by its primary structure. Activity of the enzyme is dependent on a functional B subunit, therefore it is also termed the regulatory subunit. The *Manduca* B subunit primary structure closely matches other V-ATPase subunit B sequences published such as that of the lepidopteran *H. virescens* and human kidney. The 40 kDa subunit enhances ATPase activity but its main function is believed to be structural (Puopolo, 1992). The 28 kDa subunit of midgut V-ATPase exclusively binds the ATP analogue [^{14}C]5'-p-fluorosulfonylbenzoyladenosine (FSBA) resulting in ATPase activity inhibition and thus suggesting a catalytic activity.

However other studies could not detect radiolabelled ATP binding to this subunit.

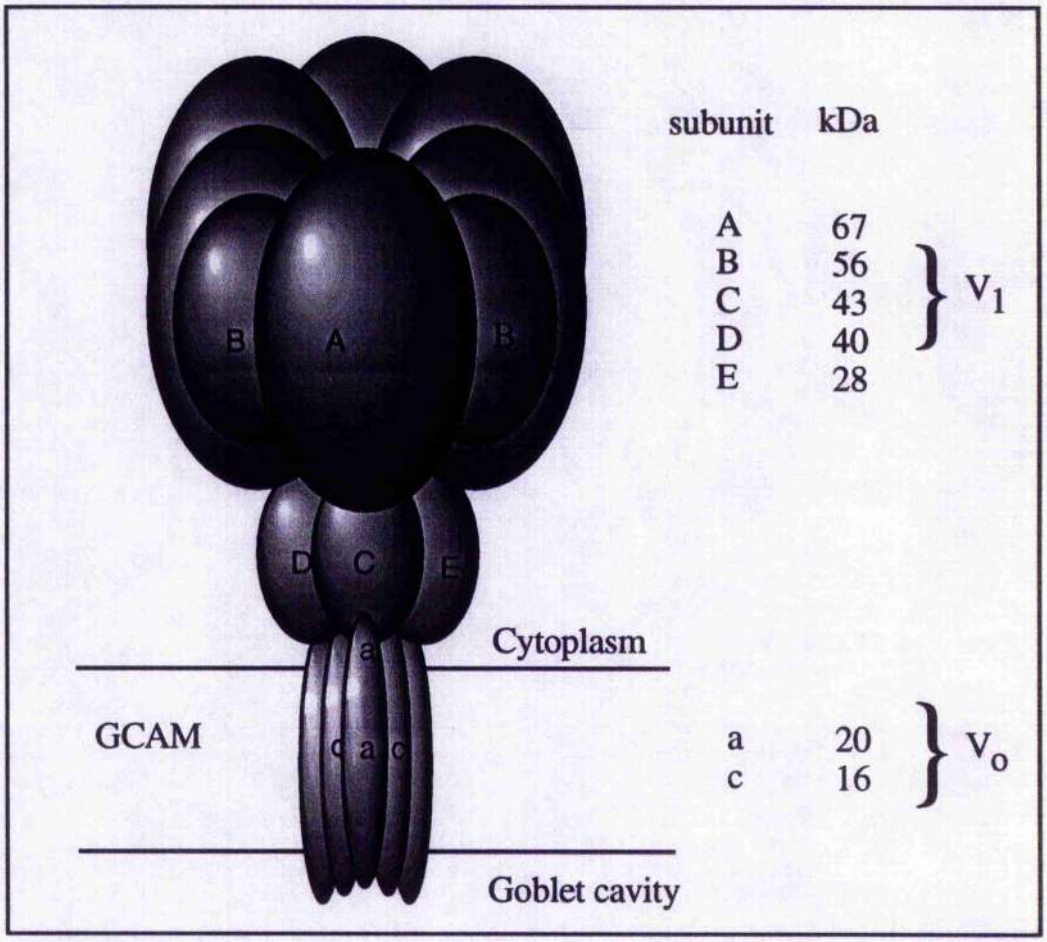

Figure 1.7. Schematic model for the minimal subunit structure of the V-ATPase. The model is composed of the polypeptides common to preparations from fungi, plants and mammals (after Nelson, 1991).

Six copies of the 16 kDa subunit constitute the transmembrane proton pore. This subunit is labelled with the hydrophobic carboxyl reagent N,N'-dicyclohexylcarbodiimide (DCCD). The 16 kDa proteolipid (subunit c) appears to have evolved by tandem duplication of the 8 kDa proton pore of the F-ATPases (Mandel, et al., 1988). The 16 kDa proteolipid of the yeast *Saccharomyces cerevisiae* is encoded by the VMA3 gene, inactivation of which leads to loss of V-ATPase activity (Nelson, Mandiyan, Noumi, Moriyama, Miedel, & Nelson, 1990; Nelson & Nelson, 1990). The

16 kDa subunit is very similar to the 16-18 kDa protein of gap junctions (Finbow, Eliopoulos, Jackson, Keen, Meagher, Thompson, et al., 1992). Recent studies have argued that the V-ATPase subunit c and the ductin protein of gap junctions are indeed the same protein (Finbow, Goodwin, Meagher, Lane, Keen, Findlay, et al., 1994).

1.3.3 Mechanism of K^+ transport

Potassium is actively secreted across the GCAM by a V-ATPase; however, all known V-ATPases are proton pumps. To address this puzzle the ion transporting properties of purified goblet cell apical membrane have been studied. The fluorescent dye acridine orange accumulates in acidic vesicles and the subsequent quench of fluorescence is used to demonstrate compartmentalised acidification. Vesicles derived from GCAM undergo ATP-dependent acidification, demonstrating proton transport, with the same substrate/inhibitor profile as the GCAM V-ATPase activity. The close correlation between ATPase and proton transport activity profile suggests that the ATPase is indeed a proton pump, rather than a K^+ pump as had previously been supposed.

In the presence of potassium ions, however, a proton gradient cannot be generated but a transmembrane potential is produced. Furthermore, the addition of K^+ to a vesicle suspension will dissipate an established proton gradient, but maintain a transmembrane potential. Is the V-ATPase actively transporting K^+? In experiments, GCAM vesicles, preloaded with high [K^+], generate an ATP-independent pH gradient in low [K^+] medium, demonstrating an ATP independent influx of H^+. A hypothesis has been developed that explains these observations, whereby primary electrogenic V-ATPase proton transport energises a secondary K^+/H^+ antiport resulting in active K^+ secretion. Polyclonal antibodies against the GCAM ATPase inhibit ATP dependent proton transport but not antiporter activity suggesting that the ATPase and the antiport are separate entities. Conclusive proof of this model came when the antiporter was inhibited with amiloride; under these conditions the membrane

generated a pH gradient even in the presence of K^+, demonstrating that the V-ATPase is exclusively a proton pump and that K^+ transport is facilitated via a K^+/H^+ antiporter. Chloride has also been shown to destroy membrane potentials indicating that there is an anion channel (see **Fig 1.8**).

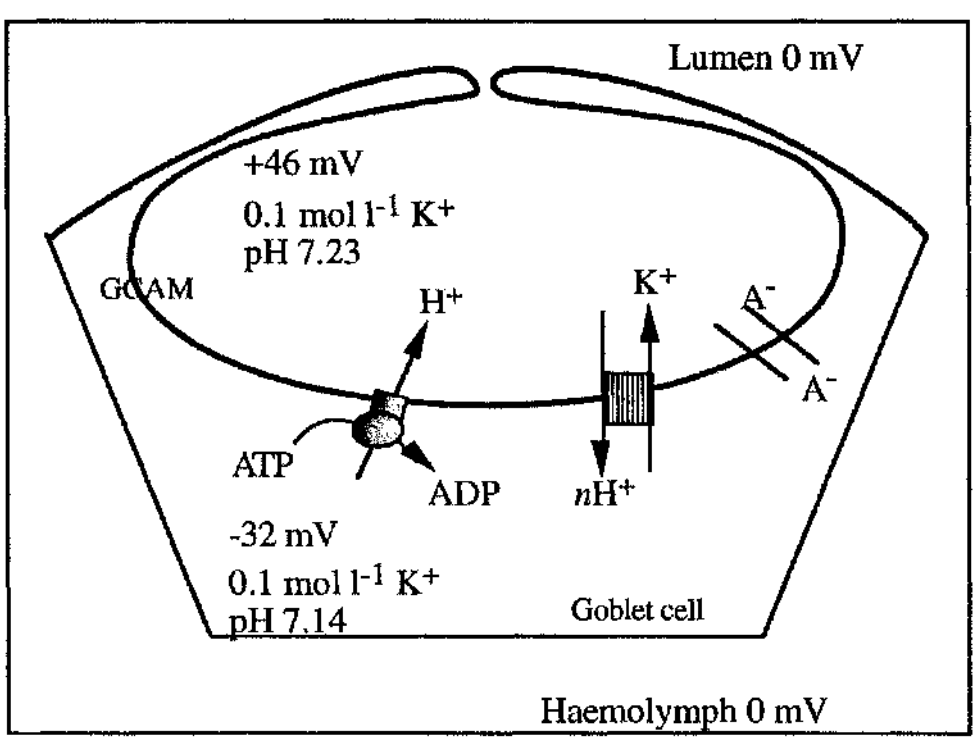

Figure 1.8. Energisation of K^+ secretion in *Manduca* posterior midgut. Voltages, pH values and K^+ concentrations are measured under short circuit conditions (after Wieczorek *et al* 1991).

1.3.4 Function of the midgut K^+ pump

The larva spends 10% of its total ATP production on K^+ transport into the gut lumen (Dow & Peacock, 1989b). The reason for this enormous effort could be K^+ excretion (Harvey & Zehran, 1972; Maddrell, 1971). This role seems unlikely because potassium is rescued from the faeces (Dow & Harvey, 1988). Also, the specialised convoluted valve at the exit of the cavity hinders K^+ transport by an estimated 5 kJ mol^{-1} K^+ (Dow & Peacock, 1989a). In addition, the major component of the electrochemical gradient against which the pump must work is the electrical gradient generated by the pump itself (Dow & Harvey, 1988; Dow &

Peacock, 1989). It is therefore unlikely that the function of the K^+ transport system is K^+ excretion. The K^+ pump does, however, drive K^+/amino acid cotransport (Giordana, Parenti, Hanozet, & Sacchi, 1985; Giordana, Sacchi, & Hanozet, 1982; Nedergaard, 1977).

The lepidopteran midgut has an extremely high pH, with a peak *in vivo* value being the highest measured in a biological system. Measurements, using pH semi-micro electrodes along the length of the alimentary canal, reveal that the gut content pH values rise above the pH of the ingested food in the anterior region of the midgut and reach a peak in excess of pH 12 in the mid-midgut region. pH levels fall rapidly in the posterior region, ultimately reaching levels when the faecal pH is similar to that of the ingested food. The reason for such a high pH is most likely to aid digestion or absorption of food. Tannins, released from plant tissue upon maceration, crosslink food proteins. The high pH may promote digestion by preventing this cross linking from occurring. The high pH also optimises the rate of enzymatic hydrolysis and may protect against microbial pathogens (see **Fig 1.9.**).

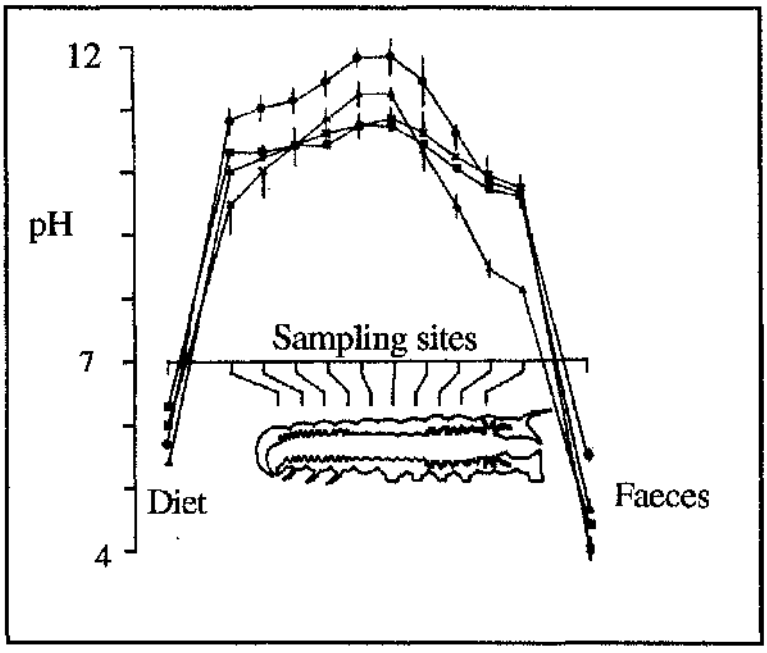

Figure 1.9. The pH profile along the alimentary canal of several species of larval Lepidoptera (After Dow, 1984). The highest pH is always found two-thirds of the way along the midgut.

1.3.5 Generation of a high pH

A significant body of evidence suggests that the K^+ transport system is involved in generation of the high pH, indeed, according to the current model, the generation of a high pH is the raison d'être for the K^+ pump (Dow, 1992b).(Dow, 1984b; Dow, 1992b; Dow & Peacock, 1989b). K^+ transport activity and high pH generation in the anterior and mid-midgut are inseparable under physiological conditions (Dow & O'Donnell, 1990). High pH generation is restricted to the anterior and middle regions of the midgut. This regional specificity is accompanied by carbonic anhydrase activity in the goblet cells (Ridgway & Moffett, 1986)., mitochondrial insertion into the GCAM 'microvillus' and an elaborate 'valve' structure. The posterior midgut, lacking these specialisations, also pumps K+ but here a high pH is not generated. These observations suggest that high pH found in the midgut is likely to be generated by a cellular process and not solely as a consequence of K+ transport into the midgut. K^+ secretion into the gut lumen is obligatorily followed by negative ions to maintain the charge balance. Carbonic anhydrase will supply HCO_3^- for export to the midgut lumen, thus somewhat compensating the positive charge. Simultaneously, a high pH is generated. In this scenario, it is essential that the goblet cavity remains neutral or acid as a slight alkalinity would inhibit the H+/K+ exchanger (Dow, 1992b; Dow & Peacock, 1989a). The goblet cavity is isolated from the highly alkaline 'protophile' gut lumen by the elaborate cavity 'valve'. One may speculate that the valve is the structure in which the pH is generated (see **Figure 1.10.**). In this way a proton transporting ATPase generates the highest known pH in a biological system!

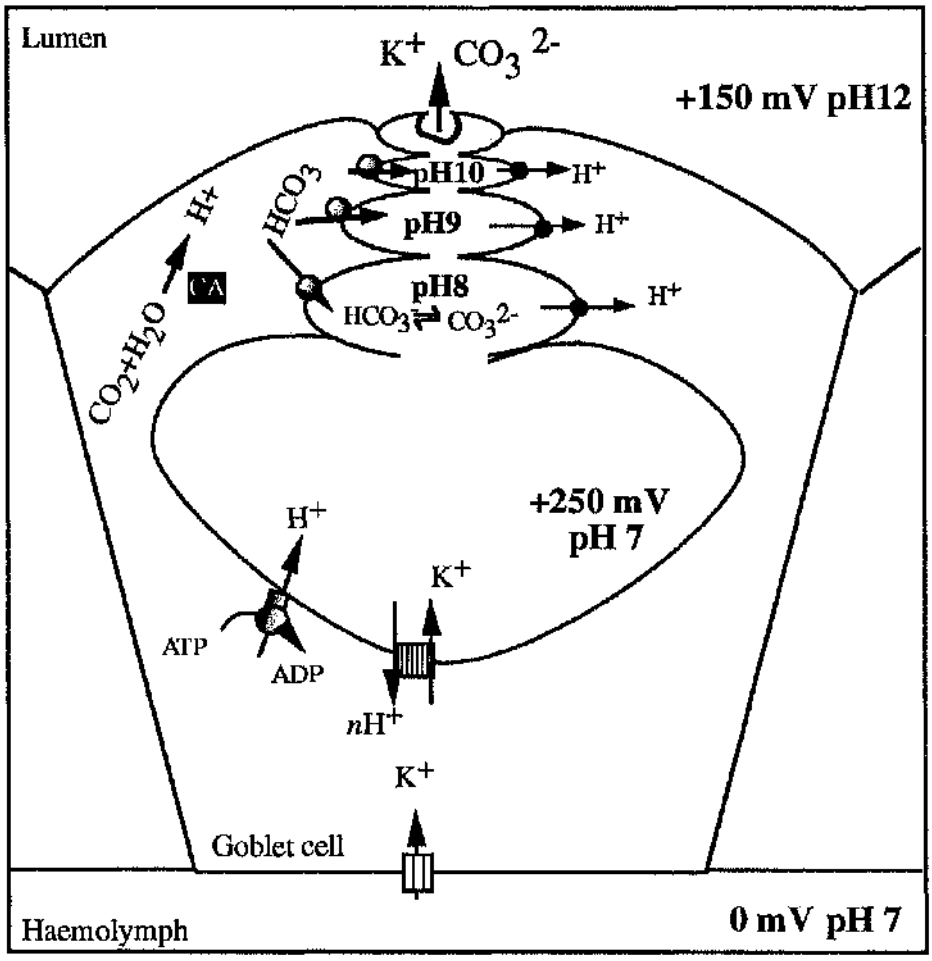

Figure 1.10. Model for high midgut pH generation by the goblet cell 'valve' structure. It is tempting to speculate that the elaborate valve structure that separates the goblet cavity (pH 7 or less) and the midgut lumen (pH 12) is involved in pH generation. The valve is described in Flower & Filshie, 1976 as a complex interdigitation of membrane projections. In the model described here, the valve is considered to be a series of compartments which are tightly separated from the goblet cavity. Protons are progressively forced out of the valve compartments by the huge electrochemical potential across the GCAM.

1.4 Aims

Ion transport is one of the most fundamental processes in biology. The *Manduca* midgut ion transport system is an ideal model to study this phenomena. Transport can be studied on the level of net transport across the epithelium, transport by the components of the

K^+ pump or at the molecular level of these components. The emphasis of this thesis will be the regulation of ion transport. I aim to demonstrate that ion transport is modulated during specific periods of the larva's growth. Evidence will be provided that strongly suggests that the V-ATPase component of the transport system is the specific target of hormonal control. An investigation will follow into the mechanism of V-ATPase regulation in *Manduca* midgut.

CHAPTER 2 MATERIALS AND METHODS

2.1 Ion Transport Methods

2.1.1. Obtaining and rearing larvae

Manduca sexta larvae were reared on a standard artificial diet (Yamamoto, 1969) (**Table 2.1**). Larvae were maintained in a Scotlab-VSL incubator in a 16h light: 8h dark photo period at 25°C and ambient humidity. *Manduca* eggs were either kindly supplied by Dr Stuart Reynolds at the University of Bath or were from the Munich laboratory culture.

Wheatgerm	150g
Casein	70g
Sucrose	60g
Dried bakers yeast	30g
Wesson's salt mix	20g
Cholesterol	4g
Sorbic acid	3g
Choline chloride	2g
Methyl hydroxybenzoate	2g
Boiling dH_2O	700 ml
Stir ingredients until suspended, then add...	
Melted Agar	40g
in dH_2O	1000ml
Linseed oil	4ml
Corn oil	4ml
10% formaldehyde	8ml
Cool to 60°C then add..	
Ascorbic acid	8g
Vanderzant vitamin mix	0.2g
Chlortetracycline	0.2g

Table 2.1 Composition of artificial diet

2.1.2 Staging of larvae

Larvae were studied during the fourth instar to fifth instar larval moult and then up to the wandering stage. Growth and development rates varied between individuals, therefore larvae were staged upon development of external morphological features (Baldwin & Hakim, 1991) as summarised below. Fourth instar intermoult larvae feed and gain mass until they attain approximately the weight of 1.5 g (stage A). The larvae stop feeding upon entry into the moult (stage B). Development of a green head capsule was the first external indication of entry into the moult (stage C). The following processes up to ecdysis take approximately 24 hours; the base of the head capsule becomes clear (stage D), then the head capsule clears and the mandibles are present but unpigmented (stage E), the mandibles become pigmented (stage F) and finally ecdysis occurs. Ecdysis was recorded, when the skin began to be shed, at the moment when the larvae lost their head capsule. After the moult, the larvae resumed feeding and were then considered to be 5th instar intermoult larvae (see **Figure 2.1**)

2.1.3 Physiological saline

Physiological saline used was modified from that used by Cioffi and Harvey (1981) which was based on the ionic composition of *Manduca* sexta larval haemolymph (Cioffi & Harvey, 1981; Florkin, 1974). Certain metabolic substrates were added after stimulatory properties had been reported (Chamberlin, 1989; Dow & O'Donnell, 1990). For convenience the solution was termed *Manduca saline* and was composed of 200 mM Sucrose, 5 mM Glucose, 5 mM Succinic acid, 5 mM Caproic acid, 22 mM KCl, 1 mM $CaCl_2$, 1, mM $MgCl_2$, 5 mM Tris and KOH/HCl to pH 6.7.

A more complex saline was used for periods lasting in excess of 1 h on the Ussing chamber. This saline contains physiological levels of haemolymph ions, amino acids and sugars. This saline maintains midgut function over several hours (Chamberlin, 1989; Chamberlin, 1990). The saline is composed of; 6.0 mM Na_2HPO_4, 5.0 mM $MgCl_2$, 1.0 mM $CaCl_2$, 5.8 mM KOH, 7.7 mM Potassium citrate, 2.8 Sodium succinate, 2.0 mM Glucose, 27 mM Trehalose,

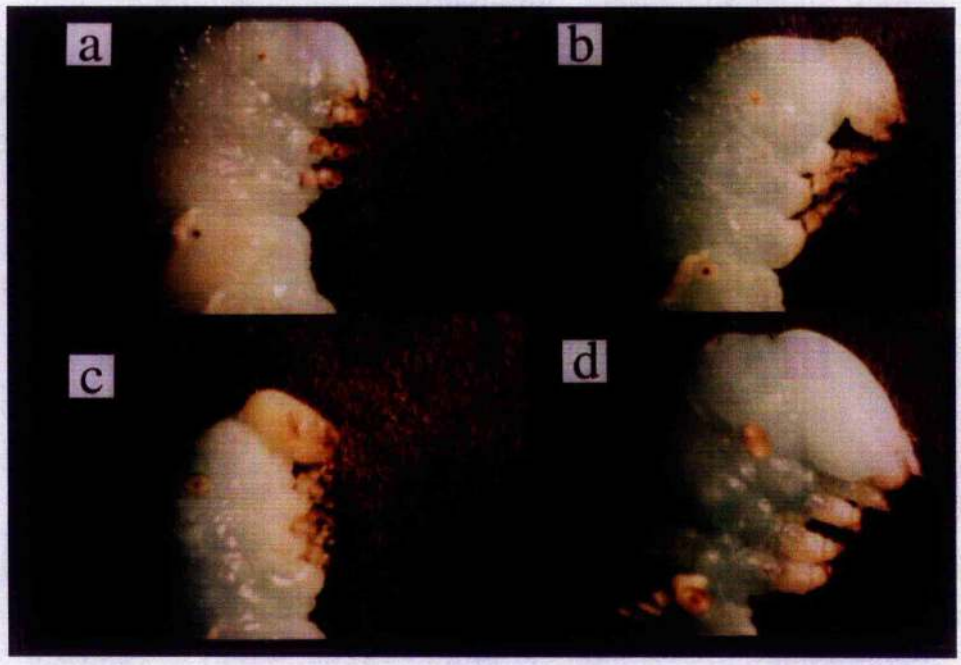

Figure 2.1. Developmental changes in head capsule morphology during the 4th to 5th instar moult. Numbers in parenthesis refer to hours prior to ecdysis. **a**, 4th instar head (-40 h); **b**, development of green head capsule indicates entry into the moult (-36 h); **c**, development of colourless headcapsule and pigmented mandibles (-12 h); **d**, 5th instar head (+1 h).

9.4 mM glutamine, 8.9 mM serine, 7.4 mM Proline, 12.8 mM Glycine, 9.7 mM Histidine, 5.6 mM Malic acid, 4.6 mM Threonine, 6.6 mM Alanine, 140 mM Polyethylene glycol (Mr 400), pH 6.7.

2.1.4 Dissection

Larvae were cold anaesthetised on crushed ice for 15 min prior to dissection. This numbs the animal and prevents contraction of the muscles underlying the midgut once isolated. Cross sectional cuts were made between segments 2 and 3 and between segments 8 and 9 of the larvae. A blunt ended probe was inserted longitudinally through the centre of the midgut lumen. The body wall was carefully dissected away leaving the midgut intact around the probe. The midgut was cut along one of the longitudinal muscles and opened out into a flat sheet. The dissection is similar to that described by Cioffi and Harvey (Cioffi & Harvey, 1981).

2.1.5 Transepithelial voltage measurements

In-vitro trans epithelial potential difference (TEP) measurements were made upon single, isolated mid-midguts using an Ussing-type chamber (Dow, et al., 1985). Measurements were made on a flat sample of mid-midgut stretched across an aperture 6 mm in diameter. This was inserted into the chamber using a "lollipop" type holder. *Manduca* saline was oxygenated and circulated on either side of the epithelium by using an oxygen gas lift pump system. Open circuit voltage was measured using silver chloride electrodes and displayed on a chart recorder via x1 high impedance pre-amplifier. Stable TEP readings were noted ten minutes after mounting the midgut in the chamber. Midguts were removed from the larvae and the TEP immediately measured at hourly time points across the time course of the 4th to 5th instar moult.

2.1.6 pH Measurements

The pH of the gut contents was measured using a Russell semi-micro electrode. The larvae were chilled on ice for 15 min then bled by piercing the prolegs. Haemolymph was absorbed onto a paper tissue. The larvae were dissected between segments 8 and 9

and the gut contents were allowed to exude. pH of the fluid was measured immediately in a modified microfuge vial. The vial contained approximately 200 µl candle wax, cambered to fit the pH electrode snugly. This allowed small sample volumes (≈100 µl) to surround the pH and reference electrodes (see **figure 2.2**)

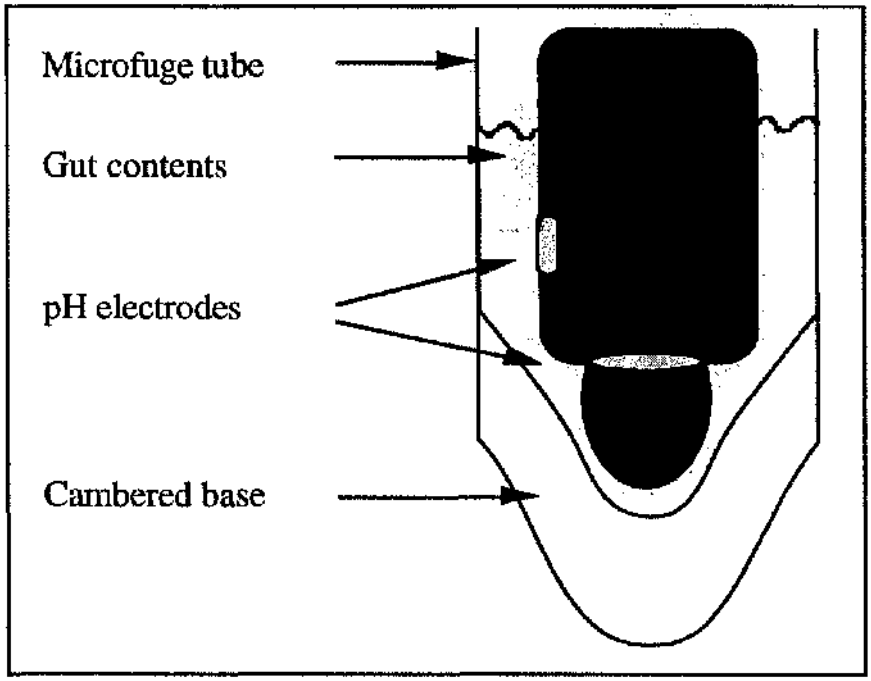

Figure 2.2 Modification to allow pH measurement of small volumes

2.1.7 Indicator dyes

Rosolic acid (red above pH 8- yellow below pH 6.8), was added to the diet in concentrations between 0.001%w/v and 10% w/v. The larvae were fed on diet impregnated with dye from hatching. The pH state of the midgut could be determined non-invasively by shining a pen-light torch through the larva and estimating the degree of colour saturation. In early instars, gut colour was directly visible without trans-illumination.

2.2 GCAM Purification and Analysis

2.2.1 Crude preparation of midgut membranes

Posterior midguts were removed from three larvae and immediately frozen in liquid nitrogen. The midguts were pooled and homogenised in 5 mM Tris HCl, 5 mM Na_2-EDTA, pH 8.1,. The homogenate was centrifuged at 4°C for 5 min at 15 000g, after which the supernatant was discarded. The pellet was washed twice by resuspension in the above buffer followed by centrifugation as above. The pellet was solubilised in 125 mM Tris- HCl, 2% SDS, 2% β-mercaptoethanol, pH 6.8 and heated for 5 min at 95°C. Any insoluble material was pelleted by a further 5 min centrifugation at 15 000g, only the supernatant was retained. At this stage the protein concentration of the supernatant was determined. The solubilised membranes were finally diluted to 5 µg/µl in Laemmli buffer: 125mM, Tris-HCl (pH 6.8), 2% SDS, 10% sucrose, 2% β-mercaptoethanol and 0.001% bromophenol blue.

2.2.2 Partially purified goblet cell apical membrane

GCAM was purified from either moulting stage E larvae approximately 12-18 h after development of a green head capsule, or 5g (mid stadium) fifth instar intermoult larvae. GCAM had not previously been isolated from fourth instar.

Preparation of GCAM from 5th instar larvae weighing 5-7 g was carried out by the method according to (Cioffi & Wolfersberger, 1983), (Wieczorek, Cioffi, Klein, Harvey, Schweikl, & Wolfersberger, 1990) (see **Figure 2.3**). GCAM purification procedure. The preparation of membranes from the much smaller 1.5 g moulting larvae required some subtle modifications from that of the standard fifth instar preparation (modifications for fourth instar preparations appear in parenthesis after the description for fifth instar). Posterior midgut regions were isolated as described above. The Malpighian tubules, which are attached to the midgut, were gently removed using forceps. The

tissue was then cut along each side of each longitudinal muscle and the strips of epithelial tissue were unfolded. The strips were cut into small pieces and stored on ice in SET buffer (SET buffer: 250mM sucrose,5 mM Tris-HCl, 5 mM Na2 EDTA, pH 8.1). The tissue pieces from three larvae (or from six moulting larvae) were collected in one tube until a total of twelve larvae (thirty moulting larvae) were processed.

The tip of the sonicator probe was placed in the middle of a suspension of tissue squares. The sonicator was set at power level 2.5 and the tissue pieces were sonicated for 20 s at a 40%/s 'on' pulse. Sonication was reduced by approximately 30% for moulting larvae to 10 s at power level 1.5. The tissue pieces were allowed to settle and the cloudy solution, consisting of columnar cell apical microvilli, was removed by aspiration. The tissue pieces were washed three times in cold SET buffer and finally resuspended in 2 ml of SET buffer. The suspension was drawn into and expelled from a Pasteur pipette 15 times, or until the tissue pieces failed to sink to the bottom of the tube. This action broke off the GCAM from the cell. The suspension was filtered through 4 layers of surgical gauze that were saturated in SET buffer. The residue was discarded and the filtrate was spun at 250 g for 2 min. The supernatant was discarded and the pellet was stored on ice while the other tissue squares in the other tubes were disrupted. The total elapsed time from the beginning of the dissection to the collection of 250 g pellets should not exceed 1.5 h.

The pellets were combined and layered onto a 45, 41, 37% w/w discontinuous sucrose density gradient and spun overnight at 77 000g. Three bands were visible after the spin. Band 2 contained the partially purified GCAM. Band 2 was collected and diluted stepwise with four times its volume of 5 mM Na-EDTA, 5 mM Tris-HCl, pH 8.1. The suspension was centrifuged at 10 000 g, after which the supernatant was removed and discarded. The pellet was believed to be composed of partially purified GCAM.

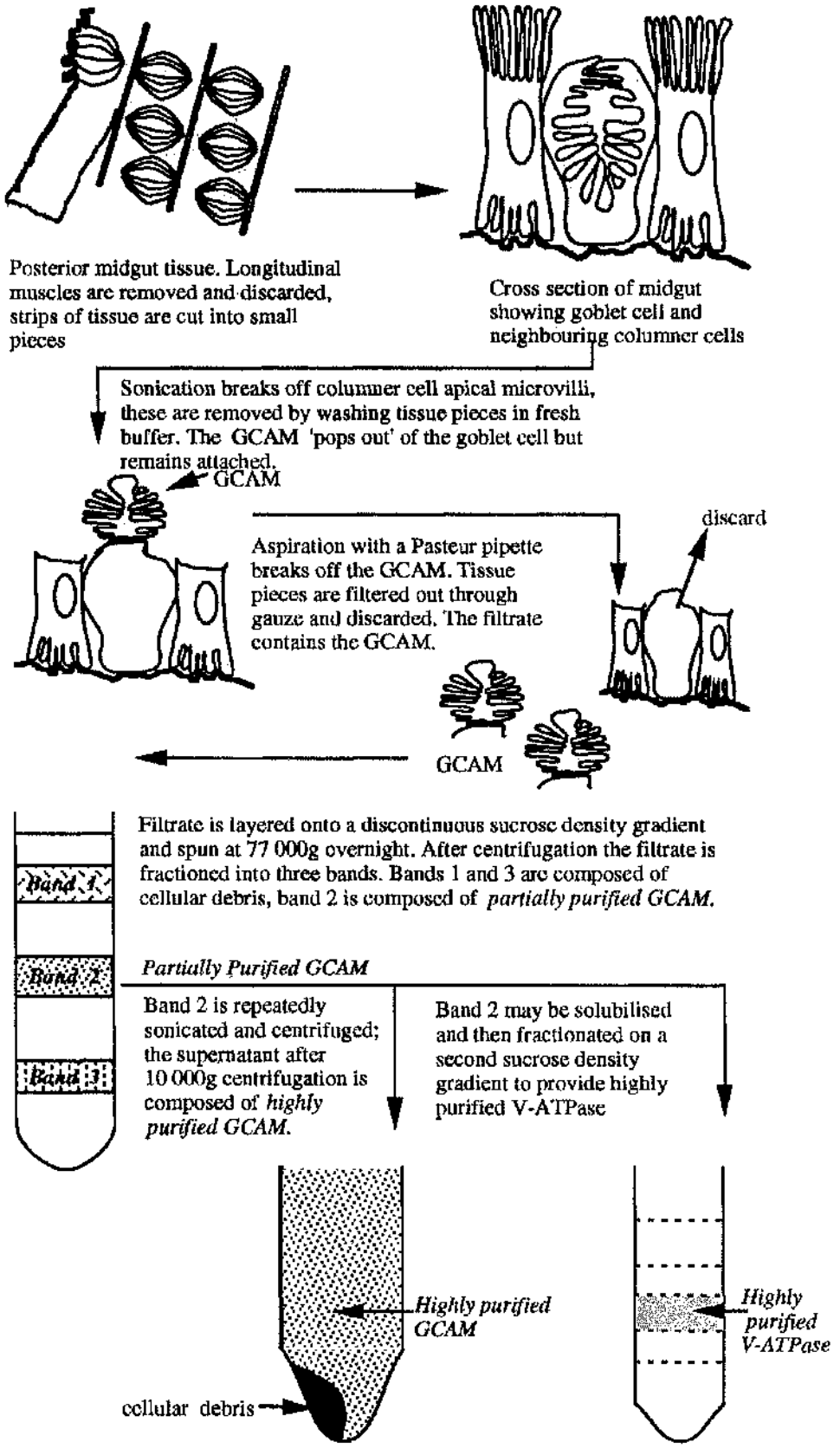

Figure 2.3. Goblet cell apical membrane (GCAM) purification procedureby the methods according to Cioffi and Wolfersberger (1983) and Wieczorek, Cioffi, Klein, Harvey, Schweikl & Wolfersberger (1990).

Method for isolation of highly purified GCAM

The diluted band 2 suspension was divided into aliquots of approximately 4 ml. Each aliquot was sonicated at a low setting. The sonicated suspension was centrifuged at 10 000g for 30 min. The supernatant, which contains the highly purified GCAM, was decanted and kept on ice. The pellet was resuspended in 4 ml of SET buffer and then sonicated and centrifuged as described above. The supernatant was combined with the 10 000g supernatant collected earlier. This process was repeated up to four times. The combined 10 000g supernatants were centrifuged at 30 000g for 1 h. After centrifugation the supernatant was removed and discarded, the pellet remaining was believed to be composed of highly purified GCAM.

2.2.3 Protein determination

Protein concentrations were determined using Amido Black according to the method of Popov *et al.*, 1975.

300µl of Amido Black solution (26 mg Amido Black in 100 ml 10% acetic acid/90% methanol) is added to 50µl of protein sample in a 1.5 ml disposable microfuge tube and incubated for 5 min at room temperature. After incubation the mixture is centrifuged at 14, 000 rpm for 5 min. The supernatant is discarded, the pellet is resuspended in 500 µl 10% acetic acid/90% methanol and centrifuged as before. This washing procedure is repeated twice. The washed pellet is dissolved in 350 µl of 0.1 N NaOH and the absorbance of the solution at 615 nm is determined. The absorbance is compared against a standard curve of known bovine serum albumin concentrations (for typical standard curve see appendix).

2.2.4 Membrane bound V-ATPase activity

The V-ATPase activity present in partially purified GCAM vesicles was assayed according to (Wieczorek, et al., 1990) in a buffer composed of 10 mM MOPS-Tris, 0.5 mM NaN_3, 0.1 mM Na_3VO_4, pH 7.0. Incubation mixtures had a total volume of 160 µl and were prepared in clean 1.5 ml disposable microcentrifuge tubes. Approximately 5 µg of membrane protein was used per assay. The mixture was pre incubated without

substrate for 10 min at an ambient temperature of 24-27°C.The reaction was started by the addition of 1 mM Tris-ATP/1 mM $MgCl_2$ and incubated for 5 min. The reaction was stopped by immersion in liquid nitrogen. Time-zero controls were dropped into liquid nitrogen immediately after addition of substrate. Standard curve samples contained the above buffer, membrane sample plus known concentrations of KPi. The standards were frozen prior to addition of the substrate, upon which they were immediately re-frozen to prevent any enzyme-catalysed ATP hydrolysis. The standards had a final volume of 160 µl.

2.2.5 Detection of ATPase activity

Inorganic phosphate, produced by ATP hydrolysis, was measured as a complex of phosphomolybdate with Malachite Green using the method of Wieczorek, et al, 1990.

Stock solutions; Acid molybdate solution: On day of use, one part 24% sulphuric acid was added to three parts 200mM sodium molybdate to six parts dH_2O. Malachite Green solution: 18.5g Malachite Green were added to 25 ml 1% polyvinylalcohol.

The timing of the procedure was critical. At time zero 50 µl of TCA was added to the frozen ATPase reaction mixture. The sample was placed in a 70°C water bath for 15 s, mixed, and centrifuged at 14 000 rpm for 1 min. 60 µl of supernatant was transferred to a corresponding tube containing 100 µl acid molybdate solution, mixed, and incubated for exactly 15 s. After the short incubation 30 µl of Malachite Green solution was added, mixed and incubated for a further 2 min. After this incubation, 200 µl of 7.8% sulphuric acid was added to stop the reaction. The mixture was allowed to stand for 70 min at room temperature for colour development.

The absorbance of each sample was read at 625 nm and the inorganic phosphate content was calculated using a standard curve of known Pi concentrations (for typical standard curve see appendix).

2.2.6 V-ATPase dependent proton transport

Acidification of partially purified GCAM vesicles by the V-ATPase was measured by the quench in fluorescence of acridine orange at the excitation wavelength of 493 nm and at the emission wavelength of 530 nm (Wieczorek et al., 1989; Wieczorek, Putzenlechner, Zeiske, & Klein, 1991). Fluorescence changes were monitored at an ambient temperature of 24-27°C by a Kontron SFM 23/B spectrofluorometer, and data acquired with a MacLab™ microprocessor A/D interface (AD Instruments Ltd, UK). Assays, in a final volume of 800 µl, consisted of 20 µg of membrane protein, 1 mM Tris ATP, 1 mM $MgCl_2$, 10 mM MOPS-Tris (pH 7.0), 0.5 mM sodium azide, 0.1 mM sodium orthovanadate, and 0.9 µM acridine orange. The reaction was started with the addition of 1 mM $MgCl_2$. pH gradients were dissipated after 120 s with 20 mM NH_4Cl.

2.2.7 ATP independent proton transport

Acidification of partially purified GCAM vesicles by the K^+/nH^+ antiporter was also measured by the quench in fluorescence of acridine orange at the excitation wavelength of 493 nm and at the emission wavelength of 530 nm, using similar methods to those described above (Wieczorek et al., 1989; Wieczorek, et al., 1991). However, there were some modifications to the technique. Fluorescence changes were monitored at an ambient temperature of 24-27°C and data was recorded on a chart recorder. Partially purified GCAM vesicles were resuspended to a concentration of 1µg membrane protein/µl of 10 mM Tris-HEPES, 20 mM K^+ gluconate, pH 8.1. The vesicles were allowed to equilibrate with this buffer for 3 h at 4°C and a further 1 h at room temperature. Reactions were started with the addition of 10 µl of this suspension to 790 µl of a K^+ free buffer consisting of: 10 mM Tris-HEPES, 20 mM tetramethylammoniumgluconate, 0.9 µM Acridine Orange, pH 8.1. Total dissipation of the pH gradient was achieved by the addition of 10 µl of 240 mM NH_4Cl (final concentration 3 mM).

2.2.8 SDS-PAGE analysis

Principle of SDS-PAGE analysis

Upon application of an electric field to a solution containing a protein molecule, the protein will migrate at a rate that depends on its net charge and its size and shape. Sodium dodecylsulphate polyacrylamide gel electrophoresis (SDS-PAGE) is the method of choice for separation of proteins on the exclusive basis of the molecular weight. SDS is an anionic detergent which denatures proteins by wrapping around the polypeptide backbone. This confers a net negative charge to the polypeptide in proportion to its length. During electrophoresis the negatively charged proteins will migrate through the polyacrylamide matrix towards the positive electrode; however, in the mesh of the polyacrylamide gel, large proteins are retarded much more severely than small ones. This results in the fractionation of a complex mixture of proteins into a discrete series of protein bands arranged in order of molecular weight. Distinct protein bands can therefore be identified and compared between samples.

In forming a gel, acrylamide monomers polymerise into long chains that are covalently linked by a crosslinker, usually N,N'-methylene-bis-acrylamide (bis). The pore size of the gel is adjusted by the concentration of acrylamide. The total percentage of acrylamide in the gel, i.e. acrylamide monomer plus bis crosslinker, is expressed as %T. As the %T increases the pore size decreases. In addition, pore size can be adjusted by varying the amount of crosslinker, or %C, as a percentage of the total %T. Therefore, a 20%T 5%C gel is composed of 20% acrylamide in total, of which 5% is crosslinker. Above and below 5%C the pore size increases.

SDS-PAGE Gels

The separating gel was poured first, over which 500 µl of 50% isopropanol was layered. After the gel had set the isopropanol was removed and the comb was inserted. The stacking gel was layered on and allowed to set for 20 min. The gel cartridges were inserted into the tank and submerged in running buffer (12.1g Tris; 7.5g

Glycine; 1g SDS in 1 l dH_2O (pH 8.8)). After removal of the comb the wells were rinsed with running buffer and the gel was now ready for the application of the samples.

Stock soloution	17.5% separating gel µl	5% stacking gel µl
30% Acrylamide	5 250	670
1% Bis-acrylamide	660	520
1.00M Tris-HCl, pH 8.7	3 030	---
0.25M Tris-HCl, pH 6.8	---	2 000
20% SDS	45	20
H_2O	---	780
10% Persulphate	30	30
Temed	10	4
Tank buffer was composed of: 0.1M Tris, 0.75% glycine, 0.1% SDS (pH 8.8).		

Table 2.2. SDS Page Gel recipe.

Sample preparation for SDS PAGE

For SDS-polyacrylamide gel electrophoresis, pellets of partially or highly purified GCAM were resuspended in 125 mM Tris-HCl (pH 6.8), 5% sucrose, 2% SDS, 0.05% Bromophenol Blue and 2% β-mercaptoethanol. The samples were heated for 5 min (or 30 s for highly purified membranes) at 95°C and run on a 17.5% total, 0.4% cross linker, polyacrylamide gel at 10 mA for 10 min then 20 mA for 60 min. according to Schweikl et al. (1989), on a Bio-rad Mini-Protean II electrophoresis cell. The gel size was 8 x 7.3 x 0.075 cm.

2.2.9 Protein detection methods on SDS gels

Coomassie blue staining

Gel was impregnated in dye solution (0.25% w/v Coomassie blue R-250 in 50% methanol/10 % acetic acid) for 1 h to overnight. The gel was destained in destain solution I (25% isopropanol/10% acetic acid) for at least 1 h, then followed a further destain for 1 h in destain solution II (7.5% Methanol/10% acetic acid)

Silver stain

Protein was visualised by silver staining (Merril, Goldman, Sedman, & Ebert, 1981). The gel was fixed for 1h-overnight in fix solution (50% methanol/12% acetic acid with 0.5 ml/l 35% formaldehyde).The gel was then washed for at least 3 x 20 min in 30% ethanol. Following this, the gel was incubated for exactly 1 min in sodium thiosulphate solution (0.2 g/l $Na_2S_2O_3$. $5H_2O$) and immediately rinsed three times in dH_2O. The gel was then incubated for 20 min in silver solution (2g/l $AgNO_3$ with 0.75 ml/l 37% formaldehyde). The silver solution was rinsed away in dH_2O for 2 x 20 s. Colour was developed by incubation for a maximum of 10 min in developing solution (60g/l Na_2CO_3 with 0.5 ml/l 37% formaldehyde) The reaction was rapidly stopped, upon band visualisation, by immersion in stop solution (50% methanol/12% acetic acid). The gels were then dried either by vacuum gel drier or air-dried between layers of cellophane.

DCCD labelling

Labelling with N, N'-dicyclohexylcarbodiimide (DCCD) was performed according to Zheng *et al.* (1992).

Highly purified goblet cell apical membranes were pelleted in a microfuge tube at 13 000 rpm for 10 min at 4°C. GCAM was then resuspended in 50mM Tris-MOPS, 1mM $MgCl_2$, 1 mM β-mercaptoethanol, 0.1 mM EDTA, pH 8.1 to a protein concentration of 10 µg/ml. N'N dicyclohexyl-[14c]carbodiimide was added to a final concentration of 10 µM and incubated with the membranes for 30 min at 30°C. The membranes were pelleted at 14 000 rpm for 10 min and the highly radioactive supernatant was transferred to a waste bottle. The pellet was washed once with

the above buffer to reduce the free radioactivity on the gel. The pellet was resuspended in Laemmli buffer to a concentration of 0.5 µg/µl. The membranes were solubilised and the proteins denatured by incubation at 37°C for 1 h. 5µg protein per lane were run on an SDS PAGE gel following normal procedures. After electrophoresis the gel was stained with Coomassie and destained as described above. The gel chamber and glass plates were thoroughly decontaminated with Deconex, the radioactive lower tank buffer and first Deconex soaking solution were collected for safe disposal. The destained gel was incubated with enhancer for 1 h at room temp, following which the gel is rinsed in dH_2O for 1 h. The gel was dried onto Whatman paper by vacuum pump, after which it was exposed to Kodak X-ray film at -70°C for 4 days. The film was developed in the usual manner to reveal the labelling pattern.

2.2.10 Western blots

Proteins were transferred from SDS PAGE gels to nitrocellulose membrane by electrophoretic transfer.

2 sheets of Whatman blotting paper (which act as ion reservoirs), cut to the exact size of the gel, were soaked in blot buffer I (300 mM Tris-HCl, pH 10.4; 20% methanol; 0.1% SDS) and placed on the anode electrode of the Bio-rad Trans-Blot Semi-Dry Transfer Cell. A further 2 sheets of blotting paper were soaked in blot buffer II (30 mM Tris HCl, pH 10.4; 20% methanol; 0.1% SDS) and placed on top of the previous sheets. The nitrocellulose membrane was cut to the correct size and soaked in blot buffer II for 10 min and placed on the assembly, making sure there were no air bubbles between filter paper and membrane. Following electrophoresis the SDS PAGE gel was soaked for 5 min in blot buffer III (40 mM e-amino-n-caproic acid; 25 mM Tris, pH 9.4; 20% methanol; 0.1% SDS) and placed on top of the membrane. The assembly was completed with the addition of 2 sheets of filter paper soaked in blot buffer III and the connection of the cathode electrode. Electroblotting took place for 1 h at 1 mA/cm^2 of gel (50 mA or 5 V).

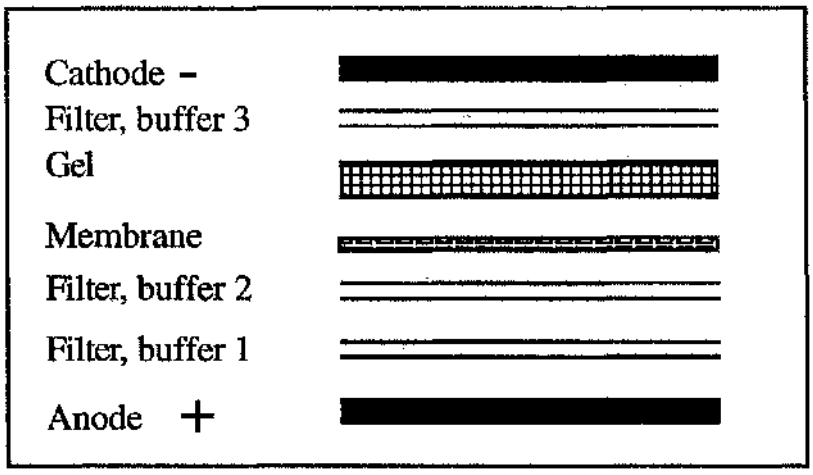

Figure 2.4. Semi dry western blot
Electrophoretic transfer assembly of buffer soaked filter paper, polyacrylamide gel and nitrocellulose membrane.

2.2.11 Protein detection methods on Western blots

Ponceau stain
This reversible stain was used to check that transfer had occurred correctly and was also used to label the standard molecular weight markers. The working solution was 0.02% (v/v) Ponceau in 2% w/v trichloroacetic acid. The blot was incubated in the stain for 2 min and then rinsed in H_2O.

Immunolabelling
This specific and highly sensitive technique required several manipulations. Firstly the membrane was blocked with a non specific protein, then the membrane was exposed to specific primary antibody. The primary antibody was detected and amplified with an alkaline phosphatase-conjugated secondary antibody which was capable of catalysing a colour producing reaction.

The membrane was blocked for 60 min in TBSN-Tween containing 3% w/v fish gelatin (TBSN-Tween: 20 mM Tris-HCl, pH 7.5; 500 mM NaCl; 0.02% NaN_3; 0.05% Tween 20). The primary antibody was diluted 1:10 000 in TBSN-Tween with 1%

fish gelatin and incubated with the membrane for 1 h at room temperature. Following this, the membrane was rinsed for 3 x 5 min with TBSN-Tween. The alkaline phosphatase conjugated secondary antibody was diluted 1:10 000 in TBSN-Tween with 1% fish gelatin and incubated with the membrane for 1 h at room temperature. The membrane was then rinsed for 3 x 5 min with TBSN-Tween and finally with dH_2O. Fresh colour reaction mix had to be made up from stock solutions of reagents. Stock Nitroblue Tetrazolium (NBT; stock: 75 mg/ml in 70% DMF) and stock 5-Bromo-4-Chloroindoxylphosphate (BCIP; stock: 50 mg/ml in 100% DMSO) were both diluted to 0.2 mg/ml in reaction buffer (100 mM Tris HCl, 5 mM $MgCl_2$, 0.01 mM $ZnCl_2$). The dilutions were 4.5 µl NBT/ml reaction buffer to which was added 3.5 µl BCIP/ml reaction buffer. The colour reaction mix was incubated with the membrane, in the dark for up to 1 h, by which time the bands were visible.

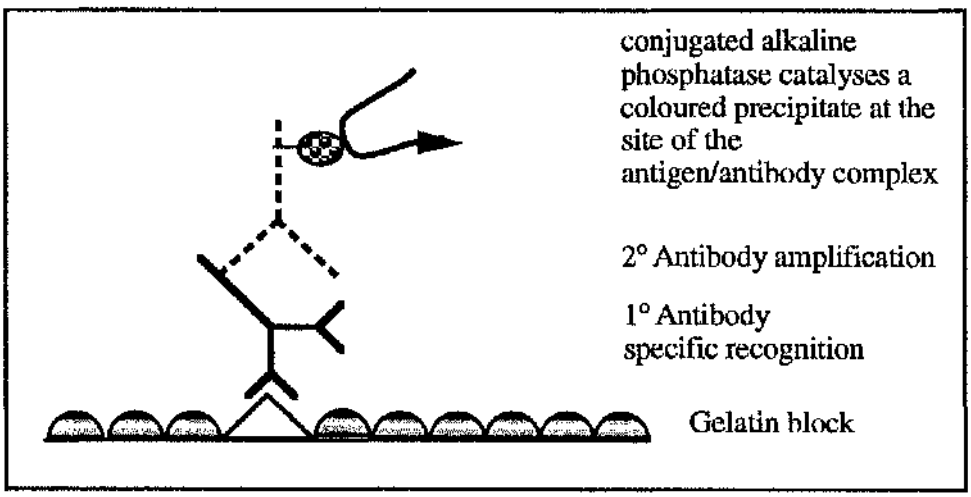

Figure 2.5 Specific enzymatic detection of membrane bound antigens.

2.2.12 Dot-blots

Band 2 membrane pellets were suspended in 125 mM Tris-HCl, 2% SDS, 2% β-mercaptoethanol at a concentration of 2 mg/ml and heated at 95°C for 5 min. 2-fold serial dilutions of the protein were made in the above buffer. 1 µl of each dilution was spotted onto nitrocellulose membrane (BA85, Schleicher & Schuell) and allowed to air dry. The blots were blocked in Tris buffered saline

(TBS: 20 mM Tris, 0.5 mM NaCl, pH 7.5) with 3 % gelatin for 1 h. The blots were incubated with the primary antibody for 1 h in TBS with 1% gelatin then washed three times for 5 min in TBS-Tween 20 (0.3% w/v). The secondary antibody probe was (depending on primary antibody used) either goat anti-rabbit IgG or goat anti-mouse IgG, conjugated to alkaline phosphatase (Sigma; Poole, Dorset). The blots were washed in TBS-Tween 20. NBT/BCIP colour was developed as described above for Western blots.

2.3 Northern Blots

2.3.1 RNA purification

Fifth instar apical, mid, posterior and moulting fourth instar whole midguts were isolated and the Malpighian tubules removed. Upon dissection the tissue pieces were frozen immediately in liquid nitrogen. Each sample was homogenised straight out of liquid nitrogen in a polytron homogeniser at full speed for 5 s in 5 ml of RNAzol™ B (Biotecx, Texas USA). 1 ml chloroform was added to the suspension to extract the RNA. The samples were left on ice for 30 min and then spun at 12 000 g for 15 min. The aqueous phase was carefully removed, to which an equal volume of isopropanol was added. The samples were centrifuged for 15 min at 4°C during which the RNA precipitate formed a pellet at the bottom of the tube. The pellet was vortexed in 75% ethanol and centrifuged at 7 500 g for 8 min. The RNA was then stored, in the ethanol, at -70 °C.

2.3.2 RNA quantification

The RNA pellet was dissolved in 100µl of dH_2O. 10 µl of this was added to 1 ml of dH_2O and measured spectrophotometrically at 260 nm and 280 nm. H_2O was used as a blank. The optical density at 260 nm (OD_{260}) of 1 is equivalent to an RNA concentration of 40 µg/ml.

2.3.3 Agar Gel electrophoresis

Agar gel mix (1.2 g agarose type V, 73 ml ddH_2O, 10 ml 10x MOPS)(10x MOPS: 41.2g MOPS in 1600 ml of 0.1 M NaAC, adjust to pH 7 with 10 N NaOH, 20 ml 0.5 M EDTA (pH 8) and adjust to 2 l with ddH_2O) was heated in a microwave at high power for 2.5 min, after which 17 ml formaldehyde was added. The gel was allowed to cool to approximately 60 °C prior to being poured. After the gel had set it was placed in the gel apparatus under running buffer (1x MOPS).

The RNA sample was prepared for electrophoresis as follows. To 10 µl of 1 µg/µl RNA, 5µl of RNA-mix was added (RNA-mix: 1250 µl deionised formamide, 400 µl formaldehyde, 250 µl 10x MOPS). The sample was incubated at 65 °C for 10 min after which the sample was kept on ice. 2 µl of ethidium bromide dye (1/10 ethidium bromide, ddH_2O) was added to each sample. The sample was applied to the gel and run at 60 V for 2-2.5 h.

2.3.4 Northern blot

Tank was filled with 2x SSC (1xSSC: 0.1 M NaCL, 14.8 mM sodium citrate, pH 7.0). A wick of 3 sheets of Whatman 3MM paper was soaked in 2x SSC. The gel was added to the assembly followed by the nylon membrane. A further sheet of Whatman paper was assembled on top of the membrane, followed by a wad of absorbent paper and finally a weight. The assembly was allowed to blot overnight.

2.3.5 DNA probes and detection

^{32}P labelling of DNA probe

2 µl of the 16 kDa DNA probe was added to 32 µl ddH_2O, boiled for 5 min and then placed on ice. 10 µl of reagent mix, 5µl ^{32}P labelled CTP and 1µl of Klenow fragment (all reagents from the Pharmacia Oligolabelling Kit) were all added to the probe in the fume hood and incubated for 1 h at 37°C. After incubation the probe was purified on a G50 sephadex column. Purified probe, after filtration through the column, was detected as the fraction with the highest level of radioactivity.

Detection of RNA bands

After blotting, the membrane was rinsed in 1xSSC and UV crosslinked for 30 s. 250 µl of salmon testes DNA was added to 25 ml of Pre-hybridisation mix and the membrane was then incubated in Pre-hybridisation Mix for 4 h at 65°C to block non-specific binding of the probe to the membrane (Pre-hybridisation Mix: 5g dextran sulphate, 2.5 ml 10% SDS, 5 ml 50X Denhardts solution, 12.5 ml 20xSSC; 50x Denhardts solution: 1g polyvinylpyrrolidine, 1g ficoll, 1g bovine serum albumin in 100 ml H_2O). The ^{32}P labelled probe was boiled for 5 min and put on ice. After pre-hybridisation the probe was added to the pre-hybridisation mix and allowed to hybridise at 65°C overnight. After, hybridisation the probe was poured off and the membrane rinsed with 1xSSC at 65°C. The membrane was then washed to medium stringency in 1xSSC for 20 min at 65°C. A further wash to high stringency in 0.5xSSC at 65°C for 20 min was required. X-ray film was exposed to the membrane for 4 h. The autorad was developed as for the DCCD labelling.

2.4 Secondary Messengers and Ion Transport

2.4.1 Ecdysone injection of larvae

For investigation of ecdysone-mediated ecdysis and gut switch-on the larvae were staged according to morphological markers described previously (section 2.1.2). Injections of ecdysone took place upon appearance of pigmentation in the new crochets, about two hours after the head capsule becomes air filled. Crotchet pigmentation occurs about 11 h prior to ecdysis. The larvae were injected with 6 µl of 0.5 µg/µl 20-hydroxyecdysone in 10% isopropanol using a fine gauge Hamilton syringe, controls were injected with 10% isopropanol only. Midgut SSC measurements were made on the Ussing chamber at 2 h intervals, starting at 10 h after injection.

2.4.2 Extraction of partially purified eclosion hormone

Partially purified eclosion hormone was isolated from prepupal larvae approximately 48 h after entering the wandering stage, 4th instar moulting larvae upon development of an air filled head capsule and post moult 5th instar approximately 1 h after ecdysis. Staged larvae were anaesthetised on ice for 20 min, then decapitated. Eclosion hormone was partially purified according to Truman *et al.* (1989). A dorsal incision was cut from the 'horn' forward. The terminal ganglia was located and the proctodeal nerve, which branches off the ganglia identified. The proctodeal nerve was isolated and immediately transferred to ice-cold acidified methanol (90: 9: 1, methanol: H_2O: acetic acid). The samples were then homogenised and the particulate matter pelleted by a brief centrifugation. The supernatant was blown to dryness under a stream of nitrogen and stored at -20°C. Prior to use, the sample was dissolved in 10% acetonitrile.

2.4.3 Eclosion hormone activity assay

Partially purified eclosion hormone was added to the Ussing chamber to investigate its effect on ion transport. Midguts were removed from larvae approximately 1 h prior to ecdysis or 1 h after ecdysis. Partially purified eclosion hormone was added after 30 min. Controls were treated with 10% acetonitrile.

2.4.4 NADPH staining method

The NADPH diaphorase (NADPHd) staining technique (according to Dawson *et al*, 1991,) allows the rapid visualisation of nitric oxide synthase. Tissue samples were dissected, fixed and permeabilised prior to NADPH/NBT labelling. Tissue was dissected out and added to formyl saline solution for 15 min (formyl saline: PBS+4% paraformaldehyde, heated to 65°C and sufficient 5N NaOH added to dissolve the paraformaldehyde. Allow to cool and re-pH to 7.4 with 5 N HCl; PBS: 8 g NaCl, 0.2 g KCl, 1.44 g Na_2HPO_4 and 0.24 g KH_2PO_4 in 1 l H_2O.). After fixation the solution was replaced with detergent solution (3 µl Triton X-100/ml PBS) and the tissue was incubated for a further 15 min. Following this incubation the Triton solution was replaced

with colour mix solution (1 mg NADPH, 2 µl NBT and 3 µl Triton X-100 in 1 ml PBS). Colour development took approximately 30 min at room temperature.

2.4.5 Native Gel electrophoresis

Gradient native polyacrylamide gel electrophoresis (PAGE) was performed on insect tissues to identify the nature of the NADPHd-reactive protein. 2% (1.4 g acrylamide/0.6g bis in 100ml) and 15% (14.7 g acrylamide/0.3 g bis in 100 ml) acrylamide were dissolved in gel buffer (0.144 mM acetic acid, 0.144 mM Tris, 3% glycerol, 0.4% octyl β-D-glucopyranoside; pH 6.4) and placed in each chamber of the gradient mixer. The gel cartridge was assembled and 100 ml of 50% isopropanol was added to the chamber to give the gel a flat top. 25 ml of each gel solution was required to fill the cartridge. 50 µl of 10% ammonium persulfate (APS) solution was added to the 2% acrylamide solution and 10 µl APS was added to the 15% acrylamide solution. 12 µl of TEMED was added to each chamber. The solutions were allowed to mix and flow into the gel cassette. 50% sucrose was fed into the chamber to fill dead space and force the acrylamide between the glass plates. Gels were left overnight to set. The electrode buffer was composed of 25 mM Tris, 192 mM glycine pH 8.3.

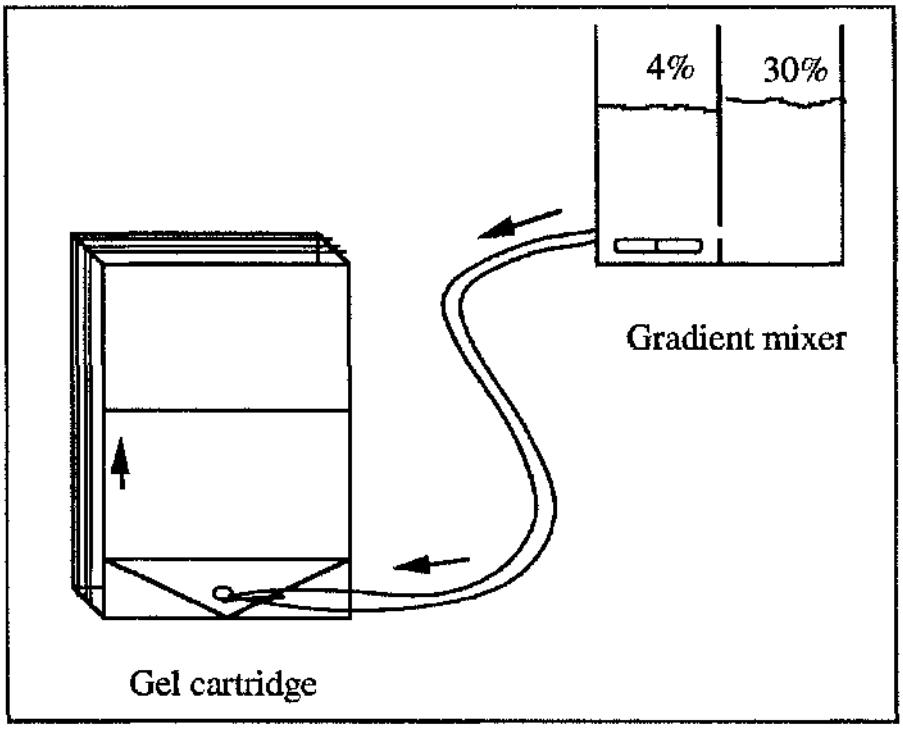

Figure 2.6. Apparatus for pouring gradient polyacrylamide gels.

2.4.6 Sample preparation for native PAGE

Posterior, mid and apical regions of the 5th instar midgut were removed, homogenised in 500 µl SET buffer, and spun at 13 000 rpm for 15 min. The pellet was washed by aspiration in 500µl of set buffer and re-spun. Samples were solubilised in 2% β-mercaptoethanol, 0.04% Bromophenol blue, 50% sucrose, 1% Triton X-100 and spun for 10 min. The supernatant was applied to the gel.

2.4.7 NADPHd labelling of native gels

The gel was labelled by incubation in 10 mg NADPH, 20 µl NBT in dH_2O for approximately 2 h.

CHAPTER 3
ION TRANSPORT IN MANDUCA

3.1 Introduction

3.1.1 Growth and staging of larvae

In order to accommodate the growing tissues, larvae shed their cuticle at intervals termed moults. *Manduca* larvae undergo a strict sequence of events over the time course of each moult. The first step of entry into the moult is the cessation of feeding and the larva becomes quiescent. Soon after, the old cuticle becomes detached from the epidermis (a process known as apolysis) and new cuticle is laid down. At this stage the larval head capsule is forced forward and is said to have "dropped". The space between the old and new cuticles becomes filled with moulting fluid, which dissolves the old cuticle. The remains of the old cuticle are now ready to be shed. The process of shedding the old cuticle is termed ecdysis. The larva contracts its abdominal muscles and increases the pressure of blood in the head. The distension causes the old cuticle to rupture along pre-determined lines of weakness. When the old skin has split the insect crawls out. The old linings of the tracheae, foregut and hindgut are left behind with the old skin (exuviae). Soon after ecdysis the larva, having successfully attained a higher instar, resumes feeding. Finally, the cuticle hardens and darkens.

Many of the processes described above are internal and their precise timings difficult to determine. A convenient morphological marker for staging the development of the moult is the head capsule. The development and morphology of the head capsule has been described over the timecourse of the 4th/5th instar larval moult by Baldwin *et al.*, 1991. This description has been used in this study as a standard staging criteria and is described in the Materials and Methods section.

After ecdysis, the fifth instar larva will feed and grow for five or six days. At the end of this period of growth an abrupt change occurs in the larva's appearance and behaviour. Within a span of a few hours feeding ceases, the gut is cleared and the larvae burrows into the ground or food. Meanwhile, the epidermis along the dorsal midline becomes somewhat transparent. The heart becomes visible and a pink pigment appears along the dorsal midline. Larvae at this stage are termed "wandering larvae" and are in preparation for the moult to pupa. The wandering stage lasts for almost two days until retraction of the ocular pigment marks entry into the pre-pupal phase. Approximately three days thereafter the pre-pupa undergoes ecdysis to the pupa.

3.1.2 Growth and development of the midgut

The larval/larval moult

Between hatching and pupation the *Manduca* larvae can increase its body weight by up to 10 000-fold. Over the course of four larval moults the surface area of the midgut increases 200-fold and it has been estimated that the number of cells increases 256-fold (Baldwin & Hakim, 1991). During the moult the midgut remains intact. After apolysis, but before ecdysis, regenerative cells proliferate and differentiate into goblet and columnar cells. Existing goblet and columnar cells are not replaced by the new cells; instead new epithelial cells grow between existing cells maintaining a constant ratio of one goblet cell to five columnar cells (Baldwin & Hakim, 1991).

The larval/pupal moult

The fate of the midgut in the fifth, and final stage is different from that of earlier larval stages. The larval epithelium is destined to be replaced by a pupal midgut that has a different structure and function (Russel & Dunn, 1991). Approximately five days after ecdysis to fifth instar, the regenerative cells proliferate to form a nascent pupal midgut which lies beneath the larval epithelium. By the time the larval midgut cells are sloughed into the lumen at ecdysis, the pupal midgut has fully differentiated into a columnar

epithelium (Russel & Dunn, 1991). The ion transporting activities of the midgut during these changes are obscure.

Although morphological studies reveal that the midgut undergoes dramatic structural changes during the growth and development of the insect, functional changes are less well understood. Loss of midgut ion transport activity was known to be associated with the moult and pre-pupal stages (Cioffi, unpublished results, discussed in Cioffi, 1984) however the mechanism of transport shutdown was not elucidated. In this investigation I will endeavour to improve the resolution of these early measurements of midgut function in the later stages of the fifth instar, in earlier instars and during larval/larval moults.

3.1.3 Ion transport measurements

The presence of an electrogenic K^+ pump has been shown to be ubiquitous among insect tissues, being found in midgut, Malpighian tubules, salivary glands and cuticular sensillae (Harvey, et al., 1983a; Harvey, Cioffi, & Wolfersberger, 1983b). Of these, the caterpillar midgut is probably the most accessible to study as it can be mounted on an Ussing chamber.

The chamber used was a modification by Dow *et al.*, 1985, of the classical Ussing design. The epithelium is stretched across a narrow aperture which is then inserted between two halves of the saline filled chamber. This allows access of the oxygen rich saline to the tissue. The saline is oxygenated and circulated using oxygen gas-lift pumps. There are two silver current electrodes, one at each end of the chamber and three voltage sensing electrodes located near to, and equidistantly from, the epithelium. The three electrode assembly compensates for the resistance of the saline, when the low resistance tissue is short-circuited (Wood, 1978). During short-circuit measurements the current applied to the chamber is adjusted until the TEP between the sensing electrodes becomes zero. Under such conditions, only actively transported ions move across the tissue, and the short-circuit is a precise measure of the net flux of charged species. By using the TEP and

SSC measurements I will be able to assess the ion transporting activity of the midgut.

3.1.4 pH techniques

The extremely high pH found in the midgut lumen is believed to be a consequence of, and a reason for, the K^+ pump (Dow, 1992a). The relationship between the K^+ pump and high pH generation is illuminated when one or other of these processes is modified. The ability of the midgut to generate a high pH will be studied at various stages in the development of the larvae and be compared with the K^+ transport activity at these stages. The characteristic pH peak in the mid-midgut region was revealed using pH semi-micro electrodes (Dow, 1984b). A similar technique has been used here with some modifications to take account of the small sample volumes found in moulting fourth instar larvae.

3.1.5 pH indicator dyes

One disadvantage of dissection and direct analysis of the body fluids is that, after a sole initial measurement, the development of the animal is terminated permanently. For this reason a non-invasive method was developed for investigation of changes in gut pH. pH indicator dyes applied directly to the midgut via the food would undergo a high pH generated colour change and thus demonstrate midgut activity. Dyes were chosen that would undergo colour changes within the ranges expected in the midgut.

3.2 Results

3.2.1 Growth of larvae during 5th instar

Upon ecdysis to 5th instar *Manduca* larvae resumed feeding within 2 ± 0.1 h (SEM, n=4) and fed continuously until the cessation of feeding indicated entry into the wandering phase. There is a 6-fold increased in weight during the 5th instar; from 1.39 ± 0.01 g (SEM, n=20) upon ecdysis to 5th instar to 8.40 ± 0.39 g (SEM, n=14) on the day of entry into the wandering phase **Figure 3.1.** After entry into the wandering phase the weight slowly decreased, partly because the larvae had stopped feeding. The growth and development of larvae was not necessarily synchronous, therefore

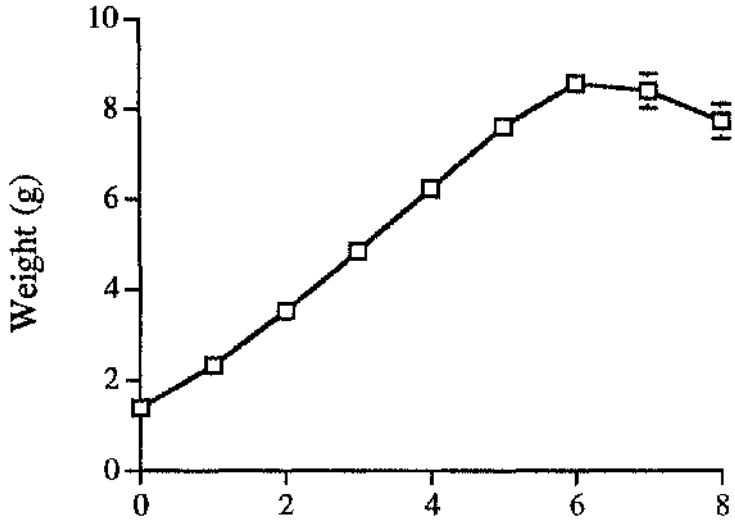

Figure 3.1. Growth of 5th instar

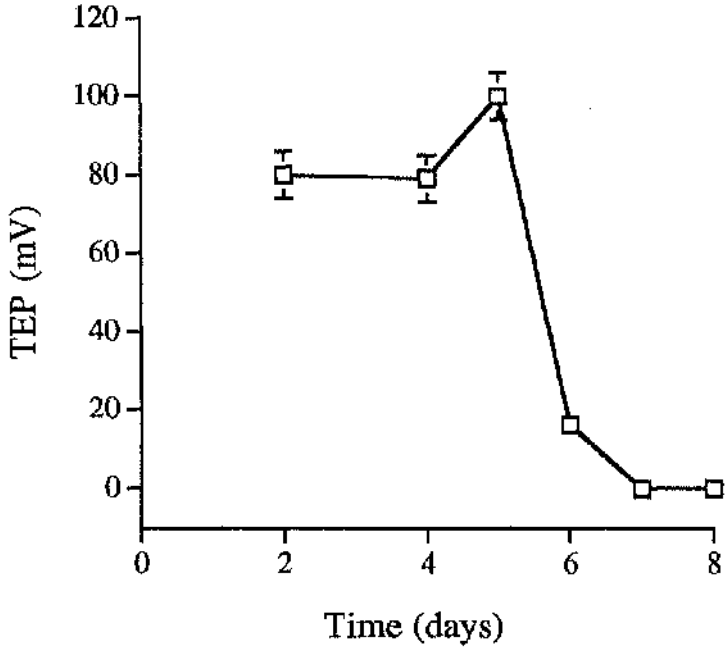

Figure 3.2 TEP during 5th instar

Ecdysis to 5th instar

Entry into wandering stage

this data has been standardised whereby only the larvae that entered the wandering phase on day 6 were used. Weight of larvae was important, with 90% of larvae entering the wandering phase within 24 h of reaching 8 g.

3.2.2 Ion transport is high during 5th instar

The remarkable transport capabilities of the epithelium are usually studied during the feeding phase of the fifth instar. During this stage the larvae are relatively large and the epithelium is most easily manipulated. The transport properties of 5g feeding larvae were designated as standard active epithelium, against which transport activities at other stages are compared. The trans-epithelial potential (TEP) generated by a midgut isolated from a 5 g larvae was typically in excess of 80 mV (see **Figure 3.2**)

3.2.3 Ion transport is switched off irreversibly upon entry into the wandering stage

The weight of the larvae was used to estimate the developmental stage relative to entry into the wandering stage (see **Figure 3.1.**). A larva was designated as being approximately 24 h prior to entry into the wandering stage upon reaching 8 ± 0.25 g. On day 5 the larvae weighed 8.56 ± 0.33 g (SEM, n=14) and displayed a TEP of 104 ± 8 mV (SEM, n=7). Within 24 h the larvae had entered the wandering phase and the TEP dropped to 16 ± 3 mV (SEM, n=12). By day seven the TEP had dropped to 0 ± 0 mV (SEM, n=8) and remained permanently inactive.

There is therefore a control mechanism at the end of the 5th instar that regulates ion transport which causes the permanent switch-off of the K^+ pump.

3.2.4 Ion transport undergoes reversible switch off over larval-larval moult

Fourth instar feeding larvae generated a transepithelial voltage of +91 ± 10 mV (n = 4, mean ± SEM), lumen side positive (see **Figure 3.3.**). The high TEP indicated that active electrogenic K^+ transport across the goblet cell apical membrane (GCAM) to the midgut lumen was about as intense as it is in fifth instar

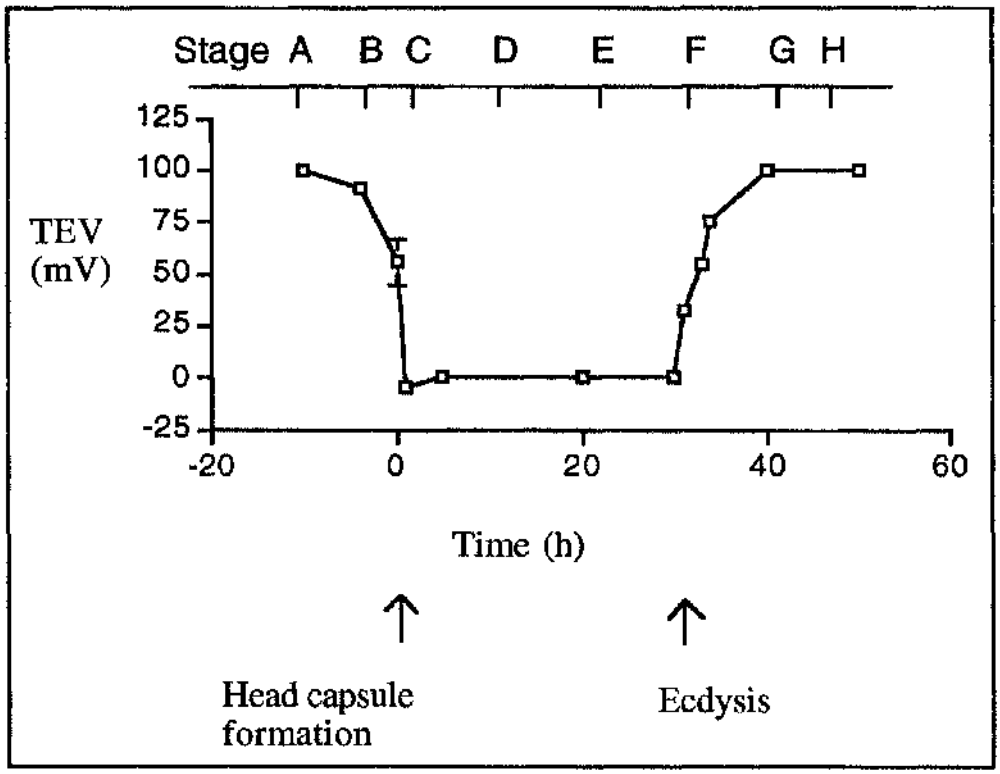

Figure 3.3. Time course of transepithelial voltage (TEV) during moult.

Timings are relative to formation of the head capsule at time zero, corresponding to stage C. Each time point is the mean of at least 4 independent measurements. Error bars indicate standard error of the mean; when not visible, they are smaller than the plot symbols.

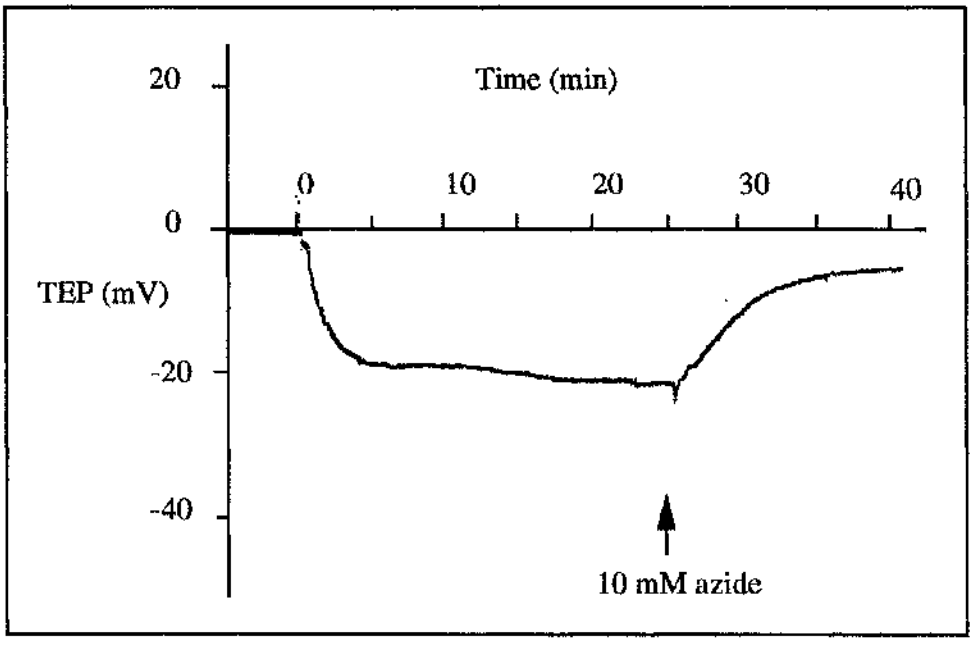

Figure 3.4. Ussing chamber trace of residual ion transport during gut shut-down. There is a sustained negative potential on entry into the moult.

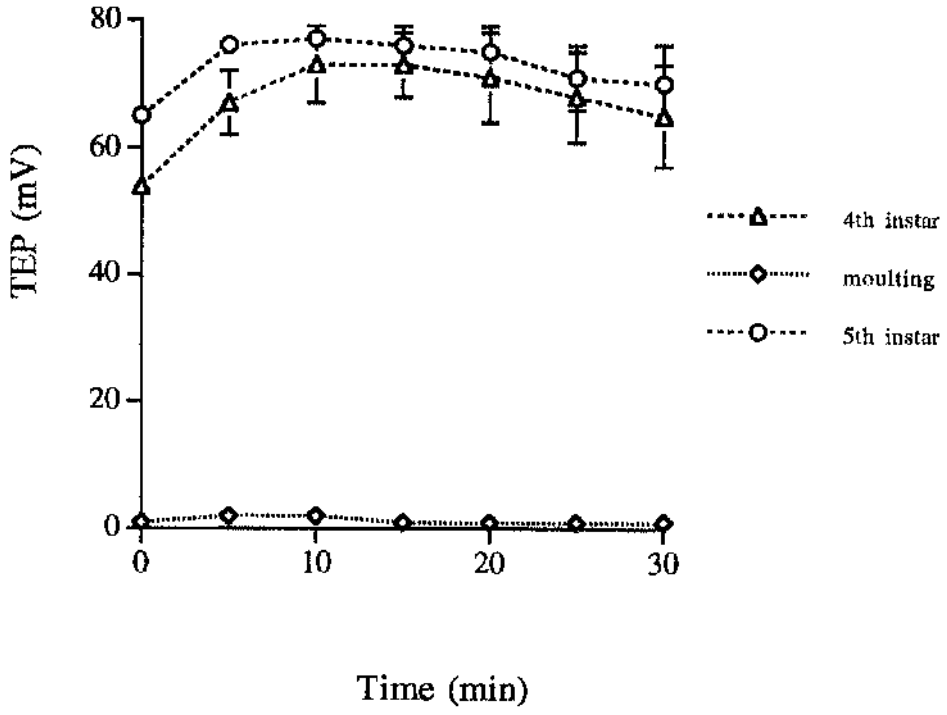

Figure 3.5. Ussing chamber trace of 4th, moult and 5th instar midgut

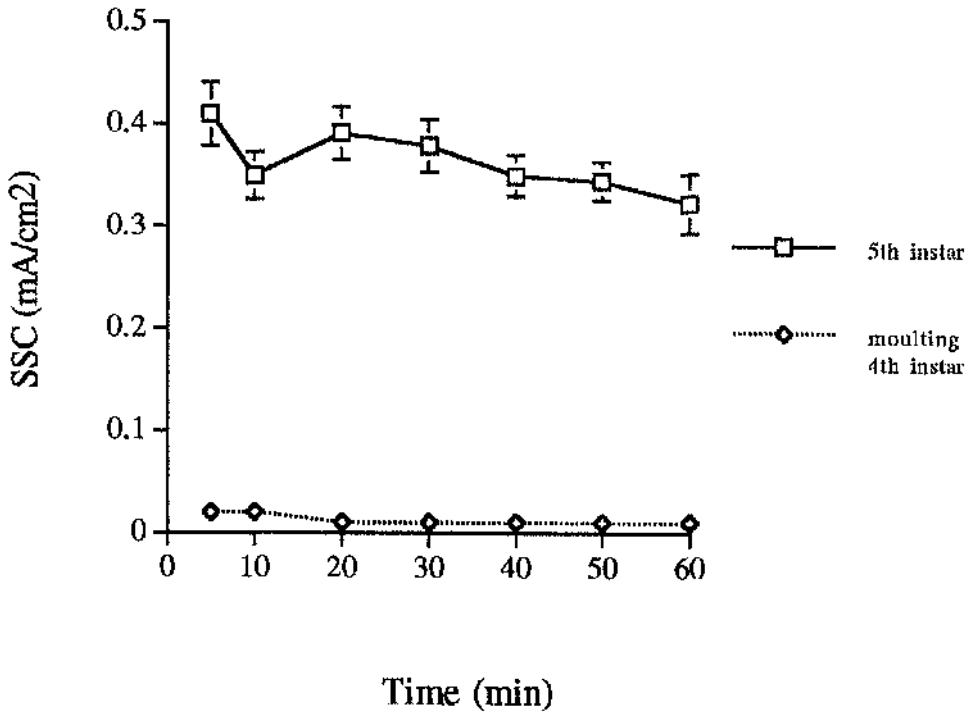

Figure 3.6. SCC generated by either moulting or 5th instar larvae

intermoult larvae. Approximately 2 h before development of the head capsule, the larvae stopped feeding and purged the gut lumen of food (stage B). This behaviour, the first sign of entry into the moult, did not affect the TEP which remained stable until development of the head capsule (stage C), whereupon it fell abruptly to -5 ± 4 mV (n=4, mean ± SEM), lumen side negative. Approximately 1 h after head capsule development the TEP had stabilised at 0 mV and remained at zero until ecdysis (stages D to F). Upon ecdysis the TEP rose to +32 ± 13 mV (n=5, mean ± SEM), lumen side positive. The TEP continued rising steadily until it levelled off at approximately +100 mV some 4 h after ecdysis.

The slightly negative residual voltage, presumably due to unknown ion transport processes in the epithelium which take longer to shut down, was reproducible and could be inhibited with 10 mM azide (see **Figure 3.4.**).

Modulation of ion transport activity was confirmed by short circuit current (SSC) measurements. The short circuit current was high during the 5th instar and generated 0.39 ± 0.2 mA/cm^2 (SEM, n=4), demonstrating vigorous K^+ active transport. This was a 20-fold increase compared with moulting fourth instar larvae which generated a negligible 0.02 ± 0.01 mA/cm^2 (SEM, n=4) (see **Figures 3.5. and 3.6.**).

3.2.5 pH drops reversibly over a larval/larval moult

Feeding fourth instar day two larvae generated a gut lumen pH of 9.9 ± 0.1 (SEM, n=8), **Figure 3.7.** This extremely high alkalisation dropped from pH 9.9 ± 0.3 (SEM, n=4) upon head capsule formation to pH 9.5 ± 0.2 (SEM, n=4) approximately 4 h after head capsule formation. The pH continued to fall gradually until a minimum pH 8.1 ± 0.2 (SEM, n=4) was reached, 24 h after head capsule formation. Approximately 1 h prior to ecdysis to 5th instar the pH is 8.4 ± 0.2 (SEM, n = 7), rising to 9.0 ± 0.2 (SEM, n=8) during ecdysis. Four hours after ecdysis the pH gradient is fully regenerated at 10.0 ± 0.2. (SEM, n=7).

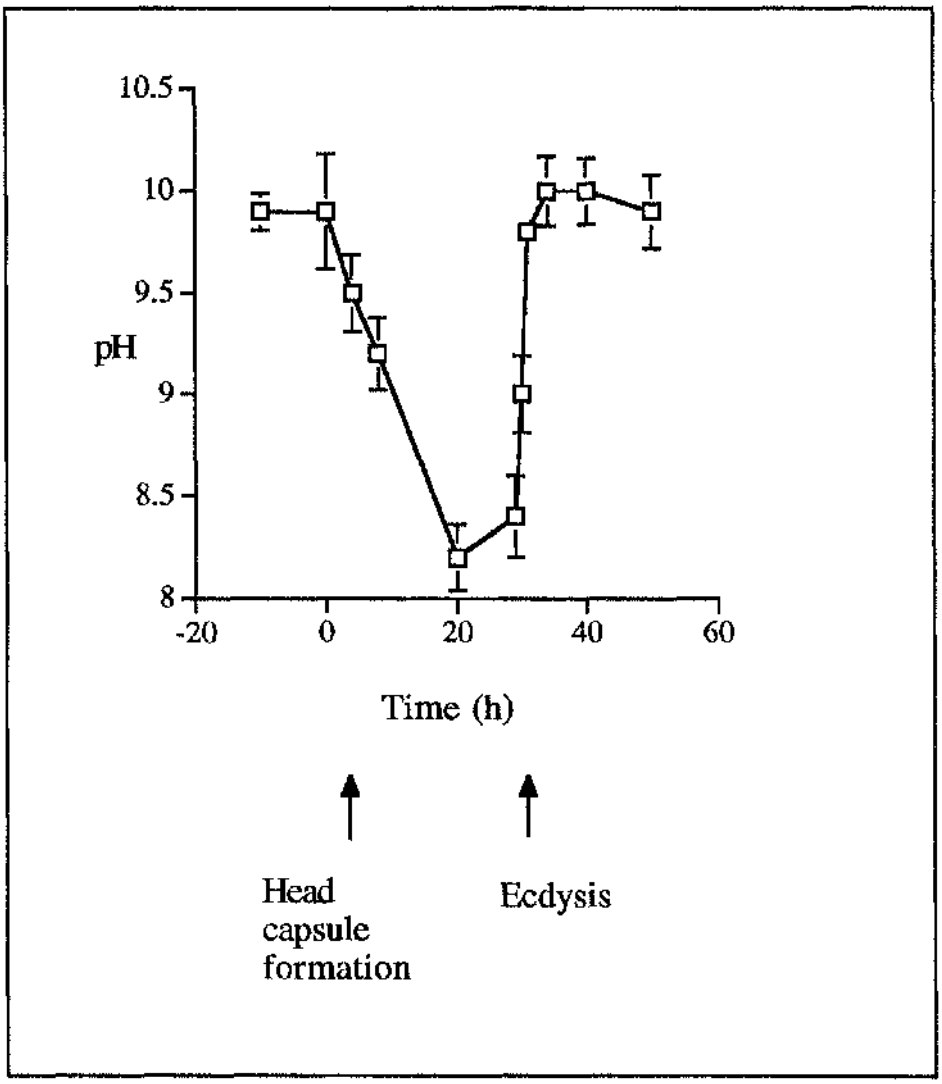

Figure 3.7. pH levels over timecourse of the moult
Each time point is the mean of at least 6 independent measurements. Error bars indicate standard error of the mean; when not visible, they are smaller than the plot symbols.

3.2.6 Switch-off can be predicted using pH indicator dyes

Dye was added to the dry food ingredients as a percentage of dry weight of food i.e. %w/w. The final concentrations of the dye were between 0.001 %w/w and 10 %w/w. All the dyes tested were non-toxic up to the maximum concentration of 10% w/w, with the exception of naptholbenzein which was lethal at the lowest concentration tested of 0.001 %w/w. The colour changes were viewed by transmitted light, dissection and examination of the midgut under bright field microscopy.

Rosolic acid is yellow at or below pH 6.8 becoming red at or above pH 8. Concentrations of 0.01%w/v - 0.05% w/v were found to work best for *in vivo* observations. Dye concentrations of 0.001 %w/v were too faint to quantify by sight, concentrations at 10% were too dark to be seen by transmitted light. Gut contents of feeding, intermoult larvae show deep red with transmitted light, indicating that the pH is above pH 8. (The dye does not appear to enter the tissues; however the dye would be colourless/yellow in pH 7 haemolymph) **Figure 3.8** . Rosolic acid was non-poisonous at all concentrations tested, and did not interfere with the growth or development of the larvae.

The red colour in the midgut is lost upon entering the moult. On day 3, three hours before head capsule slippage, the red gut colour fades to pink. By head capsule slippage all gut indicator colour has disappeared. The indicator remains colourless until 2 h after ecdysis to 5th instar. The gut colour returns within 5 min of the larva ingesting food containing the dye.

Similar results were found with the pH indicator phenolphthalein; pH range from 8.2-10.0, colour change from colourless to pink. The dye was pink in the midgut of feeding larvae and could not be visualised in the tissues. The midguts of moulting larvae fed on diet containing this dye were colourless.

In conclusion, high pH generated colour changes were found to dissipate approximately 2 h prior to head capsule development.

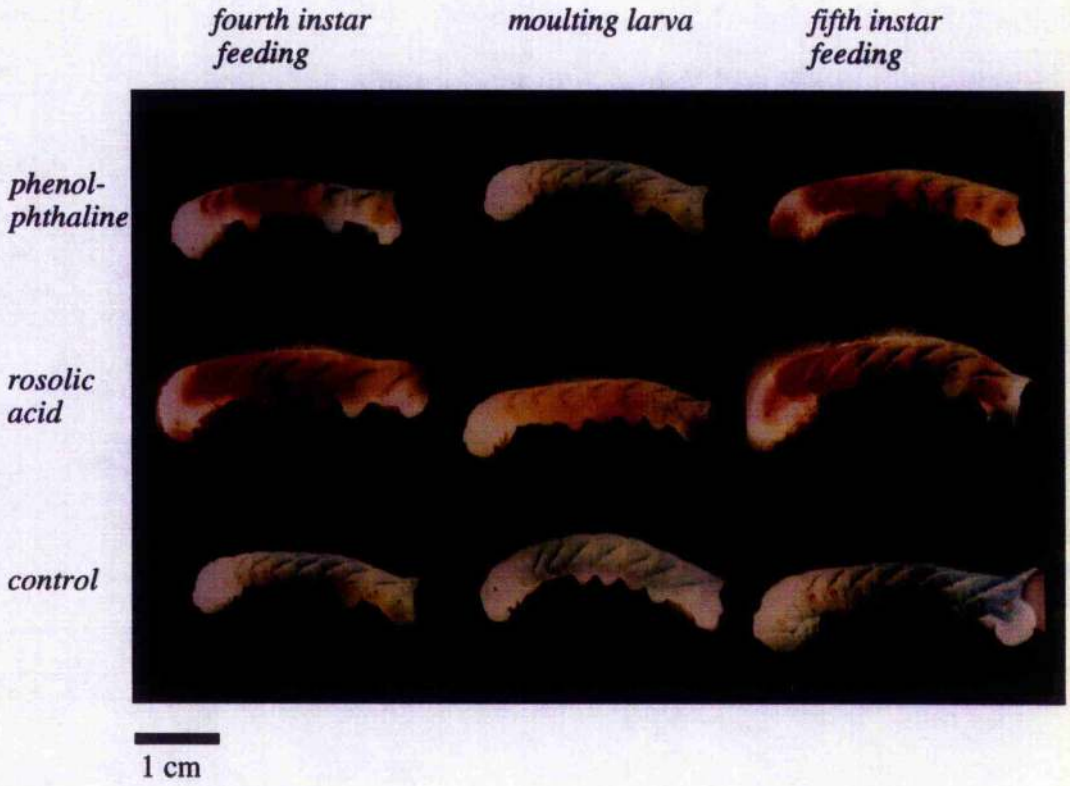

Figure 3.8. Non invasive monitoring of gut pH. Larvae were fed on a diet containing 0.2% w/w pH indictor dye. Stages shown are: feeding fourth instar, moulting larvae just prior to head capsule formation, feeding fifth instar 5 min after resumption of feeding. Note the anterior and middle midgut regions maintain a high pH as seen by a dramatic dye colour, dye is colourless in the posterior region.

The loss of colour from the midgut occurs approximately 2 h prior to loss of K^+ pump activity. The loss of colour can be used as a non-invasive technique for the prediction of K^+ transport shutdown upon entry into a moult.

3.3 Discussion

Active transport was found to be high in feeding 4th and 5th instar larvae. However, during periods when feeding did not occur, at the 4th/5th instar moult and during the wandering stage, the active transport levels dropped. External conditions were identical between samples. This demonstrates that the larvae regulate the level of K^+ pump activity in the midgut during periods of non-feeding.

During the moult the K^+ pump itself may be capable of transport but changes in the environment surrounding the pump may conspire to affect its performance indirectly. Changes in midgut ion transport may be due to changes in oxidative metabolism. Studies of moulting larvae reveal that respiration falls during the moult from fourth to fifth instar (Dahlman & Herald, 1971). This may be due to the moulting of the tracheal system (Wigglesworth, 1984) and impaired oxygen delivery to the tissues. The resulting hypoxia would be expected to impair active transport in the metabolically demanding midgut. Indeed, *in vitro* studies have eloquently demonstrated the tight coupling of oxygen supply and active transport. If the cessation of ion transport was solely regulated by availability of oxygen one may expect activity to return upon insertion into the oxygenated environment of the Ussing chamber. The TEP and SSC generated by midguts isolated from moulting larvae was found not to increase with time in the Ussing chamber (Figure 3.5 and 3.6). This result indicates that the availability of oxygen alone is insufficient to reverse the inhibition of active transport in the tissue.

Various morphological changes in midgut cell structure during the moult have been reported. During the moult from fourth to fifth

instar the columnar cell apical cytoplasm becomes inexplicably filled with mitochondria (Cioffi, 1984), meanwhile the anterior region goblet cell shape is modified in such a way as to distance the base of the goblet cavity from the haemolymph (Cioffi, 1984). The posterior goblet cell shape is not modified during the moult, however, the goblet cavity becomes filled with an electron dense granular material. In both anterior and posterior regions the goblet cell valve which appears in feeding larvae as a tortuous pathway between cavity and lumen, becomes sealed during the moult (Cioffi, 1984). It is unknown if these ultrastructural events seen during the moult are directly related to ion transport regulation.

The K^+ transport system is switched off rapidly upon entry into the moult. Half maximal K^+ transport activity is reached within approximately 1 h. In comparison with the rapid K^+ gradient dissipation, the pH gradient *in vivo* drops slowly and requires ten hours to reach its half maximal value. The slow reduction in pH gradient suggests that there is no mechanism to break down the pH gradient. The K^+ pump is rapidly re-activated upon ecdysis and reaches its half maximum level within 1 h of ecdysis. The pH of the midgut begins to rise upon ecdysis and has reached its half maximal level also within 1 h of ecdysis.

The decrease of pH levels upon entry into the moult begins at the same time as K^+ transport ceases. Re-generation of a high pH occurs in synchrony with the re-establishment of a potential difference. These results highlight the intimate relationship between K^+ pump activity and the generation of a high pH.

The gut contents are expelled prior to head capsule formation and during the moult the midgut only contains a watery fluid. There was some concern that the observed drop in pH was due to the absence of gut contents and not an actual decrease in pH generation. However, during ecdysis the pH gradient began to return prior to ingestion of a meal. This confirmed that the measurement of the luminal fluid gave a reliable representation of the state of pH generation in the midgut during the moult.

In many systems ion transport activities are triggered by the ingestion of a meal. The return of ion transport after the moult occurred at similar rates with or without the presence of food in the gut. This result demonstrates that activation of the K^+ transport mechanism is not triggered by the ingestion of a meal.

The striking indicator colours generated by the high pH are lost approximately 2 h prior to head capsule development and cessation of ion transport. The colour loss is not, however, due solely to the collapse in pH, as the pH collapse occurs a further 10 h after colour loss. Simultaneous with pH indicator colour loss the midgut contents are expelled prior to the moult. The colour loss recorded at this time is likely to be due to the indicator being expelled from the midgut and not solely an implication of the pH state of the midgut.

At high concentrations of rosolic acid some dye particles remain in the folds of the midgut for the duration of the moult. In these cases the strong coloration is lost during midgut purge leaving a residual faint pink colour. Upon head capsule formation the indicator fades, not to return until ecdysis, indicating the pH state of the midgut. After ecdysis the colour begins to return prior to feeding, demonstrating that dye particles have been present throughout the moult and that pH generation capabilities return prior to feeding.

In this chapter I have provided evidence that the K^+ transport system is under an element of control depending on the developmental stage of the larvae. The K^+ transport system is reversibly switched off during a larval/larval moult, simultaneously the generation of a high pH is down-regulated. In the next chapter, the control of ion transport during a larval/larval moult will be studied at the level of the components of the K^+ pump.

CHAPTER 4. V-ATPase ACTIVITY AND STRUCTURE IS MODIFIED DURING THE MOULT

4.1 Introduction

The V-ATPase, situated on the goblet cell apical membrane, drives the K^+ transport process. ATP is hydrolysed by the V_1 catalytic sector of the ATPase and fuels proton transport from cytoplasm to goblet cavity via the V_O proton channel. The ensuing generation of an electrochemical proton gradient across the goblet cell apical membrane (GCAM) energises the K^+/nH^+ antiporter, resulting in K^+ secretion. The V-ATPase, as the primary site of ATP hydrolysis and active transport, is a prominent target for any control mechanism exerted to regulate K^+ transport and associated procedures.

This chapter will describe the isolation of goblet cell apical membranes from moulting and feeding larvae, and subsequent analysis of the V-ATPase activities on this membrane and the ion transport mechanisms. An investigation into V-ATPase activity and protein structure will analyse the membrane bound V-ATPase structure and subunit composition when isolated from feeding and moulting larvae.

4.1.1 GCAM purification procedure

The V-ATPase and the K^+/nH^+ antiporter are located on the goblet cell apical membrane (GCAM) (Wieczorek, et al., 1991). The process (Cioffi & Wolfersberger, 1983) of specific separation of plasma-membranes, including purification of the GCAM, has allowed the biochemical properties of these membranes to be studied. The posterior midgut is the only suitable area for this procedure since the GCAM is situated towards the apical extremity

of the cell making it more accessible for extraction. Additionally, mitochondria do not associate closely with the goblet cell apical membranes in this region thus reducing mitochondrial membrane contamination of the GCAM during purification. The technique involves sequential disruption of the tissue by dissection, sonication and aspiration. The subcellular fractions are then separated by discontinuous sucrose density centrifugation resulting in three bands. The middle band (also known as Band 2) is composed of the *partially purified* GCAM, identified by the presence of 10-12 nm particles called portasomes on the membrane. This fraction can be studied directly or purified further to make *highly purified* goblet cell apical membranes. The V-ATPase can be extracted from Band 2 by selective solubilisation and further sucrose density centrifugation resulting in *highly purified V-ATPase* (Wieczorek, et al., 1990).

4.1.2 Discrimination between ATPases

The three groups of ion transporting ATPases (P-, F- and V-ATPases) are classed and identified by, among other characteristics, their sensitivity to various inhibitors. During ATP hydrolysis, the P-ATPase forms a phospho-enzyme intermediate. Consequently, micromolar concentrations of the transition-state phosphate analogue, vanadate, will inhibit ATP hydrolysis by the P-ATPases. Vanadate, however, does not inhibit the F- or V-ATPases since they do not have a phospho-enzyme intermediate stage. The F-ATPases, responsible for ATP synthesis in mitochondria, are selectively inhibited by the potent metabolic inhibitor, azide. Azide does not inhibit the P- or V-ATPases. Recently, the antibiotic bafilomycin A_1 was described by Bowman et al (1988) as a specific inhibitor of the V-ATPases. Bafilomycin A_1 inhibits V-ATPases at nanomolar concentrations yet, is required in concentrations of 100-1 000 μM to inhibit F- or P-ATPases. A concentration of 1μM bafilomycin A_1 resulted in over 90% inhibition of the membrane bound *Manduca* midgut V-ATPase activity (Wieczorek, et al., 1991). Addition of one or more of these inhibitors to an ATPase activity assay will selectively knock out specific classes of ATPases revealing the presence and activity of others.

4.1.3 Measurement of ATPase activity

V-ATPase hydrolyse ATP in the presence of Mg^{2+} to produce ADP and inorganic phosphate (Pi). The rate of ATP hydrolysis can be calculated by measuring the amount of inorganic phosphate produced. In the assay, the inorganic phosphate is determined as a complex of phosphomolybdate with Malachite Green, and the subsequent colour development is measured using a spectrophotometer. The inorganic phosphate liberated by ATPase activity is compared with a standard curve of absorbance at known phosphate concentrations (*see appendix for typical standard curve*). Thus ATPase activities can be calculated and compared.

In addition to the biochemical determination of ATPase activity, the activity can be functionally assayed using ATP dependent proton transport across the membrane. In the absence of K^+, but in the presence of Mg^{2+} and ATP, partially purified GCAM vacuoles will acidify the vacuolar space.

The properties of the fluorescent dye, acridine orange, have been exploited to study acidification of membranous compartments . Acridine orange has an excitation wavelength maximum at 493 nm, and an emission maximum at 530 nm. Acridine orange is a weak base: at neutral pH the dye is uncharged and can readily cross biological membranes. Upon entry into an acidic compartment the weak base becomes protonated and forms positively charged, weakly metachromatic red, dimers. The positively charged dye cannot cross the hydrophobic membrane and hence is trapped in the compartment. Consequently, non fluorescent, acridine orange dimers accumulate in the lumen of the acidic vesicle. Additionally, because non fluorescent acridine orange is accumulating in the vesicles, the available dye in the medium at the neutral fluorescence of 530 nm is depleted, causing a fluorescence quench detected at this wavelength. In summary, acridine orange accumulates and alters its fluorescence wavelength in acidic vesicular compartments, this results in a fluorescence quench of the neutral extravesicular dye. The rate and final amount of fluorescence quench at 530 nm is a measure of the

acidification state of the vesicle. The ability to sustain the quench demonstrates that the vesicle's low pH is being continually generated and maintained.

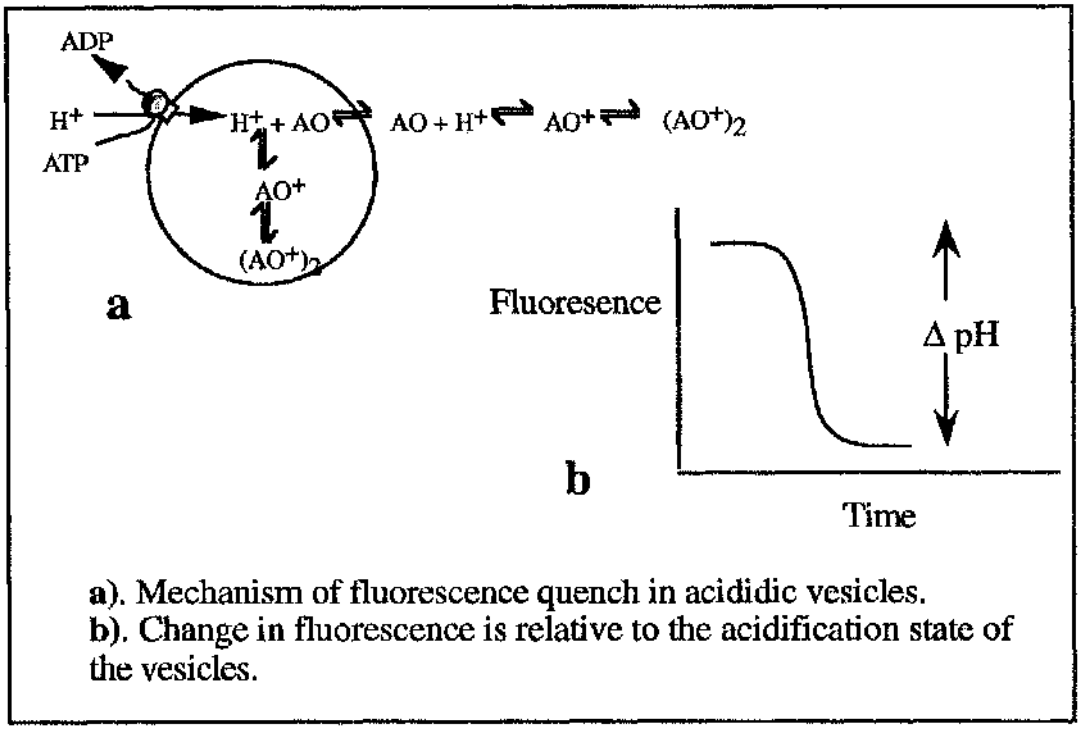

a). Mechanism of fluorescence quench in acididic vesicles.
b). Change in fluorescence is relative to the acidification state of the vesicles.

Figure 4.1. Detection of vesicle acidification using the fluorescence quench of acridine orange.

Antiporter activity can also be studied using the quench in acridine orange upon vesicular acidification. Vesicles, pre-loaded with potassium, then resuspended in a potassium free medium, will exchange the potassium for protons via the K^+/nH^+ antiporter. This results in acidification of the vesicles which can be measured using the fluorescence quench of acridine orange.

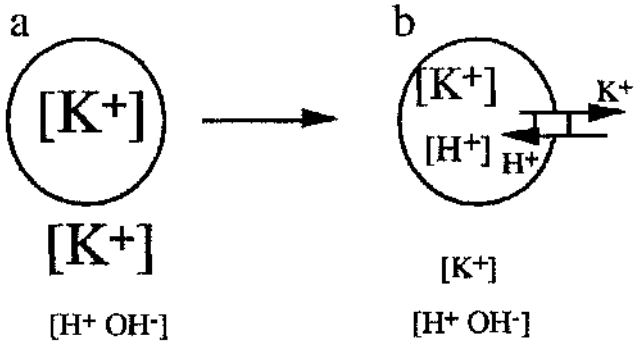

(a) GCAM vesicles are pre-loaded with K^+ by equilibration in a high $[K^+]$ buffer. (b)When the vesicles are then placed in a buffer containing very low $[K^+]$ the potassium ions flow down the concentration gradient via the K^+/nH^+ antiporter, simultaneously leading to vesicle acidification.

Figure 4.2. Mechanism of ATP independent, antiport generated vesicle acidification.

4.1.4 Proteins on the membrane.

Control of ion transport may be reflected in the structural properties of the membrane. The protein complement and structure of the membrane can be studied using a variety of techniques. Polyacrylamide gel electrophoresis is one of the standard methods for the separation and analysis of proteins.

4.1.5 Analysis of the gel and detection methods.

There are many detection methods available for the visualisation of proteins, some of which were used in this investigation. Direct detection of bands on the gel after electrophoresis is accomplished by immediately treating the gel with dye, such as Coomassie blue. Coomassie blue is a triphenylmethane anionic dye which preferentially forms dye complexes with proteins in the gel matrix. This method is rapid and will detect protein as low as 2 ng per band. For increased sensitivity, silver stain is used which will detect protein between 0.5 and 2 ng per band. Autoradiography is the process whereby the sample is labelled with a radioactive

marker either before or after electrophoresis. The radioactive label is then detected by exposing a photographic film to the dried gel, the bands are visualised upon development of the film. Specific antibodies raised against a target polypeptide provide a specific detection system for polypeptides separated by SDS-PAGE. Polyacrylamide gels, however, cannot be probed with antibodies because the probe is too large to diffuse through the gel to bind with the antigen. Transfer of protein from the gel to a nitrocellulose membrane increases the sensitivity of such detection systems. Protein transfer from gel to membrane is termed a Western blot and is often done electrophoretically for speed. When the gel containing the protein is placed under a nitrocellulose membrane and an electric field is applied perpendicular to the assembly, the sample moves out of the gel and onto the membrane. This results in an exact copy of the gel.

In this chapter the techniques described above were used to study the activity of the V-ATPase and other transport systems on the membrane. The results indicate that the V-ATPase activity, in terms of ATP hydrolysis rates and ATP dependent proton transport, is selectively down-regulated during the larval moult from fourth to fifth instar. Concurrent with V-ATPase activity down-regulation, the V-ATPase structure is modified by the loss of the catalytic V_1 domain from the GCAM.

4.1.6 Northern blots

Northern blots allow the study of the expression of a specific gene by the presence of mRNA in the tissue. In this study a ^{32}P radiolabled cDNA probe encoding the 17 kDa subunit has been utilised to specifically demonstrate the expression of the 17 kDa subunit.

4.2 Results

V-ATPase ACTIVITY IS MODIFIED DURING THE MOULT

4.2.1 GCAM purification

Following the methods in the literature production of three clear bands after sucrose density purification was unsuccessful (Cioffi & Wolfersberger, 1983). After advice from Helmut Wieczorek, a discontinuous gradient was employed. This proved a success and three bands were clearly visible. Band 2 is the fraction enriched with GCAM and is referred to as partially purified GCAM. This preparation yielded 122 ± 13 µg (SEM, n=5) protein per feeding fifth instar larvae of 7g. Not surprisingly, the yield was much lower from 1g moulting larvae at 6 ± 1 µg (SEM, n=8) per larvae, a 20-fold reduction in comparison to feeding larvae. The wet weight of the posterior midgut tissue was 104 mg ± 2 for fifth instar and 19 mg ± 1 for moulting larvae, thus, there is approximately 1/5 the starting material per moulting larvae. The specific yield is thus 1.2 µg band 2 protein/mg wet weight tissue, and 0.3 µg band 2 protein/ mg wet weight tissue. The yield of partially purified GCAM protein in band 2 from moulting larvae is reduced by approximately 75% in comparison to band 2 extracted from feeding larvae.

4.2.2 V-ATPase is the target for regulation

Partially purified GCAM was extracted from either fourth instar moulting larvae or feeding fifth instar larvae, following which, the membrane bound ATPase capabilities were assayed and compared. The specific activity of ATPases in the absence of inhibitors on membranes extracted from feeding fifth instar larvae was 51 ± 4 µM phosphate/mg protein/hour (U). On membranes extracted from fourth instar moulting larvae the specific activity of ATPases in the absence of inhibitors is 27 ± 2 U, an approximate 50% reduction in comparison with the activity from feeding larvae (see **figures 4.3.** and **4.4.**).

In the presence of azide and vanadate the F- and P- type ATPase activities were eliminated respectively; any remaining activity was considered to be due to V-ATPases. The assay was conducted using membranes from feeding larvae, in the presence of azide (0.5 mM) and vanadate (0.1 mM). In this case, the ATPase activity measured was reduced from the total ATPase activity of 51 ± 4 U to 28 ± 3 U. Therefore, approximately 50% of the total ATPase activity of partially purified GCAM from feeding larvae is composed of either azide or vanadate sensitive ATPases, the remaining 50% being V-ATPase. In comparison, ATPase activity isolated from moulting larvae is reduced from a total of 27 ± 2 to 3 ± 1 in the presence of azide and vanadate. Here, approximately 90% of the ATPase activity is either azide or vanadate sensitive and is not, therefore, V-ATPase. The remaining azide and vanadate insensitive activity is the V-ATPase component of the membrane and is dramatically reduced to 10% that of the V-ATPase activity of feeding larvae.

The V-ATPase was inhibited directly with 1μM bafilomycin A_1. 50% of the total ATPase activity from feeding larvae is inhibited by 1μM bafilomycin and is therefore V-ATPase. Thus the total ATPase activity is composed of 50% P- and F- ATPases, and 50% V-ATPase. Membranes isolated from moulting larvae still retain approximately 100% of their total activity in the presence of bafilomycin. This demonstrates that the V-ATPase makes up an extremely small proportion of total ATPase activity in these membranes.

It becomes apparent that the 2-fold difference in the total ATPase activity between moulting and feeding larvae is due to V-ATPase inactivation during the moult. However, contaminating P- and F-ATPases display equivalent specific activities when isolated from either moulting or feeding larvae and are therefore not inhibited during the moult.

	Moulting Larvae	Feeding Larvae
ATPase ACTIVITY (no inhibitors added)	27 ± 2 (n = 6)	51 ± 4 (n = 4)
V-ATPase ACTIVITY (incubated with 0.5 mM azide and 0.1 mM vanadate)	3 ± 1 (n = 4)	28 ± 3 (n = 3)
OTHER ATPase ACTIVITIES (incubated with1μM bafilomycin)	31 ± 6 (n = 3)	27 ± 5 (n = 3)

Table 4.3. Specific ATPase activities (mean ±SEM) are expressed as μmol Pi/mg protein/h. Numbers of independent preparations are given in parentheses.

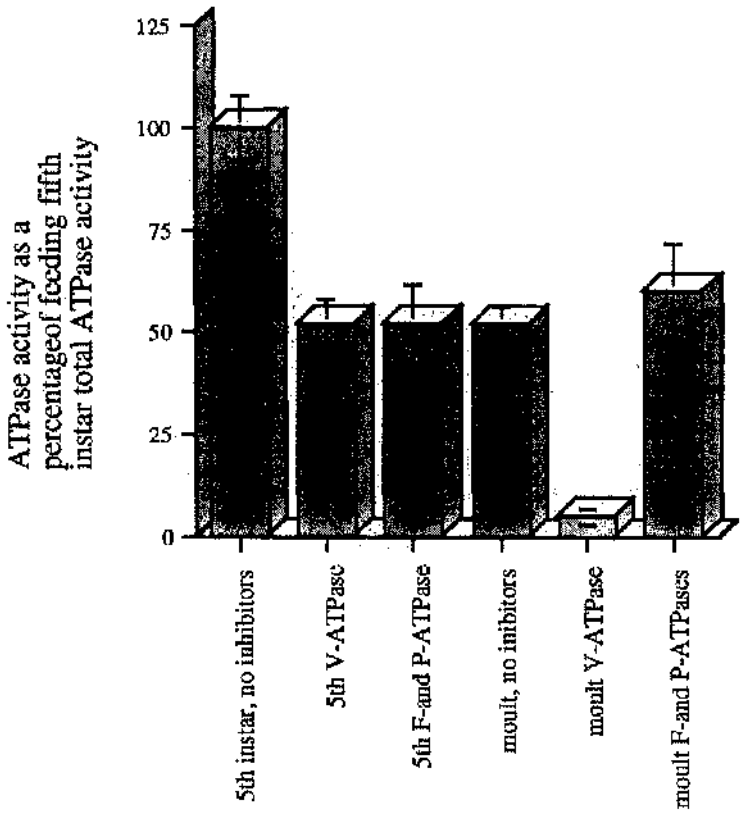

Figure 4.4. Relative ATPase activities on partially purified GCAM

4.2.3 V-ATPase dependent proton transport

In addition to ATPase activity, ATP dependent proton transport across the membrane was used to measure V-ATPase activity. Acridine orange fluorescence quench, upon vesicular acidification, is detected by a spectrofluorometer. Experiments were conducted in the presence of Mg^{2+} and ATP but in the absence of K^+, consequently, disconnection of the antiporter resulted in V-ATPase driven vesicular acidification.

At the beginning of the experiment the cuvette contains vesicles, ATP, azide, vanadate and acridine orange; a stable baseline is set. The reaction is started with the addition of $MgCl_2$ which is essential for activity. Subsequently, vesicular acidification is displayed as a downward deflection in fluorescence. The reaction is allowed to continue until a steady state is reached when the quench has reached is maximum and has levelled off. The pH gradient is dissipated with NH_4Cl. The difference between the potential when NH_4Cl was added and its final point is the true measure of the vesicle acidification. The initial velocity or rate was calculated as the relative quench 20 s after the start of the reaction.

ATP dependent proton transport was compared between partially purified GCAM vesicles isolated from feeding fifth instar and moulting fourth instar larvae. Initial velocity of acidification in vesicles was found to be 40- fold greater in vesicles derived from feeding larvae compared with vesicles from moulting larvae. The maximal specific fluorescence quench using vesicles from feeding larvae was 65 ± 2 mV (SEM, n=4), compared with the vesicles from moulting larvae figure of only 5 ± 2 (SEM, n=4). The ATP dependent V-ATPase proton transport derived from moulting larvae is reduced to 8 ±2 % (SEM, n=4) that of vesicles derived from feeding larvae. This result demonstrates that the V-ATPase is severely inhibited during the moult, see **Figure 4.5**.

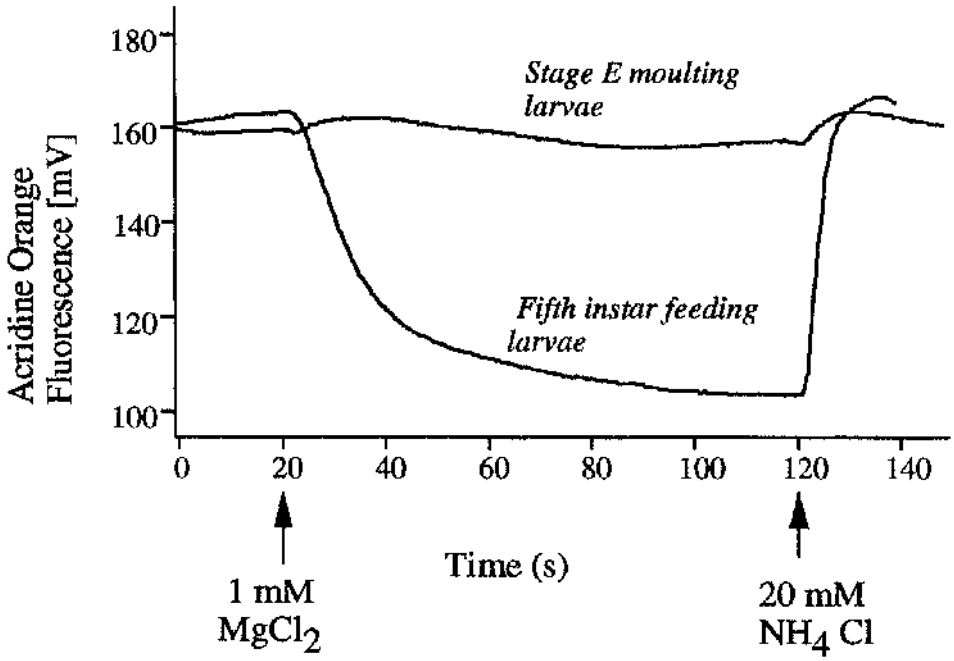

Figure 4.5 ATP dependent proton transport measured using the fluorescence quench of acridine orange. Curves shown are original data from representative experiments on goblet cell apical membrane vesicles. The reactions were started by the addition of 1mM $MgCl_2$ and stopped by the addition of 20mM NH_4Cl (final concentrations). Equal amounts (20μg) of membrane protein were used in each assay. Reduction in fluorescence corresponds to acidification of the vesicles.

4.2.4 ATP independent proton transport

Vesicles, pre-loaded with potassium, then resuspended in a potassium free medium, will exchange the potassium for protons via the K^+/nH^+ antiporter. This results in acidification of the vesicles and can be measured using the fluorescence quench of acridine orange.

Partially purified vesicles isolated from either moulting or feeding larvae were pre-incubated for 2-3 h in 10 mM Tris-Hepes, 20 mM potassium gluconate, pH 8.1. This manipulation pre-loads the vesicles with K^+. The cuvette contains a non ionic buffer and acridine orange and the baseline is standardised. The experiment is started with the addition of the vesicles. A drop in fluorescence deflection indicates ATP independent acidification: however, this deflection is partially due to non-specific quench by the vesicles themselves. The true degree of acidification is demonstrated when the pH gradient is dissipated with NH_4Cl.

Comparisons were made between vesicles isolated from moulting and feeding larvae, see **Figure 4.6.** The initial velocity of fluorescence quench was equal between the two groups of vesicles. Also, the maximal fluorescence quench was equal between the two groups. Most importantly, the level of acidification, revealed when the pH gradient was dissipated with NH_4Cl, was equal in both groups. The GCAM K^+/nH^+ antiporter is, therefore, equally functional in vesicles isolated from moulting larvae and feeding larvae. These experiments demonstrate that the antiporter remains functional during the moult and that the V-ATPase component of the K^+ transport system is the focus of pump activity regulation.

THE V-ATPase STRUCTURE IS MODIFIED UPON INACTIVATION

4.2.5 Protein components of the partially purified GCAM

To investigate the structural properties of the membrane and V-ATPase, partially purified GCAM membranes were denatured with SDS and run on a 17.5% polyacrylamide gel. Preparations

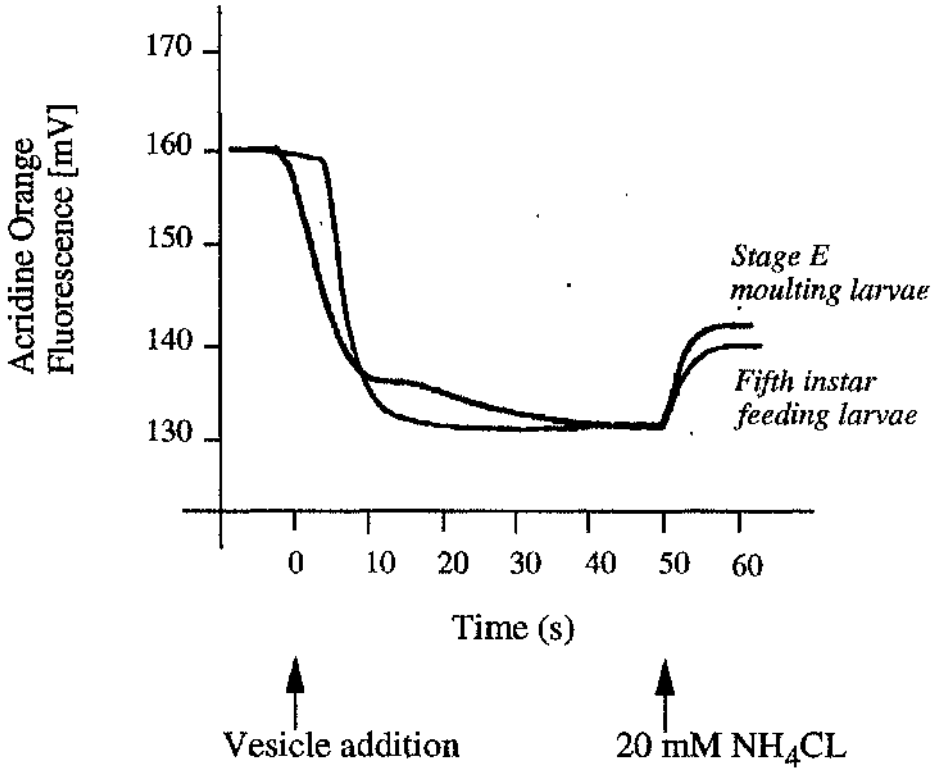

Figure 4.6 ATP independent proton transport measured using the fluorescence quench generated by a suspension of K^+ loaded vesicles. Curves shown are original data from representative experiments on goblet cell apical membrane vesicles. The reactions were started by the addition of 15 µg vesicle protein. The proton gradient was dissipated with the addition of 20 mM NH_4Cl.

from moulting larvae were compared with feeding larvae. Initially, the membranes extracted from feeding larvae were analysed. The partially purified membrane samples contained bands that were associated with the GCAM and the V-ATPase. A 100 kDa protein, normally found to associate with the GCAM and used as a marker for this membrane, was clearly present in this preparation. In addition, many of the most prominent bands coincided with the molecular weights of the V-ATPase subunits. These bands were found to have molecular weights of 67, 56, 43, 40, 28 and 16 kDa (identified with arrows). The prominence of these bands demonstrated an enrichment of GCAM membranes in this preparation, see **Figure 4.7**.

Comparison between SDS gels containing GCAM from moulting larvae with GCAM from feeding larvae suggested that there was equivalent amounts of protein in each lane, see **Figure 4.9**. A 100 kDa band was present in both samples and generally the banding patterns were similar. However, examination of the putative V-ATPase subunits revealed that there were major differences in the presence of V-ATPase subunits between the samples. The sample isolated from feeding larvae contained putative V-ATPase bands at 67, 56, 43, 40, 28 and 16 kDa. In comparison, the sample isolated from moulting larvae appeared to be lacking the 67, 56, 28 and 16 kDa V-ATPase components. These subunits were evidently either missing or under represented in partially purified GCAM from moulting larvae. The 40 and 43 kDa subunits appeared to be present in equal amounts in both samples.

4.2.6 Analysis of western blots.

Western blots were undertaken to identify the bands on the SDS gel. The primary antibody used was a polyclonal antibody directed against highly-purified V-ATPase. The antibody heavily labelled bands heavily at 67, 56, 43, 28 and 16 kDa. This verified that these bands are components of the V-ATPase and that the GCAM has been partially purified from fifth instar feeding larvae, see **Figure 4.8**.

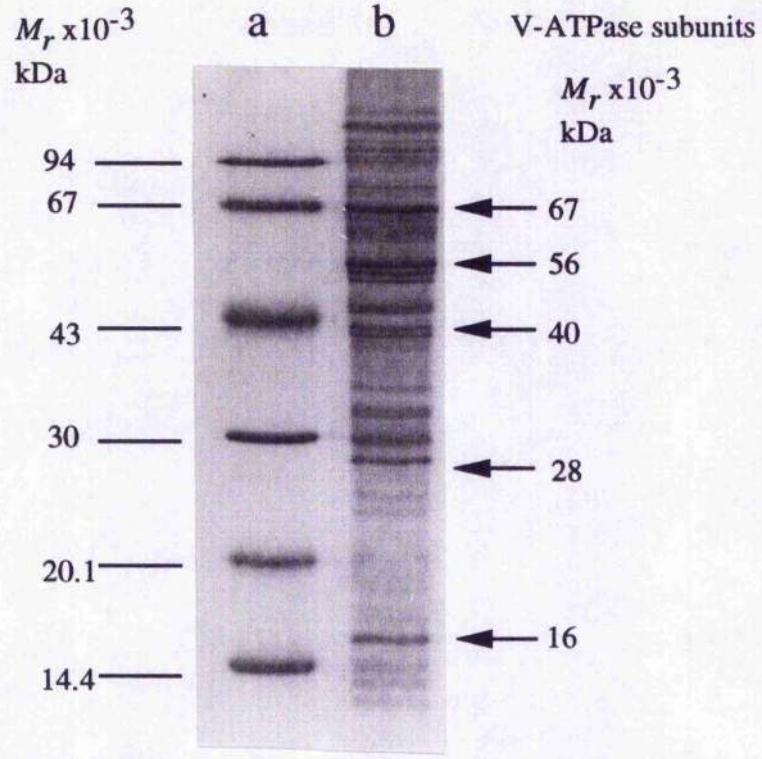

Figure 4.7. SDS PAGE of GCAM partially purified from feeding larvae labelled with Coomassie blue. **Lane a**, 5 µg Low molecular weight standards; **Lane b**, 5 µg 5th instar partially purified GCAM. V-ATPase subunits are arrowed.

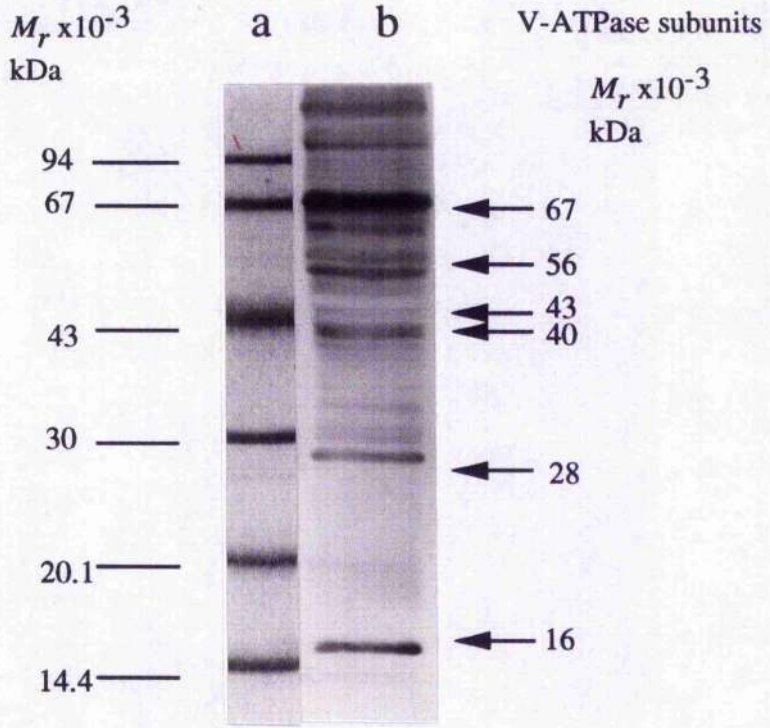

Figure 4.8. Western blot of GCAM partially purified from feeding larvae. **Lane a**, Ponceau labelled STD; **Lane b**, V-ATPase Polyclonal antibody labelling.

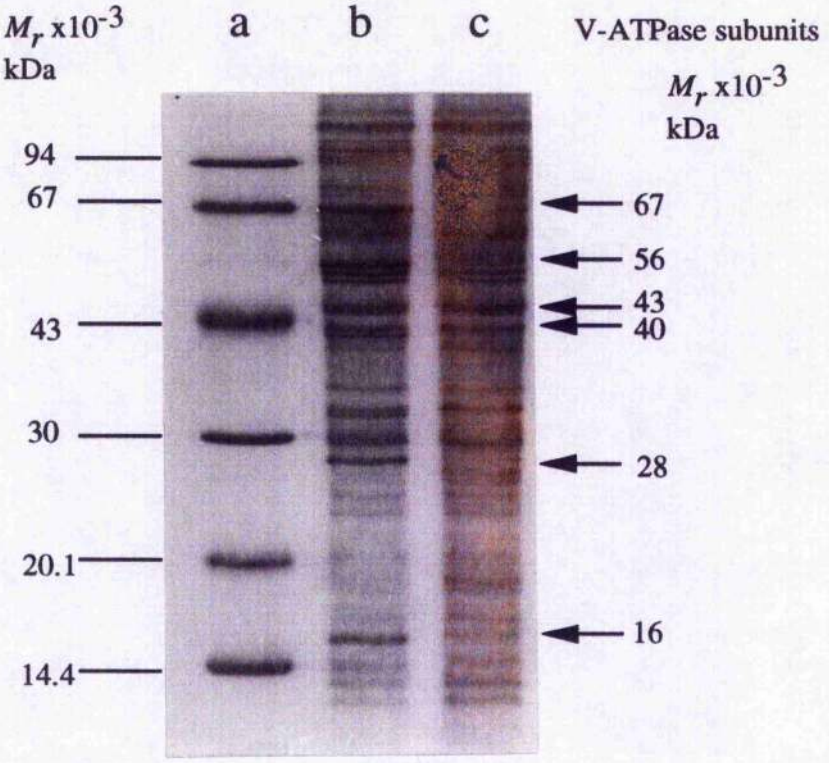

Figure 4.9. Coomassie stained SDS PAGE of partially purified GCAM. **Lane a**, STD; **Lane b**, 5 µg band 2 from feeding larvae; **Lane c**, 5 µg band 2 protein from moulting larvae.

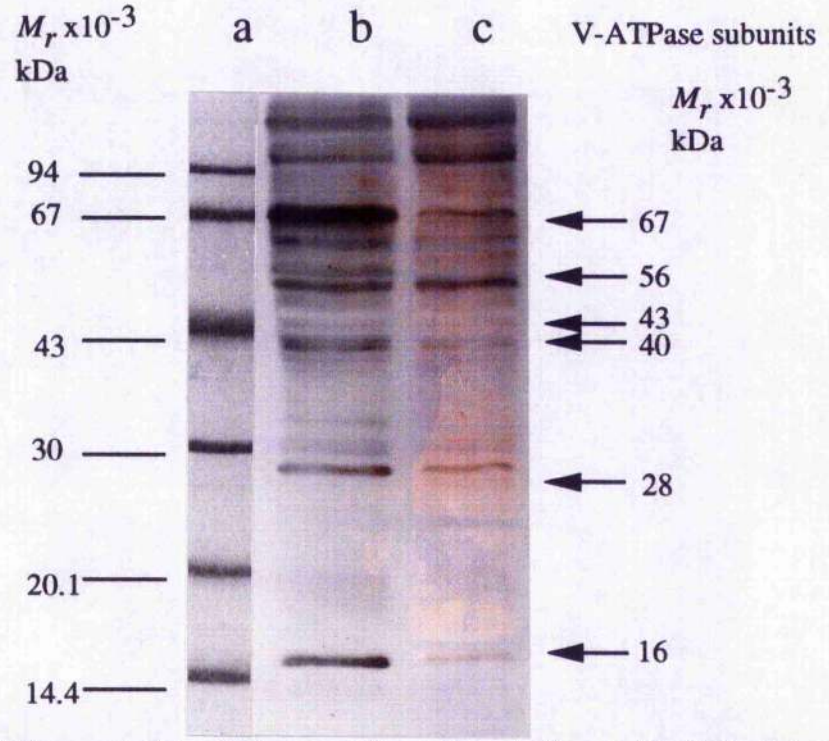

Figure 4.10. Western blot of partially purified GCAM **Lane a**, Ponceau STD; **Lane b**,band 2 from feeding, **lane c**, band 2 from moulting. Probed with polyclonal antibodies raised against the V-ATPase.

Polyclonal antibodies, directed against the highly purified ATPase, label subunits in membrane samples from both feeding and moulting larvae. The degree of labelling of the V-ATPase subunits, however, is greatly reduced on membranes isolated from moulting larvae. V-ATPase subunits of molecular weight 67, 56, 43, 28 and 16 kDa are prominently labelled on membranes isolated from feeding larvae. These subunits are labelled when membranes are isolated from moulting larvae but to a much lesser extent, indeed, the 28 and 16 kDa subunits are labelled only marginally stronger than the background. This result demonstrates that these V-ATPase subunits are present in a lower concentration on the GCAM during the moult. The background labelling pattern and intensity indicates that the isolates are similar in composition, except with regard to the V-ATPase, see **Figure 4.10**.

4.2.7 Highly purified GCAM membranes

For a higher degree of clarity, the protein components of highly purified goblet cell apical membranes were analysed by SDS-PAGE. Overall, the peptide compositions of the membrane samples were similar; however, there were differences in the subunit profiles of the V-ATPase. The fifth instar highly purified membrane had the full complement of known insect V-ATPase subunits; 67, 56, 43, 40, 28, 20, 17, 16 and 14 kDa. In comparison, the inactivated membrane clearly contained the 43, 40, 20 and 17 kDa subunits; however, the 67, 56, 28 and 16 kDa subunits appeared to be under-represented. The 14 kDa subunit is reduced in concentration on membranes isolated from moulting larvae. The 100 kDa peptide, which has an unknown function but is a marker for the GCAM, was present in both samples. It becomes apparent that specific subunits are consistently absent from membrane preparations from moulting larvae, whereas others remain on the membrane. Thus, there appears to be a structural modification to the inactivated V-ATPase, see **Figure 4.11**.

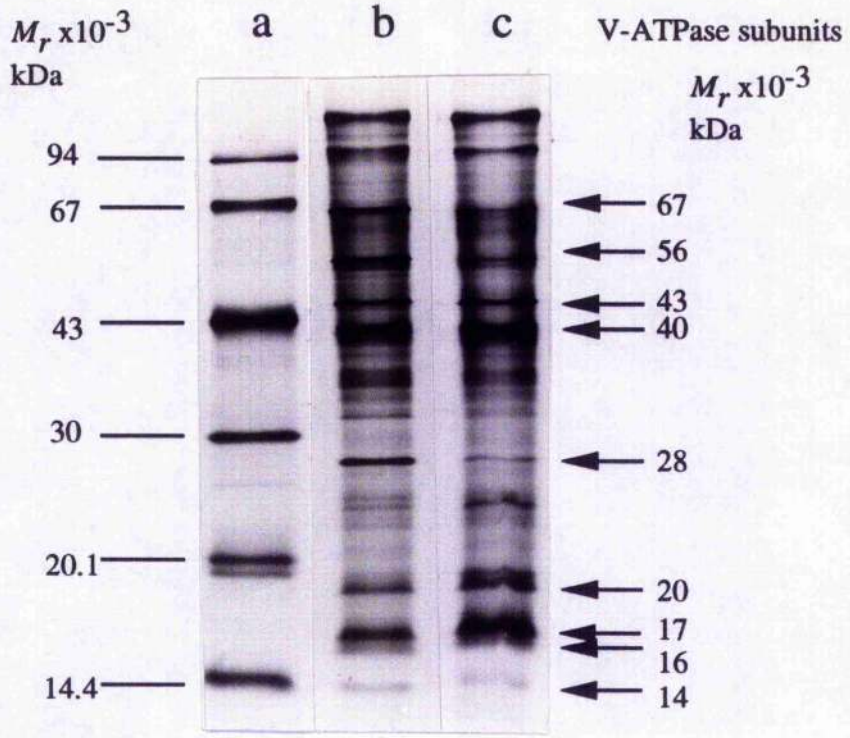

Figure 4.11. SDS PAGE of highly purified GCAM membranes. **Lane (a)** molecular weight standard, **lane (b)** highly purified GCAM isolated from feeding larvae, **lane (c)** highly purified GCAM isolated from moulting larvae. 5µg of protein were added per lane and the protein was detected using silver stain. Note the absence of specific V-ATPase subunits on membranes from moulting larvae.

4.2.8 Analysis of distinct V-ATPase subunits

The evidence above suggests that the V-ATPase molecule is not down regulated in its entirety, rather, that specific components of the molecule are lost from the membrane. Techniques were available to investigate the levels of specific subunits on the membrane. Hydrophobic proteins were labelled with radioactive DCCD to reveal the lipoproteins. Additionally, monoclonal antibodies highlighted the discrepancy of subunit concentrations between different groups of membranes. Dot-blots were used to investigate the amount of specific subunits on the two groups of membranes, whereby, monoclonal antibodies were employed to assess the concentrations of specific subunits on the membrane, relative to the total ATPase protein.

4.2.9 DCCD labels the 17 kDa subunit

Specific labelling of the 17 kDa proteolipid membrane pore by DCCD demonstrates that this subunit is present in both membrane preparations. Compared with active membranes, the DCCD labelling on inactive membranes is more intense suggesting that the 17 kDa proteolipid is present as a higher proportion of total membrane protein, see **Figure 4.12**.

4.2.10 Monoclonal antibodies demonstrate subunit depletion

Western blots of partially purified GCAM were probed with monoclonal antibodies against the 67 kDa subunit or monospecific polyclonal antibodies against the 14 kDa subunit. Polyclonal antibodies against the holoenzyme were also used in some experiments. The results show that, when probed with the polyclonal against the holoenzyme, there is a general decrease in V-ATPase isolated from moulting larvae. The 67 kDa subunit is specifically labelled on active membranes from feeding larvae but is undetectable on membranes from moulting larvae. Polyclonal antibodies directed against the 14 kDa show that this subunit is reduced in membranes from moulting larvae. These results

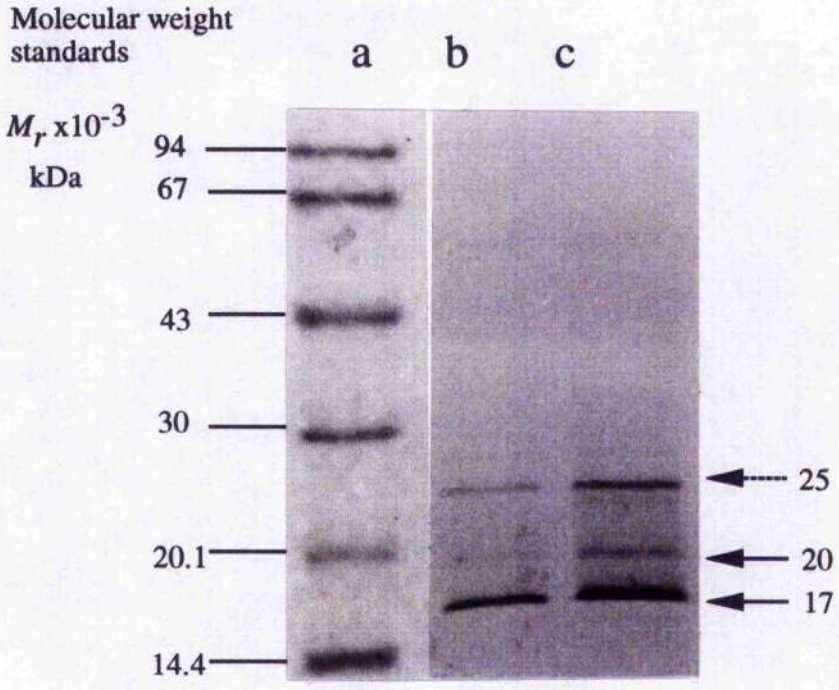

Figure 4.12. DCCD labelling of highly purified GCAM membranes. N,N'- dicyclohexylcarbodiimide labelling of highly purified GCAM membranes from either **lane (b)** feeding fifth instar or **lane (c)** moulting larvae. Bands at 25, 20 and 17 kDa are labelled in both samples. Notice, however, that the degree of labelling is greater in the moulting sample, indicating that these proteins constitute a greater proportion of the membrane than in feeding larvae. **Lane (a)** contains Coomassie labelled standard molecular weight proteins.

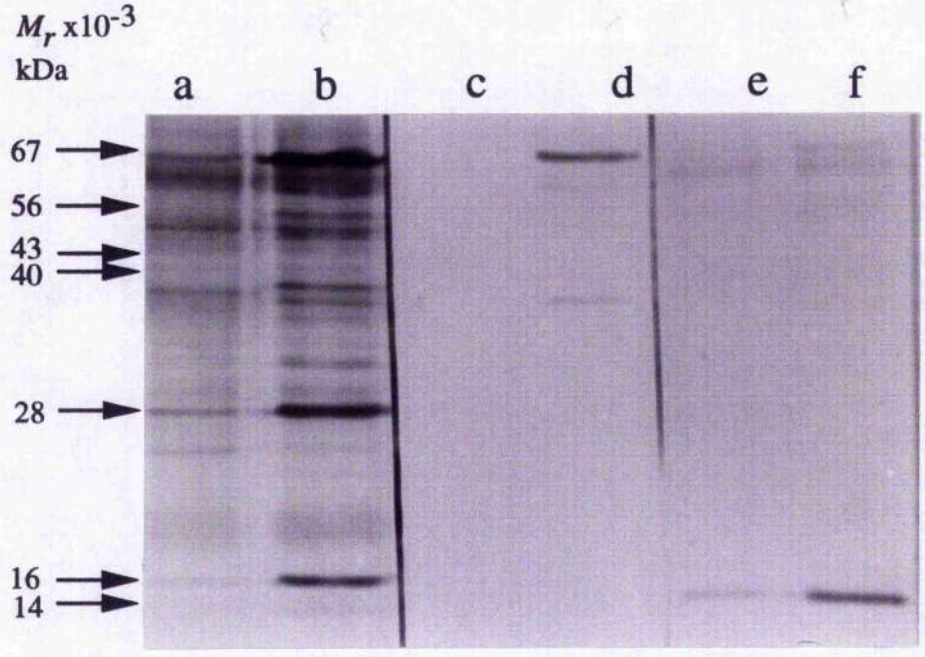

Figure 4.13. Antibodies are monospecific for V-ATPase subunits. **Lanes a, c** and **e**, GCAM isolated from moulting larvae; **lanes b, d** and **f**, GCAM isolated from feeding larvae. Primary antibodies were; **lanes a** and **b**, anti- 14 kDa monospecific antibody; **lanes c** and **d**, anti- 67 kDa monoclonal antibody; **lanes e** and **f**, polyclonal anti-V-ATPase holoenzyme.

confirm that specific subunits are missing from the membrane in moulting larvae and demonstrate the capability of the antibodies to differentiate between distinct subunits, see **figure 4.13.**

Dot blots were used to measure directly the relative amounts of specific V-ATPase subunits. Two fold serial dilutions of partially purified GCAM were dot-blotted onto nitrocellulose and probed with various antibodies against the V-ATPase. Polyclonal antibodies against the holoenzyme indicated that membranes extracted from moulting larvae contained approximately 50% less V-ATPase when compared with identical amounts of GCAM protein from feeding larvae.

GCAM blots were also probed with monoclonal antibodies against either the 67 kDa or 28 kDa subunits. Both the 67 and 28 kDa subunits were reduced ten-fold on inactive membranes compared with active membranes.

Monospecific antibodies against the 14 kDa subunit revealed that this subunit appeared to be reduced five fold on inactive stage E membranes.

The dot blot data are consistent with the banding pattern on the SDS gels, where the 67 and 28 kDa bands are greatly reduced on stage E larvae, whereas the 14 kDa subunit appears to be an intermediate and is not as readily lost as other subunits, see **Figure 4.14**.

4.2.11 Western blot of crude tissue homogenate confirms previous results

Posterior midgut tissue was homogenised and the membranes were washed in buffer. The membranes were solubilised with SDS, run on a gel, and then western blotted. The blot was probed with polyclonal antibodies directed against the V-ATPase holoenzyme molecule. The bands detected on feeding fourth and feeding fifth instar membranes are similar. The main V-ATPase subunits are clearly detected by the antibody. The membranes from moulting larvae are not labelled heavily. This crude extract demonstrates

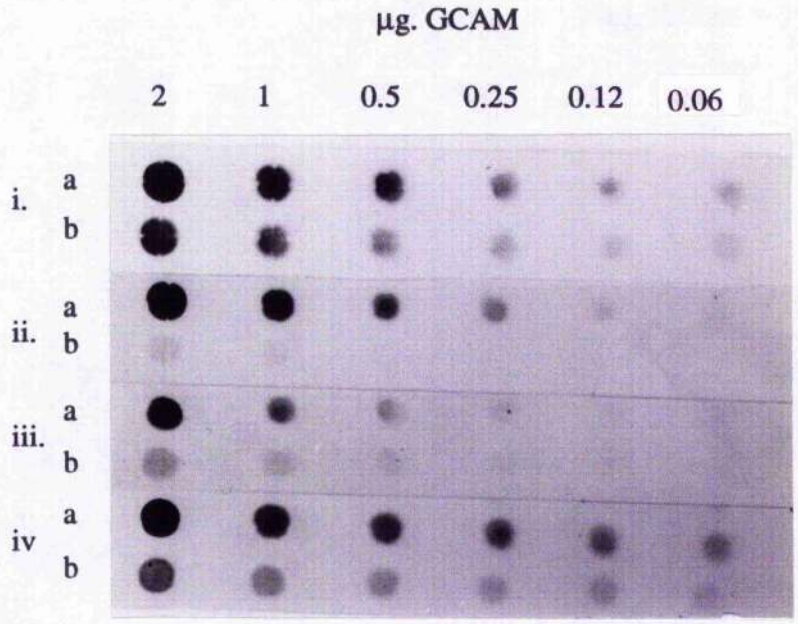

Figure 4.14. Dot blots of partially purified goblet cell apical membranes after SDS treatment. Serial dilutions of GCAM isolated from fifth instar larvae (**rows** labelled **a**) or from stage E moulting larvae (**rows** labelled **b**), spotted onto nitrocellulose membrane (1µl/spot), air dried and probed with anti- V-ATPase antibodies. **i**, polyclonal antiserum against V-ATPase holoenzyme; **ii**, monoclonal antibody against 67-kDa subunit A; **iii**, monoclonal antibody against 28-kDa subunit E; **iv**, monospecific polyclonal antibodies against the 14-kDa subunit.

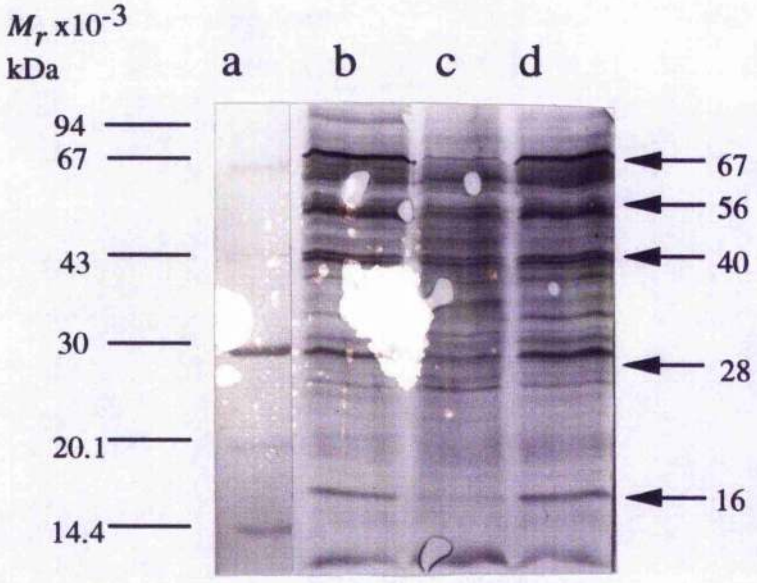

Figure 4.15. Western blot of crude extract of midgut membranes. Midgut homogenate was run on an SDS gel, from which a western blot was produced. V-ATPase components were visualised by using anti-V-ATPase holoenzyme polyclonal antibodies. **Lane a**, molecular weight standard; **lane b**, feeding fourth instar midgut membranes; **lane c**, moulting fourth instar midgut membranes; **lane d**, feeding fifth instar midgut membranes.

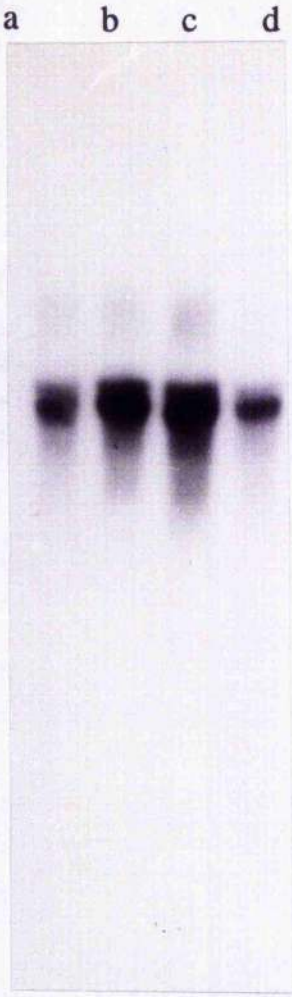

Figure 4.16. Northern blot of total RNA probed with P^{32} labelled 16 kDa cDNA. **a,** 10 µg RNA extracted from 4th/5th moulting larvae; **b,** 10 µg RNA extracted from the apical region of 5th instar feeding larvae; **c,** 10 µg RNA extracted from the mid midgut region of 5th instar feeding larvae; **d,** 10 µg RNA extracted from the posterior midgut region of 5th instar feeding larvae.

that the previous results were not influenced by the rather elaborate purification procedure, see **Figure 4.15**.

4.2.12 Northern blots

Total RNA was extracted from midguts during the moult or 5th instar. The RNA was Northern blotted and probed with a ^{32}P labelled DNA probe against the 16 kDa proteolipid proton pore. Ethidium bromide labelling of the gel prior to blotting shows that RNA has been extracted from the midgut and that it has not degraded. These samples are of total RNA, this includes ribosomal in addition to messenger RNA. The gel contained no visible ethidium bromide labelling after blotting, indicating that the blotting technique had worked efficiently.

The 16 kDa probe hybridised to the midgut isolated from moulting larvae and the apical, mid and posterior regions of the 5th instar midgut. The autorad labelling pattern was similar to the ethidium bromide labelling of the RNA on the gel suggesting that the probe is indeed specific to the insect RNA. All samples tested had a similar amount of labelling by the probe, suggesting that RNA for the 16 kDa proton pore is present in the midgut, regardless of developmental stage or region of the midgut, see **Figure 4.16**.

4.3 Discussion

4.3.1 GCAM purification from moulting larvae

GCAM had not been purified from moulting larvae prior to this investigation. There is strong evidence that the purified membrane samples being compared from moulting and feeding larvae are equivalent. Primarily, for the purification of GCAM membranes, the tissue in moulting larvae must have a similar structure to the feeding tissue, on which this technique was developed. During the moult, midgut epithelial stem cells proliferate and differentiate into goblet or columnar cells and intercalate between original mature cells. The original mature columnar and goblet cells remain intact during the moult and, significantly, the goblet cells retain the goblet cavity and the GCAM (Baldwin & Hakim, 1991;

Cioffi, 1984). Therefore, although some cell proliferation is occurring, the general organisation of the midgut, crucial for the success of isolation of GCAM, remains similar.

The amount of protein in band 2 was consistently lower per wet weight of tissue when isolated from moulting larvae. The purification procedure may not be as efficient when carried out on moulting larvae due to the small size of the tissue pieces and the relative difficulty of the dissection. An additional explanation for reduced protein yields is that there is not less membrane, but that there is less protein on that membrane!

Much of the V-ATPase, a major component of the GCAM, is found to be absent from the membranes isolated from moulting larvae, when studied on SDS PAGE gels. However, disregarding the V-ATPase, comparison of membrane samples on gels and western blots gives the impression that the samples are otherwise similar between moulting and feeding larvae. The specific levels of P- and F- ATPase contamination within the membrane samples are similar, implying the membrane samples are similar. Finally the antiport activities between moulting and feeding membranes are identical. The accumulation of this evidence argues strongly that the GCAM was purified from moulting larvae and was similar to the GCAM from moulting larvae, except with regard to the V-ATPase. The V-ATPase is specifically the metabolic target. The V-ATPase component of the potassium pump is inactive during the time course of the moult. Specific V-ATPase activity during the moult is only 10% that of intermoult larvae. The level of contaminating P- and F- ATPase activity was high in moulting larvae indicating these ATPases are not down-regulated during the moult. The specific activity of the bafilomycin insensitive P- and F- ATPases was slightly higher on membranes isolated from moulting larvae. The increased proportion of contaminating ATPases could be caused by a less pure GCAM preparation, or, on the other hand, by the loss of V-ATPase protein from the membrane, thus increasing the specific activity of contaminating ATPases. The V-ATPase was not only unable to hydrolyse ATP but was unable to transport protons across the membrane.

However, the antiporter capabilities of membranes isolated from moulting and feeding larvae were identical, which is strong evidence that the V-ATPase capabilities are directly and specifically inhibited during the moult.

4.3.2 Regulation of V-ATPases

A number of regulatory mechanisms have been described for the V-ATPases. Indirect regulation of V-ATPase activity has been demonstrated *in vitro* using V-ATPase from clathrin coated vesicles and reconstituting it in synthetic vesicles. It was found that the V-ATPase requires a specific lipid composition of the membrane for activity. These experiments also demonstrated that no additional proteins or proteolipids are required for pump activity.

However, specific regulation of V-ATPase by an inhibitor protein has been recently demonstrated. Bovine kidney cells contain a specific cytosolic V-ATPase inhibitor protein which can inhibit microsomal, brush border and lysosomal V-ATPases by up to 85%. ATPase activity and proton transporting capabilities are both inhibited by this protein. The V-ATPase inhibitor protein has a molecular weight of 6.3 kDa, which is similar to the protein inhibitors of the F-ATPases. In addition, a cytosolic V-ATPase activator protein of approximately 35 kDa has been discovered, which also affects V-ATPases specifically (Zhang, Wang, & Gluck, 1992a,b). I have found no evidence for such inhibitor, or activator, proteins stoichiometrically associated with the *Manduca* V-ATPase; nevertheless, there are many unidentified protein bands on the GCAM. However, if such a protein associated with the peripheral subunits during the inactivated phase it might be lost upon purification of the membranes.

Control of V-ATPase pump activity *in vivo* by regulation of V-ATPase molecules has been described in kidney epithelial cells (Brown, Sabolic, & Gluck, 1991b), whereby pump concentration on the membrane is modified by integration of vesicles carrying dense concentrations of V_0V_1 pump molecules. This process is signalled by a rise in intracellular calcium and is dependent on an

intact microtubule system. There is no electronmicrographic evidence for this mechanism in *Manduca*. The SDS-PAGE evidence in presented here suggests that the apical membranes are modified by the loss or gain of, not complete pumps, but V_1 domains.

Endosomal proton transport has been suggested to be under hormonal or secondary messenger control. The non-hydrolysable cAMP analogue 8-bromoadenosine cyclic monophosphate was found to have a direct inhibitory affect on the V-ATPase (Gurch & DuBose Jr, 1989). Further evidence suggests that G proteins are capable of stimulating V-ATPases of endosomes directly (Gurich, Codina, & DuBose Jr, 1991). However a structural mechanism of V-ATPase regulation has not been elucidated. Direct V-ATPase activation by protein kinase C has been suggested in neutrophils. Here, after phorbol ester stimulation, protein kinase C stimulates a phosphorylation event that stimulates the V-ATPase (Nanda & Grinstein, 1991). However there is no evidence for the structural mechanism of V-ATPase stimulation.

4.3.3 A novel mechanism for V-ATPase regulation

The V-ATPases are composed of two major domains, the catalytic "head" or V_1 domain and the membrane associated V_0 domain. Each domain is composed of defined subunits. The V_1 domain is composed of the 67, 56, 28 and 16 kDa subunits. The V_0 domain is composed of the 43, 40, 20 and, the proteolipid, the 17 kDa subunits. It is therefore interesting that only the V_0 subunits are present on the inactivated membranes, see **figure 4.17.**

The similarity of banding patterns on SDS-PAGE suggest that our GCAM preparations are, indeed, similar; however, the concentration of V_1 subunits on inactive membranes appears to be reduced. At the same time, the density of V_0 subunits appears similar between the membranes. Identification and quantification of subunits with dot blots verified that certain V_1 subunits were under represented on the inactive membrane. DCCD labelling showed that the 17 kDa proton pore subunits, components of the V_0, were present on both active and inactive membranes.

It has been demonstrated in other laboratories that the V_1V_o can be dissociated readily by treatment with chaotropic agents and ATP, resulting in the disassembly of the V_1 domain from the V_o. Dissociation of the V_1 and V_o subunits renders the enzyme unable to hydrolyse ATP or to transport protons. Upon re-association of the V_1 and V_o domains activity is restored to the V-ATPase (Puopolo & Forgac, 1990). The related F-type proton ATPases (Mandel, et al., 1988) are composed of a F_o integral proton pore and a F_1 peripheral head which, like the V-ATPase, can be dissociated from each other *in vitro* (Adachi, Puopolo, Marquez-Sterling, Arai, & Forgac, 1990). The dissociated F_o integral pore performs as a passive proton channel (Aris, Klionsky, & Simoni, 1985); however, in comparison, the dissociated V-ATPase V_o domain cannot passively conduct protons and is essentially "locked" shut until re-association of the V_1 (Zhang, Myres, & Forgac, 1992a). It has been proposed that the size of the proteolipid may be a major factor in the exclusive directionality of the V-ATPases in comparison with the F-ATPases (Nelson & Taiz, 1989). It has been demonstrated that the short 8 kDa proteolipid of F- and archaebacterial V-ATPases is capable of ATP synthesis and conducts protons when the catalytic domain is removed. The eukaryotic V-ATPase proteolipid is believed to be a duplicated and fused form of this 8 kDa protein. This event led to loss of V-ATPase capabilities for ATP synthesis and passive proton conduction (Nelson, 1992).

Evidence is accumulating that dissociation of the V_1 from the V_o occurs *in vivo* and that there is an excess population of V_o domains present on the membrane in a dissociated form (Kane, Kuehn, Howald-Stevenson, & Stevens, 1992; Zhang, et al., 1992a). Corresponding with this, there is a cytoplasmic pool of not only V_1 subunits (Nelson & Taiz, 1989) but fully assembled, enzymaticly inactive, V_1 domains (Myres & Forgac, 1993). The function of this pool of V_1 domains is still, however, unknown. The whereabouts of the missing V_1 subunits in *Manduca* is

unknown, as due to the nature of membrane purification any unattached subunits will be lost in the preparation.

Evidence from the Northern blots suggest that expression of the V_o subunits is not down regulated during the moult. This suggests that V_o subunits are continuously being produced even though the pump is inactivated. It is not known if V_o subunits produced during the moult are inserted into the membrane during this period.

The present study indicates that, in *Manduca*, the V-ATPase molecule is "switched off" by the loss of the V_1 group, whereas recovery of V-ATPase activity is accompanied with the re-assembly or re-introduction of the V_1V_o structure. This is the first demonstration of control of V-ATPase activity by regulation of assembly of the V_1 and V_o domains *in vivo*. In the following chapter I aim to demonstrate that the control of K^+ activity is under hormonal control and that control can be enforced *in vitro*.

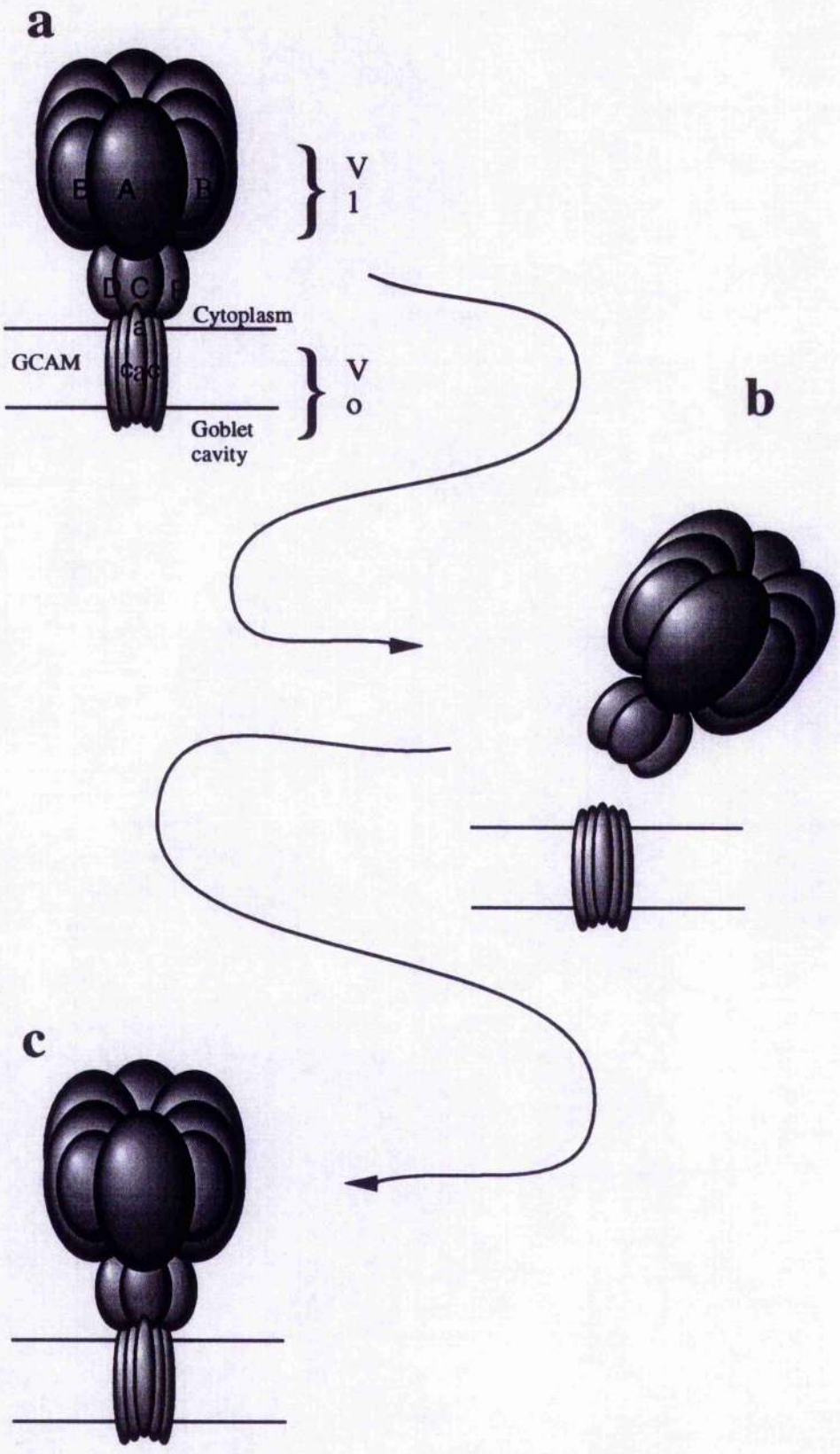

Figure 4.17. Putative model for dissasembly of V-ATPasemolecule during inactivation at the 4th/5th larval moult. **a**, holoenzyme during fourth instar feeding period; **b**, dissociation of V_1 domain during inactivation; **c**, re-assembly of holoenzyme upon re-activation of ATPase activity

CHAPTER 5

HORMONAL CONTROL OF ION TRANSPORT

5.1 Introduction

5.1.1 Regulation of ion transport occurs at the same time as hormonally controlled moulting processes

The regulation of V-ATPase activity occurs in synchrony with the hormonally mediated entry and exit from the moult. This correlation suggested that regulation of V-ATPase activity and structure may be controlled directly, or indirectly, by the hormones that control the moult. The aim of this chapter is to investigate the cellular processes that may couple the hormonally initiated entry and exit from the moult and the regulation of V-ATPase activity.

5.1.2 Mechanism of action of the peptide hormone eclosion hormone

In Lepidoptera, and other insect groups, ecdysis behaviour is triggered by eclosion hormone (EH) (Truman, 1971; Truman, Taghert, Copenhaver, Tublitz, & Schwartz, 1981). This peptide hormone acts directly on the central nervous system to evoke the stereotypical ecdysis motor programs (Truman, 1978). Once begun the ecdysis behaviour dominates all other behaviour patterns. At its completion, an array of new behaviours appropriate to the new stage are "turned on". This activation of stage specific behaviours is also caused by eclosion hormone (Truman, 1976).

Eclosion hormone activity appears about 1.5 h prior to ecdysis and reaches a peak upon ecdysis. Eclosion hormone titres then fall rapidly, so that by 1 h after ecdysis almost no activity remains (Copenhaver & Truman, 1982). Exposure to eclosion hormone alone is not sufficient to cause an insect to undergo ecdysis and the associated behavioural changes. In *Manduca* the nervous system is

responsive to eclosion hormone for only brief periods of approximately 4 h prior to ecdysis. The association of eclosion hormone sensitivity with the period of the moult suggests that ecdysteroids may be involved in regulating CNS responsiveness to eclosion hormone.

Eclosion hormone release is controlled by ecdysone
During each moult in *Manduca*, the ecdysteroid titre rapidly rises to initiate and direct the moult and then gradually declines so that ecdysis coincides with a low point in the ecdysteroid titre. During the moult from the fourth to the fifth larval instar, the ecdysteroid titre reaches peak levels at approximately 21 h prior to ecdysis and declines thereafter. If the normal ecdysteroid decline is interrupted by an injection of 20-hydroxyecdysone (20-HE), ecdysis is then delayed by a span of time that is proportional the dosage given (Curtis, Hori, Green, Wolfgang, Hiruma, & Riddiford, 1984; Truman, Rowntree, Reiss, & Schwartz, 1983). Exogenous 20-hydroxyecdysone administered during the end of the moult delayed larval, pupal (Slama, 1980), and adult moults. Continuous infusion of 20-HE into pharate adult *Manduca* blocked ecdysis for the duration of the infusion. Thus the normal withdrawal of ecdysteroids at the end of a moult appears essential for ecdysis to occur. The successive delays in ecdysis seen after steroid treatment reflect delays in the time of eclosion hormone release (Truman, et al., 1983).

Responsiveness of tissue is controlled by ecdysone
Besides showing a highly restricted time of eclosion hormone release, insects are correspondingly restricted in the times that they are responsive to eclosion hormone (Morton & Truman, 1988a; Morton & W., 1986; Truman, et al., 1983). *Manduca* are responsive to the peptide only during a very narrow temporal window that immediately precedes the time of eclosion hormone release. During the 24 h preceding pupal ecdysis, the titre of ecdysteroids declines. These insects become responsive to exogenous eclosion hormone treatment late in the decline at about 8 h prior to the expected ecdysis (Morton & Truman, 1988b; Truman, et al., 1983). This responsiveness my be delayed by an

injection of exogenous 20-hydroxyecdysone. If the ecdysone is administered less than 13 h prior to ecdysis then it does not delay eclosion hormone responsiveness. Thus steroid decline triggers some event at 13 h prior to ecdysis which results in the subsequent appearance of eclosion hormone responsiveness at 8 h prior to ecdysis.

Ecdysone appears to make the CNS responsive to eclosion hormone by inducing some of the components of the biochemical cascade that mediates eclosion hormone action. Eclosion hormone exposure results in rapid elevation in the levels of cGMP (Morton & Truman, 1985). cGMP, working via a cGMP-dependent protein kinase, then causes the phosphorylation of two endogenous substrates, the EGPs (Morton & Truman, 1988a). The nature of the EGP response is, however, unknown. The endogenous substrates are only expressed after the decline in ecdysteroid thus synchronising the responsiveness of the tissue and the release of eclosion hormone.

Timetable for events in ecdysis

A model has been suggested to explain the co-ordination of eclosion hormone release and responsiveness in neurones. An ecdysone prime is required greater than 24 h prior to the moult to stimulate the ability of eclosion hormone to generate cGMP within the neurones, possibly by the appearance of eclosion hormone receptors. After this the ecdysteroid titres decline, meanwhile the eclosion hormone receptors become functional 13 h prior to the moult. The ecdysteroid decline is required for the appearance, at 8 h prior to the moult, of the EGPs and the associated behavioural responsiveness to eclosion hormone. Ecdysone applications will prevent appearance of the EGPs provided ecdysone is applied greater than 13 h prior to ecdysis (Truman 1992).

5.1.3 Extraction of Eclosion hormone

EH originates in two pairs of cells (the VM cells) with the somata located ventromedially in the brain and axons that project the entire length of the CNS (Truman & Copenhaver, 1989). Larval and prepupal *Manduca* possess only one known peripheral EH

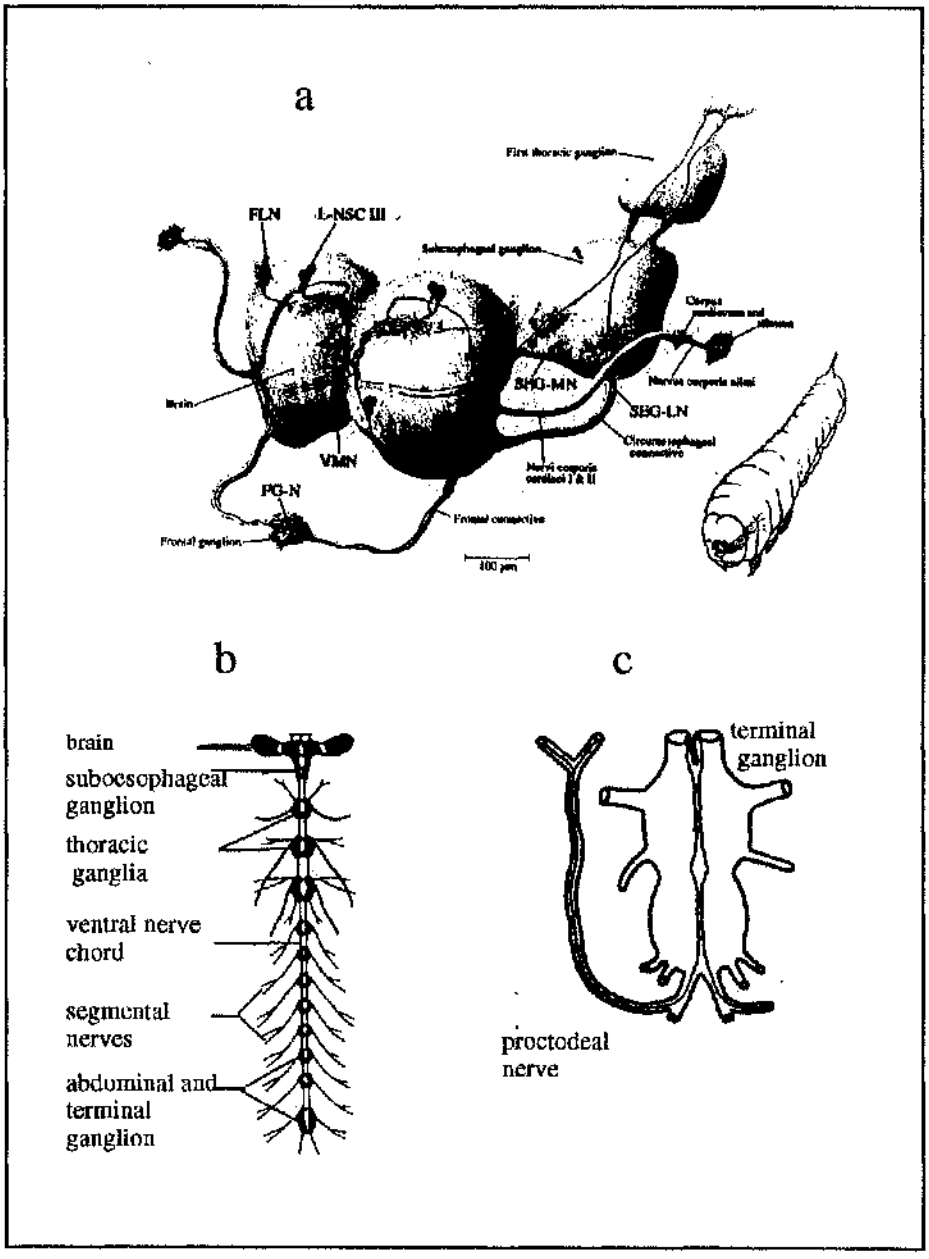

Figure 5.1. The brain-proctodeal neurosecretory system.
a. The *Manduca* brain (after Westbrook *et al*, 1993)
b. The central nervous system from brain to terminal ganglion (after Horridge 1965.) **c.** The proctodeal nerves function as a neurohaemal site for EH release. Connection of the neurohaemal site at the terminal ganglion (after Hewes *et al*, 1991).

release site, the proctodeal nerves (Truman & Copenhaver, 1989). Prior to ecdysis, this site contains more than 70% of the total EH activity measured in extracts of nervous tissue homogenates. EH activity is observed in the haemolymph in the minutes just preceding the onset of ecdysis behaviours (Truman, et al., 1981; Truman, Taghert, & Reynolds, 1980) coincident with a dramatic (>90%) release of EH from the proctodeal nerves, see **Figure 5.1** (Truman & Copenhaver, 1989). The adult brain possesses five pairs of EH containing neurones, but these cells send axons only to the corpora cardiaca/corpora allata (CC-CA) complex. EH is released from this site at adult eclosion (Truman & Copenhaver, 1989).

5.1.4 Secondary messenger mechanisms

Post-translational modifications of cellular proteins by reversible phosphorylation/dephosphorylation are important control mechanisms in a wide range of biological processes. Extracellular signals produce their effects by regulating the level of some intracellular mediators such as cyclic AMP (cAMP), cyclic GMP (cGMP), and calcium ions (Ca^{2+}). These mediators act via activation of protein kinases and the subsequent phosphorylation of specific substrate proteins.

5.1.5 Nitric oxide studies

Nitric oxide (NO) has recently been identified as an intercellular messenger with a variety of important physiological functions in vertebrates (Moncada, Palmer, & Higgs, 1991). Nitric oxide is generated by nitric oxide synthase (NOS) a 160 kDa protein. In many signalling systems NO activates a soluble cytoplasmic guanylate cyclase by nitrosylation of the haem group. This leads to accelerated intracellular formation of cGMP. cGMP may thereafter follow its more traditional pathway leading to phosphorylation of a target protein via a cGMP dependent protein kinase (PKG) (Lincoln & Cornwell, 1993).

Dehydrogenase histochemistry is based on the ability of reduced co-factors formed in the dehydrogenase reaction, in association with a second enzyme, to subsequently reduce a dye such as nitro

blue tetrazolium. The secondary enhancer enzyme, which utilises the co-factors produced in the dehydrogenase reaction, is termed a diaphorase. NADPH oxidation forms reduced co-factors which, in turn, reduces dye via NADPH-diaphorase. NADPH and nitroblue tetrazolium, when added to tissue, may react via NADPH-diaphorase to form the coloured reduced form of the dye (Scherer-Singler, Vincent, Kimura, & McGeer, 1983b). The patterns of histochemical staining for NADPH-diaphorase matches immunostaining for nitric oxide synthase very closely (Dawson, et al., 1991). In this way NADPH-diaporase labelling by tetrazolium is a convenient marker for nitric oxide activity.

5.2 Results

Insect Hormones

5.2.1 20-hydroxyecdysone prevents switch-on of gut

Mandibles became pigmented 25.1±0.1 h (SEM, n=27) after development of green head capsule. Upon mandible pigmentation synchronised larvae were injected with 6 µl of 0.5 µg/µl 20-hydroxyecdysone in isopropanol. Control larvae were injected at the same stage with 6 µl isopropanol only. Control larvae underwent ecdysis 11±0.5 h (SEM, n=5) after injection. In contrast, ecdysis occurred 15±0.8 h (SEM, n=5) after injection of ecdysone. There is an ecdysone mediated delay in ecdysis of approximately 4 h. SSC measurements on the midgut demonstrate that there is an associated delay in midgut transport activity in ecdysone treated animals (**figure 5.2.**). SSC measurements of the activity of the midgut were made at 2 hourly intervals beginning 10 h after the injections. Midgut activity returned with a delay of approximately 5 h in ecdysone treated larvae compared with controls. 12 h after injection the control midguts generated 0.15 mA/cm^2, this level of transport was acquired 17 h after injection with ecdysone, a delay of 5 h. These results suggest that the switch-on of midgut ion transport is intimately related to the hormonal environment at the time.

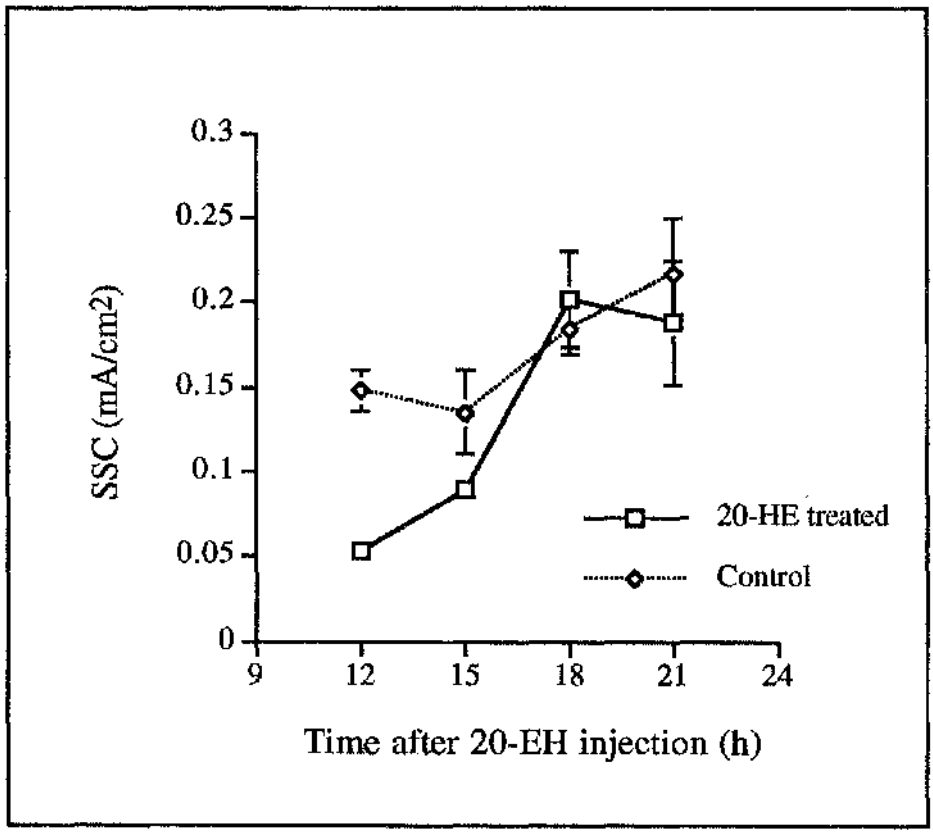

Figure 5.2. Regulation of ion transport 'switch-on' by 20-hydroxyecdysone. Ecdysone mediated delay in short circuit re~activation at the end of the moult. Experimental animals recieved 3 µg 20-HE in isopropanol, controls recieved the same volume of isopropanol only. Short circuit measurements were made between 12 and 21 h after injection. Error bars denote the SEM; where not visible, they are smaller than the plot symbols.

5.2.2 Effect of CNS extract on ion transport

Central nervous tissue extracts were found not to stimulate ion transport in midgut. Brain extract from up to 10 5th instar or 4th/5th instar larvae were applied to midgut isolated from pre-ecdysis moulting larvae. The extract did not stimulate activity. Extracts of ventral ganglia and proctodeal nerves were also applied to midgut isolated from pre-ecdysis larvae and were also found to not stimulate activity.

Cyclic nucleotides

5.2.3 cGMP stimulates ion transport

8-bromo cyclic GMP stimulated an increase in TEP by 30% within 10 min on midgut isolated from pre-ecdysis larvae. The TEP subsequently declined with time but the rate of decline was similar to the baseline decline in pseudo steady state conditions found on the Ussing chamber.

5.2.4 cAMP stimulates ion transport

100 μM 8-Bromo cyclic AMP was found to activate pre-ecdysis midguts. Addition of 8-bromo cAMP in the presence of 100 μM IBMX lead to an increase of 22 mV within 60 min
It was found that the Ussing chamber had to be thoroughly cleaned after each experiment as residual traces of cAMP had a stimulatory effect on the following midgut mounted on the chamber.

cAMP had a stimulatory effect only during a narrow temporal window. cAMP was found not to stimulate midguts isolated from larvae that were within 30 min of developing an air filled head capsule approximately 6 h prior to ecdysis. Within the next 5 h the midgut became responsive to cAMP so that by the time of pre-ecdysis behaviour 0.1 mM 8-bromo-cyclic AMP caused the resting TEP to be doubled. Midguts isolated 2 h after ecdysis displayed 90% maximal TEP values. No further stimulation was possible with 0.1 mM cAMP.

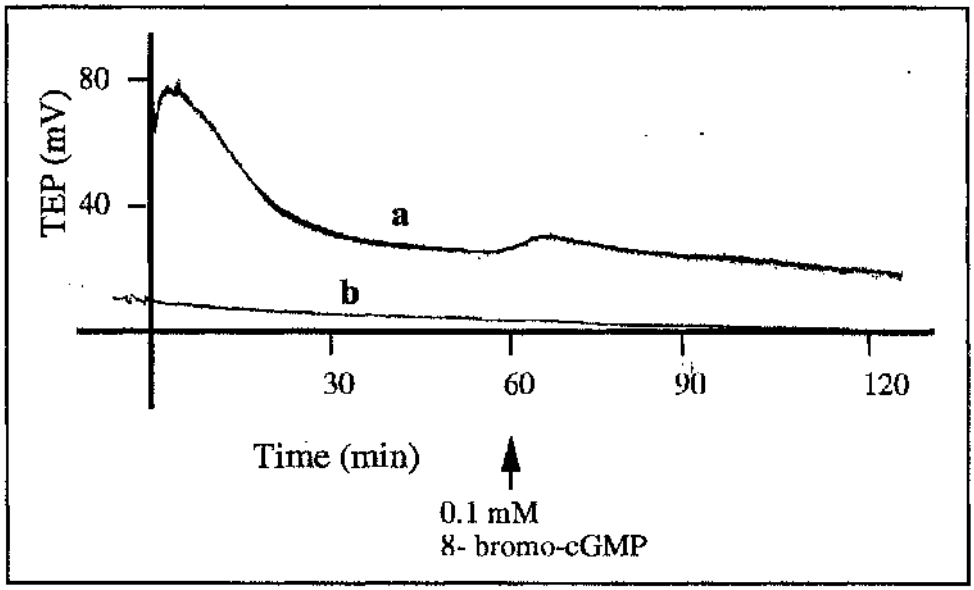

Figure 5.3. Effect of 0.1 mM 8-bromo-cGMP on transepithelial voltage. **a**, mid-midgut isolated from larvae just prior to ecdysis. **b**, mid-midgut isolted from moulting larvae with white head capsule.

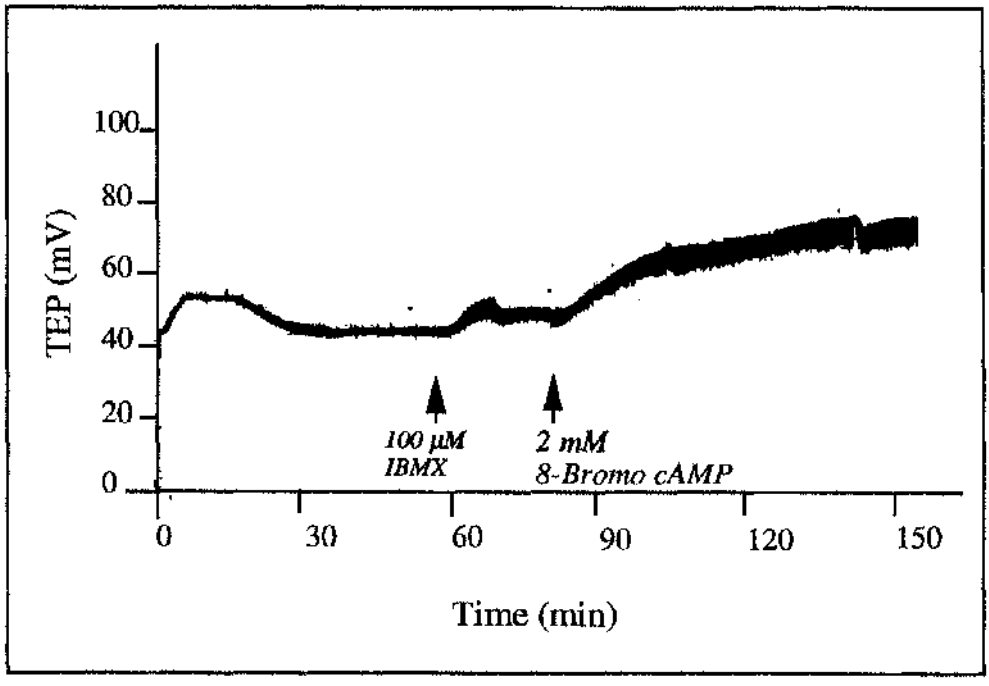

Figure 5.4. 8-Bromo cAMP stimulation of midgut activity. Midgut was isolated from larva approximatly 1 h prior to ecdysis. An air filled head capsule had developed some 3 h previously and the larva was displeying pre-ecdysis behaviour.

5.2.5 Nitric oxide and midgut activity

The ability of the tissues to generate NO requires the co-factors L-arginine, O_2 and NADPH as substrates for nitric oxide synthase. Homogenised midguts isolated from larvae undergoing ecdysis were added to the chamber. Addition of homogenised midguts resulted in a modest increase of about 6 mV. Following addition of homogenised midgut, addition of L-arginine and NADPH caused no further increase in transepithelial potential difference.

Sodium nitroprusside, which spontaneously generates nitric oxide, was added to mid-midgut 1 h after mounting the midgut onto the chamber. Midguts isolated from 4th/5th instar moulting larvae approximately 1 h prior to ecdysis during pre-ecdysis behaviour were used in all experiments. Pre-ecdysis moulting larvae had a resting TEP of 30 mV. Addition of 10 μM Na-nitroprusside was made 60 min after mounting on the Ussing chamber. Nitroprusside was found not to stimulate the midgut resting transepithelial potential.

5.2.6 NADPH-diaphorase activity in insect tissues

NADPH diaphorase labelling by tetrazolium is a convenient marker for nitric oxide activity. *Manduca* midgut, brain and ventral nerve chord was isolated from 4th/5th instar moulting larvae approximately 1 h prior to ecdysis or from larvae approximately 12 h after ecdysis. The tissues were fixed, solubilised and probed for NADPH-diaphorase activity as described earlier.

Midgut was found to label positive for NADPH diaphorase activity. Diaphorase activity was most pronounced in the posterior region of the midgut in which colour development was more rapid than in the mid or anterior regions. With more time, however the mid and anterior regions became highly coloured. The dense colouration of the posterior region was at first believed to be due

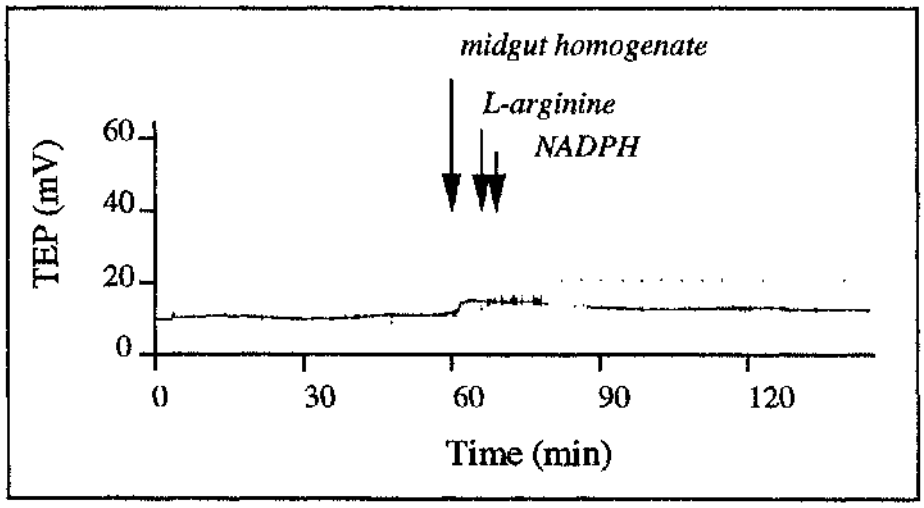

Figure 5.5. Nitric oxide synthase co-factors do not stimulate midgut activity in the presence of 5th instar midgut homogenate. Either nitric oxide is not produced due to lack of nitric oxide synthase or nitric oxide does not stimulate midgut activity

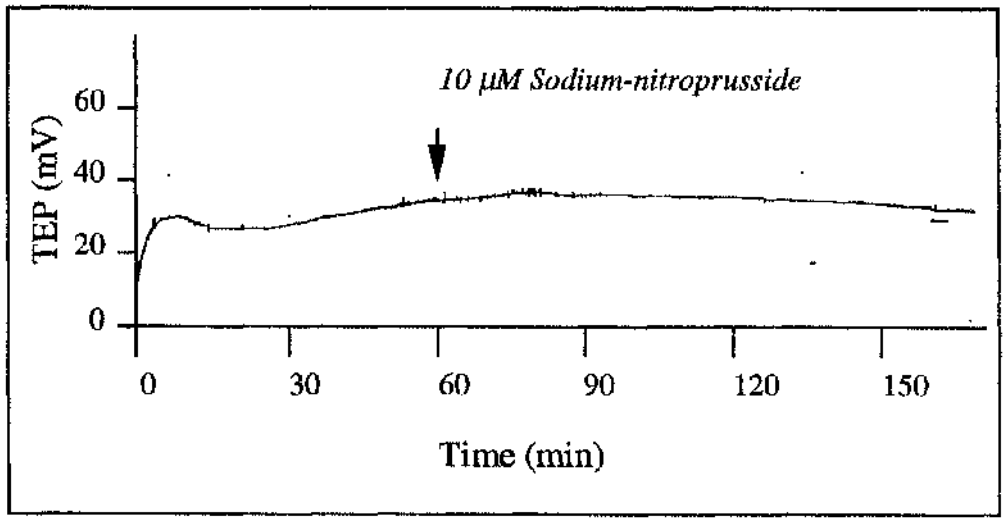

Figure 5.6. 10μM sodium nitroprusside does not stimulate midgutactivity in pre-ecdysis larvae.

to a higher degree of tissue folding. However, there is a high degree of folding in the anterior region but low staining levels suggesting that the staining pattern reflects greater specific diaphorase activity in the posterior midgut.

Nervous tissue was also found to label positive for diaphorase activity. Brain tissue was found to stain homogeneously for diaphorase activity. The ventral ganglia also labelled strongly for diaphorase activity. Labelling was not pronounced in the ventral nerve chord. The intensity of diaphorase activity in the ganglia suggests that NADPH-diaphorase is concentrated in the cell bodies and/or the synapses.

Comparisons in diaphorase labelling patterns were made between 4th/5th instar moulting larvae and 5th instar feeding larvae. There were no obvious differences between the speed of reaction, colour intensity or tissue staining patterns between the two groups. These results suggest that nitric oxide synthase is present in an active form constitutively in these tissues during moulting periods and also intermoult periods.

Control samples were prepared in an identical fashion but without the NADPH in the labelling stage. This protocol resulted in little or no labelling of the tissue. This indicates that colour development is dependent on NADPH diaphorase activity.

5.2.7 NADPH staining of native gel but not SDS gel

For non-denaturing electrophoresis the tissue samples were homogenised and the membrane bound proteins solubilised using triton X-100. The solubilised membranes were applied to a gradient native PAGE gel. Control samples were first denatured by incubation with 0.1% SDS at 95°C for 5 min. Gels were either labelled with bromophenol blue or NADPH+NBT.

Posterior midgut, mid+anterior midgut and ganglia all demonstrated similar NADPH labelling on the native gel. A dark blue band of approximately 30 kDa developed during NADPH+NBT incubation in these tissue samples. This 30 kDa was

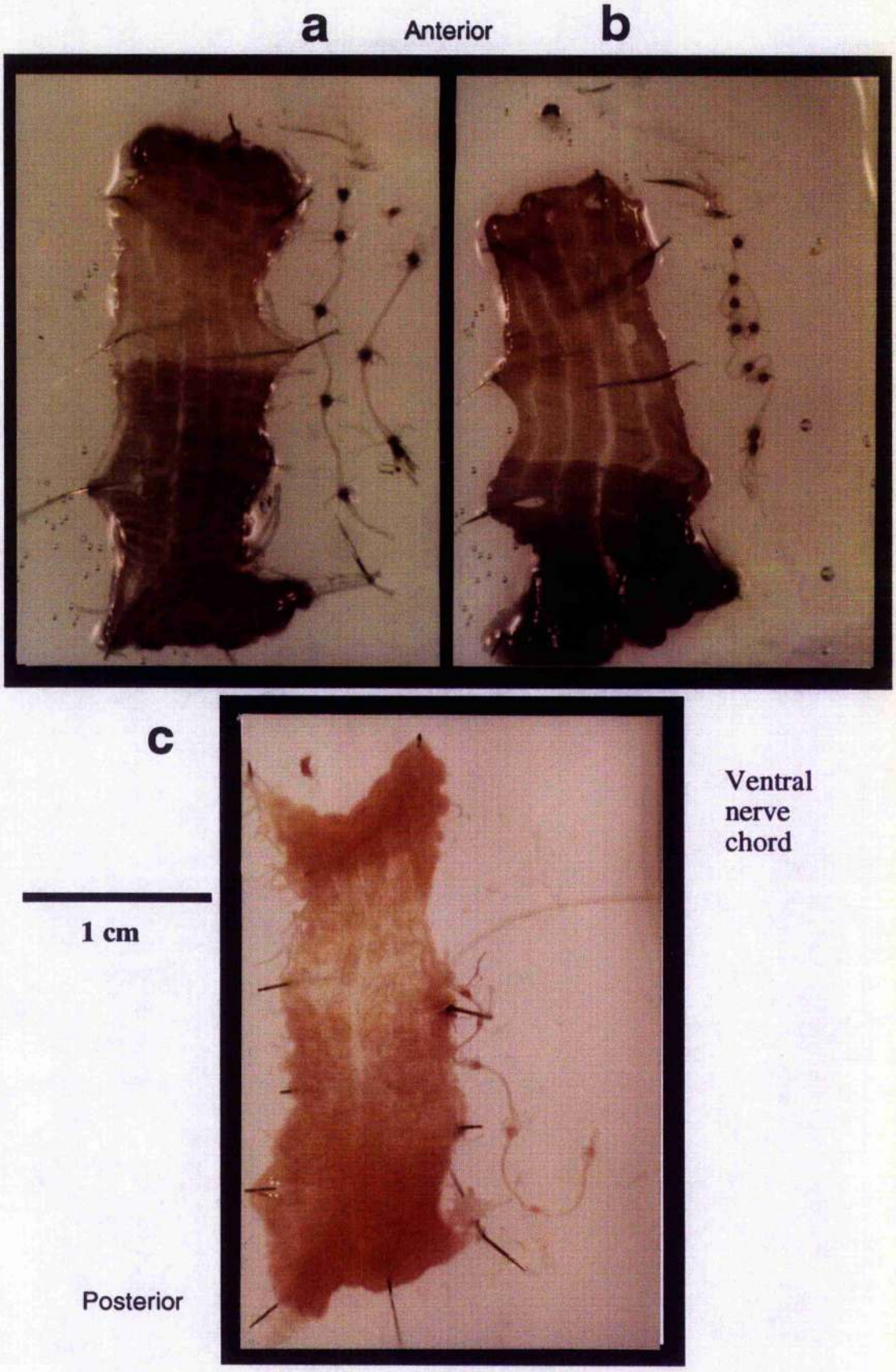

Figure 5.7. NADPH diaphorase labelling of *Manduca* midgut and central nervous system. Midgut isolated from; **a**, pre-ecdysis moulting larva; **b**, 5th instar feeding larva; **c**, Control in absence of NADPH.

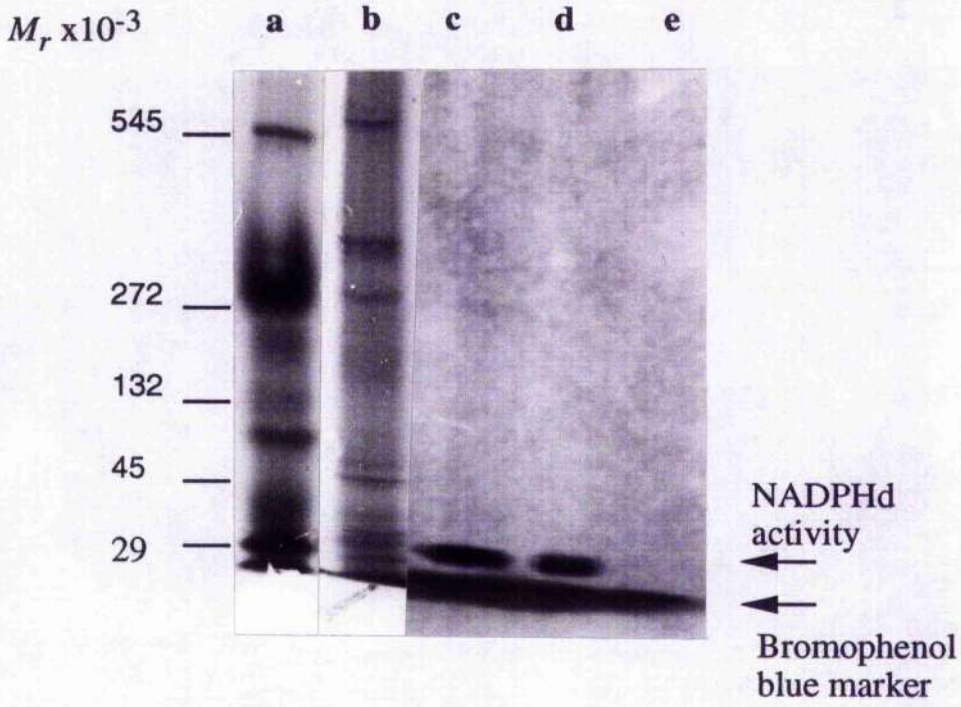

Figure 5.8. NADPH diaphorase labelling of native crude midgut membranes. **a,** Coomassie labelled native molecular weight standards; **b,** Coomassie labelled native detergent soluble midgut fraction; **c,** NADPHd activity on a midgut fraction extracted from 4th instar during larvae during ecdysis; **d,** NADPHd activity on a midgut fraction extracted from feeding 5th instar larvae; **e,** NADPHd activity on native molecular weight standard proteins.

the only band that appeared under these conditions. The standard protein lane acted as an integral control and did not contain any diaphorase activity. Some samples were first denatured by boiling with SDS. Denatured proteins did not develop NADPH mediated NBT bands. This labelling technique was dependent on the protein retaining its native conformation, denaturation resulted in the loss of diaphorase activity.

5.3 Discussion

5.3.1 Ecdysone mediated delay in re-activation

Midguts, once mounted on the chamber, display a bi-phasic decrease in transepithelial voltage and short circuit current. A consistent rapid phase in decline of the TEP occurs for approximately the first 30 minutes after mounting on the chamber. After which the TEP declines at a much slower rate (Wolfersberger, 1982). This slower rate of decline can be all but eliminated using an amino acid supplemented saline solution, resulting in a near steady state baseline activity (Chamberlin, 1990). This stable baseline activity could be maintained for several hours. The pseudo steady state resting potential was interpreted as the true level of activity of the epithelium. As described earlier, the resting potential increases in relation to the time of isolation after ecdysis. Midguts isolated prior to a complete re-activation after the moult will retain a stable, semi-activated base line, even over a matter of hours. This suggests that removal of circulating ecdysone is not sufficient to activate a dormant epithelium. Activation of midgut activity commences upon larval pre-ecdysis behaviour about 1 h prior to ecdysis. Thus the commencement of midgut activation coincides with the release of eclosion hormone (Truman, 1978).

Here, steroid-mediated delay in ecdysis was also found to delay re-activation of the midgut. This effect may be due to a number of phenomena. Firstly, midgut re-activation may be stimulated directly by eclosion hormone. Subsequently a delay in eclosion hormone release would be expected to delay midgut switch on.

Secondly, exogenous ecdysone may interfere with the midgut tissue responsiveness to stimulation.

5.3.2 Control of ion transport by a neurohaemal factor

There is much evidence in the literature that neurohaemal factors regulate physiological processes in insects. Direct transfer of neurosecretion is to specific target organs is widespread in insects. Neurosecretory axons pass directly to the salivary glands in carausis, the spermatheca of *Periplaneta*, the Malphigian tubules of *Rhodnius* and the somatic muscles in several species (Maddrell, 1974). In contrast, specialised neurohaemal organs are involved in hormonal release to the blood and subsequent circulation round the body. For instance, neurohaemal organs are present on the nerves of the peripheral nervous system in the abdomen. The neurosecretory cells branch profusely and the axon endings are devoid of any glial sheath so that they are in direct contact with the haemolymph. Fat body is absent round the neurohaemal organs so that haemolymph can circulate freely over them (Hewes & Truman, 1991). The neurohaemal proctodeal nerves are the primary site of eclosion hormone. In addition, a small amount of eclosion hormone is released by the ventral ganglia and is sufficient to trigger ecdysis. It appears that the major release of eclosion hormone at ecdysis from the proctodeal nerve may be responsible for the regulation of development of the peripheral tissues and not necessarily the specific behaviours of the process of ecdysis (Hewes & Truman, 1991).

5.3.3 Peripheral Effects of Eclosion Hormone

At the adult moult, circulating eclosion hormone has been shown to be responsible for changes in wing cuticle plasticity (Reynolds, 1977) and for the breakdown of the intersegmental muscles (Schwartz & Truman, 1982; Truman, et al., 1980). In the case of larval and pupal moults, effects of systemic eclosion hormone on peripheral tissues, such as the Version's glands has been investigated. Circulating eclosion hormone stimulates Version's gland to secrete "cement" over the newly exposed cuticle. Injection of eclosion hormone stimulates Version's gland secretion

regardless of whether the source was extracts of corpora cardiaca, proctodeal nerve extract or synthetic eclosion hormone (Hewes & Truman, 1991). Whether this is via a direct action of eclosion hormone on the tissue or by indirect action by other hormone(s) released during the course of eclosion hormone action is unknown.

Here proctodeal nerve extract and CNS extract were both found to not stimulate midgut activity. One explanation for this result is that CNS extract may not stimulate the midgut directly. It is conceivable that activation of midgut activity requires input from a variety of sources in addition to neurotransmitters isolated from the CNS and proctodeal nerves. In other words the hormonal melieu found *in vivo* may not have been reproduced *in vitro* on the Ussing chamber.

cAMP and cGMP were found to activate midgut activity prior to ecdysis. Stimulation of midgut activity was most pronounced approximately 1 h prior to ecdysis, when larvae initiated pre-ecdysis behaviour. This coincides with eclosion hormone release. Here it is suggested that the endogenous hormonal activities stimulate midgut activity at ecdysis. These processes may be delayed by treatment with exogenous ecdysone. cAMP stimulates activity during a temporal window prior to and during ecdysis which is similar to that of eclosion hormone.

Modest stimulation of midgut activity by putative secondary messengers has been reported previously. 10 mM caffine was reported to inhibit the SSC of 5th instar larvae by upto 10% (Moffett, 1983), possibly via increased Ca^{2+} levels. In the same report 1 mM, cAMP stimulated transport by 10%, suggesting that the effect of caffine is not via phosphodiesterase inhibition. In contrast the methylxanthine IBMX was found, in the results reported in this thesis, to stimulate midgut activity by 20% at 100 µM. Further investigations into the effect of caffine (Wolfersberger, 1983) found no significant effect on SSC. Studies indicated that the inhibitory effect of caffine may be due to unintentional modification of the bathing soloution pH. Wolfersberger reported that dbcAMP increased SSC of fifth

uinstar larvae in a dose dependent manner. 1 mM dbcAMP was found to increase the SSC of 5th instar larvae by upto 20%.

5.3.4 The hormonal signal does not act via nitric oxide synthase

Direct activation of *Manduca* midgut by NO generated by Na-nitroprusside was found not to occur. This suggests that the hormonal signal involved in activation of TEP generation is not mediated by nitric oxide. Homogenised midguts, in the presence of nitric oxide synthase pathway co-factors did not stimulate midgut, suggesting that either NO has no effect on transport or that NOS was not present in the homogenate and that NO was not produced. In either case we can assume that nitric oxide production does not stimulate midgut transport rates.

The nitric oxide synthase mediated transfer of two electrons from NADPH to tetrazolium dyes has long been used histochemically as a marker for nitric oxide synthase activity (Dawson, et al., 1991; Scherer-Singler, Vincent, Kimura, & McGeer, 1983a). The midgut, in addition to the central nervous system, of *Manduca sexta* displays NADPH dependent diaphorase labelling. Control experiments in which NADPH was omitted also displayed diaphorase activity, albeit at a reduced rate. Native gel electrophoresis of various tissue extracts and subsequent labelling with NADPH and NBT indicated a coloured band of approximately 30 kDa. Nitric oxide synthase has an estimated molecular weight of 160 kDa which is significantly heavier than the band isolated from *Manduca* tissue. The evidence suggests that the diaphorase activity in *Manduca* tissues is not due to nitric oxide synthase. It seems increasingly likely that the NADPH diaphorase labelling found in midgut is not due to the activity of nitric oxide synthase or if nitric oxide synthase is present then it does not affect transport activity.

CHAPTER 6. DISCUSSION

This thesis set out to investigate questions on the regulation of ion transport. Is the K^+ pump of *Manduca* regulated? At what level does regulation occur e.g. at the physiological, cellular or molecular level? What is the mechanism of regulation? Can ion transport be regulated *in vivo*? To answer these questions studies have been made at various stages in the control of transport; these include investigation of the extracellular hormonal activity, the transduction of these hormones by secondary messengers and the mechanism by which V-ATPase energised transport is ultimately regulated.

6.1 Regulation of the K^+ pump of Manduca midgut

The minimum cost of ion transport in the midgut is estimated to be 10% of the larva's total ATP production (Dow & Peacock, 1989a). The aim of such a huge effort is to aid digestion by driving an amino acid co transporter and the generation of an extremely high pH. Periodically the larva enters the moult phase, during which it stops eating. Subsequently there is no food in the gut to digest and, presumably, little requirement for the K^+ pump. During the course of this investigation evidence has been generated that K^+ transport is indeed reversibly switched off during a larval/larval moult and at other times when the gut lumen is empty. In *Manduca*, the duration between the switch 'off' and switch 'on' is many hours and is controlled by long term hormonal signals. The pump is switched off during the first set of hormonal instructions leading to entry into the moult, and is not switched on until a different set of hormones lead to ecdysis and exit from the moult. It seems that once switched off, the pump will not be switched on again until the cell receives a specific signal.

Isolation, purification and analysis of the GCAM provided evidence that the crucial, electrogenic V-ATPase was modified

during the moult. The cytoplasmic, catalytic domain of the molecule was found to be absent from the GCAM when isolated from moulting larvae. Thus it appears that the disassembly of the V-ATPase is a consequence of, or a mechanism for, the inactivation of the V-ATPase and the subsequent shut down of K^+ transport. These results support the hypothesis that proton transport may be regulated by the total number of V_1 catalytic 'heads' that are fused to the endogenous V_o transmembrane pores. This regulation of ratio between naked Vo transmembrane domains and V_oV_1 complexes may occur by a number of mechanisms. V_1V_o complexes may be replaced during periods of inactivity by membrane cycling of predominantly naked V_o domains. Upon re-activation, vesicles containing V_oV_1 complexes may be inserted into the plasma membrane. Alternatively, the V_1 domains may continuously be attaching and detaching to the Vo domains. During periods of inactivation this equilibrium may be forced in the direction of the unattached species.

Subtle differences in the properties and structure within the family of V-ATPases have been recorded. These observations have led to the hypothesis that variations in isoforms of the V-ATPase may constitute the basis for the differential targeting properties and for differential regulation of V-ATPases present in different organelles in the same cell, in different cells or in different organs (Forgac, 1989; Nelson & Taiz, 1989; Wang & Gluck, 1990). It therefore follows that there are a wide number, and combination, of control signals and mechanisms, each of which may have different effects on any one type of V-ATPase and that not every V-ATPase is regulated by the same signal and the same mechanism.

There follows a brief discussion of some of the regulatory signal pathways and control mechanisms that modulate V-ATPase activity and possible applications of this understanding.

6.2 Insect ion transporting epithelia and signal transduction

This thesis has investigated the hormonal regulation of V-ATPase generated ion transport in the midgut. The V-ATPase energises ion transport in most active insect epithelia (Klein, 1992). Many, if not all, insect epithelial active ion transport processes are regulated by endogenous hormones. (Maddrell, 1963). The following insect active transport systems are energised by the V-ATPase and demonstrate various levels of hormonal control.

6.2.1 Hormonal control in salivary glands

Salivary secretions dilute the ingested food and adjust its pH and ionic compound. The watery, alkaline saliva is a vehicle for digestive or lytic enzymes. Secretion is driven by active transport of K^+ which generates a gradient for passive movement of chloride ions and H_2O (Gupta, 1983; Hansen Bay, 1978). The general belief is that active transport is driven across the apical membrane by a V-ATPase due to a cation pump residence at this site (Klein, 1992). 5-hydroxytryptamine (5-HT or serotonin) and cAMP both stimulate fluid secretion by the salivary glands of the blowfly, *Calliphora erythrocephala.* (Hansen Bay, 1978) However, it seems that 5-HT acts upon a chloride channel to enhance chloride permeability. cAMP, on the other hand, appears to enhance the activity of the 'K^+ pump' (Smith & Wendell, 1985).

Nitric oxide (NO) is present in the salivary glands of the blood sucking bug *Rhodnius prolixus.* This acts as a vasodilator and platelet antiaggregating factor during blood feeding (Ribero, Hazzard, Nussezveig, Champagne, & Walker, 1991). Enzymatic and inhibitor studies demonstrate that nitric oxide synthase is present in salivary gland tissues. There is no evidence to distinguish between nitric oxide production for secretion in saliva and nitric oxide as a possible secondary messenger in ion transport regulation in the salivary gland.

6.2.2 Hormonal control in Malpighian tubules

The insect Malpighian tubules are thin, blind ending tubules, originating near the junction of mid and hindgut and are predominantly involved in the regulation of salt, water and nitrogenous waste excretion. The blood sucking insect *Rhodnius prolixus* may raise the rate of fluid secretion by its Malpighian tubules in excess of 1000 times its unstimulated level (Maddrell, 1991). Hormonal regulation of ion transport was first demonstrated by the stimulation of fluid secretion in *Rhodnius* using brain extract (Maddrell, 1963). Diuretic hormone has since been isolated and purified and was found to be a neuropeptide of molecular weight 2 kDa. Abdominal stretch receptors stimulate hormone release into the heamolymph of a fed *Rhodnius. The* effects of diuretic hormone are mimicked by amines such as 5-hydroxytryptamine (5-HT or serotonin) (Maddrell, 1971) and *Rhodnius* Malpighian tubule cells incorporate specific 5-HT (Maddrell, Herman, Mooney, & Overton, 1991b). It is believed that diuretic hormone and 5-HT act synergisticly to promote the high rates of fluid secretion observed (Maddrell, Herman, Farndale, & Riegel, 1991a). Diuretic hormone activity has since been demonstrated on the Malpighian tubules of many insects including *Locusta* (Mordue, 1969), *Pieris brassicae* (Nicholson 1976) and *Manduca sexta.*

Diuretic hormone is transduced in the cell to cAMP since isolated tubules of *Rhodnius* or *carausis* increase their rate of fluid secretion in the presence of 10-100μM cAMP and partially purified diuretic hormone increases intracellular levels of cAMP in *Locusta* within 1 min (Rapheli 1983) (Maddrell, 1971). Various other insect Malpighian tubule systems have been shown to be stimulated by cAMP including *Locusta migratoria* (Mordue 1972), and *Shistocerca gregaria* (Maddrell, 1973).

Recently the Malpighian tubules of *Drosophila melanogaster* have attracted intense scrutiny due to the potential for a molecular genetic approach in which the relevant ion transport and signalling pathway genes are identified, characterised and mutated. *Drosophila* Malpighian tubule secretion is energised by a

V-ATPase, demonstrated by transport inhibition at micromolar concentrations of bafilomycin. Also, in common with other insects, secretion is stimulated by cAMP (Dow, Maddrell, Görtz, Skaer, Brogan, & Kaiser, 1994).

In Malpighian tubules, cAMP is generated in response to brain extract and stimulates fluid transport via a cAMP dependent protein kinase which, presumably, phosphorylates a component if the ion transport system (Dow, et al., 1994). Fluid transport is also stimulated by leukokinins which act via inositol tri-phosphate to elevate calcium levels. Increased calcium levels leads to activation of protein kinase A and increased transport. This stimulation is additive to cAMP mediated stimulation suggesting that the two systems act upon separate distinct components of the transport mechanism.

In addition to these classical secondary messenger systems a new pathway has been elucidated in *Drosophila* tubules. Sodium nitroprusside, which generates intracellular nitric oxide, was found to elevate fluid transport via increased cGMP levels (Dow, et al., 1994). This stimulation could be blocked by methylene blue which prevents NO from stimulating guanylate cyclase. Two cGMP dependent protein kinase (PKG) genes are expressed in tubules which would be required for cGMP mediated phosphorylation of target protein(s). Finally, NADPH labelling suggests the presence of NO synthase. Thus the major elements of the NO-cGMP pathway have been found in insect tissue (Dow, et al., 1994).

D. melanogaster is open to genetic manipulation. Its genome has already been mapped to a very high resolution and many thousands of genes have been identified. Many of the genes involved in the secondary messenger or secretion pathways may have already been sequenced or mutaginised. Genes can be selectively targeted for inactivation by transposon-mediated site directed mutagenesis or site directed expression.

6.3 Regulation of V-ATPases in other systems

6.3.1 Plasmalemma V-ATPase of macrophages

V-ATPases on the plasma membrane of macrophages and neutrophils contribute to cytoplasmic pH homeostasis by extrusion of protons from the cytoplasm to the pericellular environment (Grinstein, et al., 1992). V-ATPase mediated control of cytoplasmic pH is inhibited by a product of L-arginine metabolism. Evidence suggests that the inhibitory metabolite is nitric oxide (NO). Firstly, scavengers of NO such as myoglobin and iron(II) sulphate reverse the inhibition, on the other hand, sodium nitroprusside which spontaneously generates intracellular NO mimicked the inhibition. Sodium nitroprusside was shown to increase cGMP, in turn 8-bromo cGMP was shown to inhibit transport (Grinstein, et al., 1992). These results suggest that, in macrophages, V-ATPase proton transport is inhibited by NO stimulated generation of cGMP. Gram negative, anti-inflammatory, endotoxins are believed to inhibit pump activity in macrophages by the stimulation of generation of NO and consequently the production of cGMP (Grinstein, *et al.*, 1992). On the other hand, the pro-inflammatory cytokine interleukin I enhances V-ATPase transport. These studies demonstrate that an external signal may lead to a modulation in the levels of NO and cGMP and in this way regulate V-ATPase pump activity.

6.4 Control mechanisms of other ion transport systems

6.4.1 Regulation of the F_1F_o ATPases

Unlike the V-ATPase which works in only one direction the F-ATPase catalyses both ATP-driven proton translocation and proton-gradient-driven ATP synthesis. The F_1F_o ATPases are found in the plasma membranes of prokaryotes, the mitochondrial inner membrane of animal cells and in both the chloroplast thylakoid membrane and the mitochondrial inner membrane of

plants. The F-ATPase shares many common features with the V-ATPase (Nelson, 1992). Both F- and V-ATPases are multisubunit protein complexes built of distinct catalytic and membrane sectors. The catalytic sector, F_1, is composed of five different subunits: α, β, γ, δ and ε (Nelson, 1992). The sequences of cDNAs and genes encoding the F-ATPase subunits have been compared with those encoding the V-ATPase subunits. The F-ATPase β and α subunits have homologies with the A ($72x10^3$ M_r) and B ($54x10^3$ M_r) subunits, respectively, of the V-ATPase (Forgac, 1989). The amino acid sequence homologies suggest that the α, β, A and B subunits evolved from a common ancestral gene. The property that separates the F- and V-ATPases into two distinct families of proton pumps is the lack of homology among the C, E, γ, δ and ε subunits. The F_0 proton pore subunit *c* , is similar to the proteolipid of the V-ATPase (Dow, Goodwin, & Kaiser, 1992; Mandel, et al., 1988). It is likely that the ancestral proteolipid was the $8x10^3$ M_r present in all F-ATPases and archaebacterial V-ATPases (Nelson & Taiz, 1989). The proteolipid of eukaryotic V-ATPases evolved by gene duplication of and fusion into a double sized proteolipid (Nelson & Taiz, 1989).

As discussed previously the V-ATPase V_1 domain may be removed from the membrane by incubation with chiatropic ions or cold inactivation by ATP. Similarly The F_1 region may be dissociated from the F_0 by incubation with chiatropic ions. This results in the membrane becoming extremely permeable to protons, via the F_0 proton pore (Nelson, 1992). Therefore, in contrast to the proton-impermeable V_1-depleted membranes, F_1-depleted membranes conduct protons at a rapid rate and proton conduction proceeds trough the F_0. As an F-ATPase control mechanism, dissociation of F_1 from the proteolipid F_0 would result in a rapid collapse of a proton gradient without an associated synthesis of ATP. There is no evidence that the F-ATPases are regulated in this manner, however the structural similarities between F-and V-ATPases lends weight to the argument that F-ATPases may be regulated by dissociation of the F_1 from the F_0.

The F-ATPases are known to be controlled by a regulatory protein that directly inhibits F-ATPase activity. The inhibitor peptide has a M_r of 6000 on SDS gels (Yamada & Huzel, 1988). The inhibitor has a sharp pH dependence with optimal percentage inhibition at pH <6.5. Mitochondrial inhibitor bound to the F_0F_1-ATPase is released when a proton electrochemical gradient favouring ATP synthesis is applied across the membrane (Rouslin, 1987).

6.5 Hormonal regulation and pest control

Williams first suggested (Williams, 1956) that endocrine imbalance might be an effective means for controlling pest insects through the disruption of moulting and metamorphosis. This proposal has been substantiated by the fact that several juvenile hormone analogues are commercially available for the control of flies, mosquitoes, fleas and cockroaches based on disruptions of metamorphosis and reproduction (Kenaga & Morgan, 1978). In Lepidoptera, efficient midgut function is a crucial aspect of the viability of the organism. Precocious or permanent shutdown of gut activity or even delayed return of activity after a moult would have a devastating effect on the larva's viability. It is unlikely that eclosion hormone *per se* could be used as an insecticide; however, an understanding of the biochemical mechanism by which eclosion hormone acts could be applied to insect control.

Neuroendochrine manipulation involves disrupting one or more steps in the hormonal processes of synthesis, secretion, transport, action and degradation. For example, secretion of a neuropeptide could be interfered with by development of an agent to block or over-stimulate at the release site. In *Manduca* the release site has been identified as the proctodeal nerve (Truman & Copenhaver, 1989), a possible target for insecticide action. Alternatively the peptide-mediated response at the target tissue could be blocked or over-stimulated by a peptide mimic that penetrates either the gut or the cuticle. The protein nature of neuropeptides makes them amenable to control using recombinant DNA technology and

genetic engineering. However, neuropeptides produced by transgenic crop plants or bacteria that express neuropeptide genes may be degraded in the gut of pest insects. The use of insect viruses as expression vectors for neuropeptide or 'anti-neuropeptide' genes appears to be more promising for insect control. Transgenic baculoviruses, which infect the midgut epithelium, have been used successfully to infect Lepidoptera and express modified or additional genes. In this way a baculovirus expression vector could be used to interfere with the normal regulation of gut activity.

An advantage of neuroendocrine manipulation is that some neuropeptides may be insect specific and would therefore reduce the deleterious effects on many non target organisms.

6.6 Ion transport and disease

The widespread distribution within and between cells, and the crucial roles that the V-ATPases perform, means that a malfunction in V-ATPase activity, or overall ion transport, can have disastrous consequence (Nelson, 1991).

6.6.1 V-ATPases and osteoclast function

In bone, osteoclasts acidify their pericellular milieu resulting in bone solubilisation and resorption. This process is necessary for bone growth, remodelling and repair. Several clinical conditions involve an abnormal regulation of bone resorption which can lead to local or systemic bone loss. These diseases include bone tumours, osteoporosis and osteoarthritis. The V-ATPase plays a crucial role in the pathology of these diseases (Chatterjee, Chakraborty, Liet, Neff, Jamsakellokumpu, Fuchs, et al., 1992). The osteoclast secretes several proteolytic enzymes, simultaneously, the extracellular pH is lowered by proton extrusion by use of a plasma membrane V-ATPase. The concerted action of the enzymes and the low pH lead to the extracellular digestion of the mineral and organic phases of the bone matrix (Baron, 1989; Blair, Teitelbeum, Ghiselli, & Gluck, 1989). The

control of V-ATPase mediated bone resorption is the subject of much scrutiny. The V-ATPase of osteoclast plasma membrane appears to have its own unique properties. It is sensitive to vanadate and furthermore two distinct isoforms of V-ATPase subunits *A* and *B* have been isolated (Chatterjee, et al., 1992). Strategies for the control of the osteoclast plasma membrane V-ATPase are important for the control of the level of bone absorption.

6.6.2 V-ATPases and kidney function

One of the most important functions of the kidney is to reclaim bicarbonate from the urine. This is achieved by the secretion of hydrogen ions, which leads to bicarbonate reabsorption and acid excretion. In this way the kidney maintains acid-base homeostasis. The V-ATPase plays a pivotal role in this process (Gluck & Nelson, 1992). In summary, (for review see (Gluck & Nelson, 1992) a Na^+/H^+ antiporter and the V-ATPase secrete H^+ which titrates the bicarbonate to carbonic acid. The carbonic acid is dehydrated on the brush border to CO_2 and H_2O by carbonic anhydrase. CO_2 may diffuse into the epithelium where it combines with OH^- (with help from carbonic anhydrase) to form bicarbonate and is re-absorbed. The H_2O is excreted. Over stimulated H^+ secretion will drive uptake of bicarbonate and impair the capacity to excrete excess bicarbonate. This may produce elevated serum bicarbonate concentrations (alkalosis).

Much of the observed hormonal regulation of ion transport in kidney is enforced upon the Na^+/H^+ antiporter, however regulatory factors have been identified that act on the V-ATPase. The kidney cytoplasm has been found to contain both V-ATPase activity activator and inhibitor proteins (Zhang, Wang, & Gluck, 1992b). The inhibitor protein has a Mr of 6300, similar to that of the F-ATPase inhibitor. The inhibitor protein inhibits renal microsomal V-ATPase by 70% and has a partial inhibitory effect on the F_0F_1 ATPase (Zhang, et al., 1992b). The regulation of the V-ATPase inhibitor appears to be pH dependent , with the greatest inhibition in alkaline conditions. The physiological regulation of H^+ secretion is also maintained by the microtubule dependent

redistribution of vesicles incorporating V-ATPase molecules to the plasma membrane (Brown, Sabolic, & Gluck, 1991a).

6.6.3 V-ATPases and cystic fibrosis

Cystic fibrosis is associated with a defect in a cAMP activated chloride channel in secretary epithelia which leads to decreased fluid secretion. In addition, the pH of intracellular organelles is more alkaline in cystic fibrosis cells due to a defective chloride channel in the vesicle membranes (Al-Awqati, Barasch, & Landry, 1992). Unaffected vesicles are normally acidic due to active transport of protons by a V-ATPase and subsequent charge balance by chloride via the chloride channel. In the absence of a functional chloride channel H^+ is transported in and rapidly forms a large membrane potential, this membrane potential limits further proton pumping and inhibits the generation of a large pH gradient. The absence of a low pH will have deleterious effects to pH dependant reactions such as modifications to secretary proteins. The increased pH in cystic fibrosis vesicles increases the level of sulfation and fucosylation and decreases the level of sialation within the vesicle lumen (Al-Awqati, et al., 1992). These alterations may alter the characteristics of the proteins within the vesicle. Cystic fibrosis is an example of an ailment where the overall consequences of the V-ATPase are disabled.

The cause of many diseases associated with the V-ATPase may not be a direct consequence of a malfunctioning V-ATPase, however the therapeutic regulation of the V-ATPase may alleviate the symptoms. The V-ATPases, although one family, have many structural variations and are regulated by many signals and mechanisms. These properties suggest that therapy may be targeted to selected classes of problematic V-ATPases.

6.7 Conclusions and Future prospects

This thesis has described a predictable and reversible modulation in the ion transporting activity of a V-ATPase and an associated loss of the catalytic domain of the enzyme. The ease of manipulation and extreme shift in activity conspire to make the K^+ transport system an ideal model for future investigation into the regulation of the V-ATPases and ion transport in general. In *Manduca* the V-ATPase is influenced by regulatory mechanisms, the consequence of which is the loss, and return of ion transport and ATPase activity.

The regulation of ion transport in *Manduca* provides a convenient model for the study of the cellular processes between the reception of a hormonal signal and modulation of ion transport. Using ion transport as a physiological marker, one can study the intracellular mechanisms of both steroid and peptide hormones. The intracellular secondary signals, gene expression and phosphorylation events are yet to be elucidated, and are exciting avenues for future investigations into the mechanism of hormonal transduction.

The modification to the V-ATPase that causes the disassembly of the enzyme is not entirely obvious. The timecourse of the switch from 'on' to 'off' or vice-versa is fairly rapid, occurring over a period of about 4 h. The range of mechanisms for the dis/re-assembly of the V-ATPase remains wide. Possible mechanisms include: cellular re-distribution of enzyme subunits or V_1 domains; (de)phosphorylation events leading to modification of the affinity between V_0 and V_1 domains; modulated expression of V_1 subunits/domains; or activation of inhibitor/activator proteins. The ability to control the activity of the V-ATPase *in vitro* and eventually *in vivo* is undoubtedly one of the goals of researchers of this important molecule. I hope that studies of the V-ATPase of *Manduca* will contribute to the realisation of this goal.

CHAPTER 7
REFERENCES

Adachi, I., Puopolo, K., Marquez-Sterling, N., Arai, H., & Forgac, M. (1990). J.Biol.Chem., 265, 967-973.

Adang, M. J., Spence, K.D. (1982). Biochemical comparisons of the peritrophic membranes of the lepidopterans Orgyia pseudotsugata and Manduca sexta. . Comp.Biochem.Physiol. , 73B, 645-649.

Adang, M. J., & Spence, K. D. (1981). Surface morphology of peritrophic membrane formation in the cabbage looper. Cell and Tissue Research, 218, 141-147.

Al-Awqati, Q., Barasch, J., & Landry, D. (1992). Chloride channels of intracellular organelles and their potential role in cystic fibrosis. J. Exp. Biol., 172, 245-266.

Anderson, E., & Harvey, W. R. (1966). Active transport in the Cecropia midgut II. Fine structure of the midgut epithelium. J.Cell Biol., 31, 107-134.

Aris, J. P., Klionsky, D. J., & Simoni, R. D. (1985). J. Biol. Chem., 260, 11207-11215.

Ashburner, M., Chihara, C., Meltzer, P., & Richards, G. (1974). Temporal control of puffing activity in polytene chromosomes. Cold Spring Harbour Symp. Quant. Biol., 38, 655-662.

Baldwin, K. M., & Hakim, R. S. (1981). Freeze fracture analysis of gap and septate junctions in embryos of a moth (lepidoptera). Tissue and Cell, 13, 691-699.

Baldwin, K. M., & Hakim, R. S. (1991). Growth and differentiation of the larval midgut epithelium during molting in the moth, *Manduca sexta*. Tissue & Cell, 23, 411-422.

Baron, R. (1989). Molecular mechanisms of bone resorption by the osteoclast. Anat. Rec., 224, 317-324.

Blair, H. C., Teitelbeum, S. L., Ghiselli, R., & Gluck, S. (1989). osteoclastic bone resorption by a polarised vacuolar proton pump. Science, 245, 855-857.

Bollenbacher, W. E., Agui, N., Granger, N. A., & Gilbert, L. I. (1979). In vitro activation of insect prothoracic glands by the prothoracicotropic hormone. Proceedings of the National Academy of Science., 76, 5148-5152.

Bollenbacher, W. E., Smith, S. L., Goodman, W., & Gilbert, L. I. (1981). Ecdysteroid titer during larval-pupal-adult development of the tobacco hornworm, *Manduca sexta*. Gen. Comp. Endochrin., 44, 302.

Bowman, B. J., Bowman, E. J., Allen, R., & Wechser, M. A. (1988a). Isolation of genes encoding the *Neurospora* vacuolar ATPase - analysis of Vma-2 encoding the 57-kDa polypeptide and comparison to Vma-1. J.Biol.Chem., 263(28), 4002-4007.

Bowman, E. J., Altendorf, K., & Siebers, A. (1988b). Bafilomycins - A class of inhibitors of membrane ATPases from microorganisms, animal cells, and plant cells. PNAS, 85, 7972-7976.

Bowman, E. J., & Bowman, B. J. (1988). Purification of Vacuolar Membranes, Mitochondria, and Plasma-Membranes from Neurospora-Crassa and Modes of Discriminating Among the Different H^+-Atpases. In Methods In Enzymology, 25, p100-105.

Brown, D., Hirsch, S., & Gluck, S. (1988). An H^+ -ATPase is Inserted into Opposite Plasma membrane Domains in Subpopulations of Kidney epithelial Cells. Nature, 331, 622-624.

Brown, D., Sabolic, I., & Gluck, S. (1991a). Colchicine-induced redistribution of proton pumps in kidney epithelial cells. Kidney International, 40(Suppl. 33), S79-S83.

Brown, D., Sabolic, I., & Gluck, S. (1991b). Colchicine-induced Redistribution of Proton Pumps in Kidney Epithelial Cells. Kidney International, 40(Suppl. 33), S79-S83.

Chamberlin, M. E. (1989). Metabolic stimulation of transepithelial potential difference across the midgut of the tobacco hornworm Manduca sexta. J. exp. Biol., 141, 295-311.

Chamberlin, M. E. (1990). Ion transport across the midgut of the tobacco hornworm (Manduca sexta). Journal of Experimental Biology, 150, 425-442.

Chao, A. C., Moffett, D. F., & Koch, A. (1991). Cytoplasmic pH and goblet cavity pH in the posterior midgut of the tobacco hornworm Manduca sexta. Journal of Experimental Biology, 155, 403-414.

Chatterjee, D., Chakraborty, M., Liet, M., Neff, L., Jamsakellokumpu, S., Fuchs, R., Bartkiewicz, M., Hernando, N., & Baron, R. (1992). The osteoclast proton pump differs in its pharmacology and catalytic subunits from other Vacuolar H^+ ATPases. J. Exp. Biol., 172, 193-204.

Cioffi, M. (1979). The morphology and fine structure of the larval midgut of a moth (*Manduca sexta*) in relation to active ion transport. Tissue Cell, 11, 467-479.

Cioffi, M. (1984). Comparative ultrastructure of arthropod transporting epithelia. . Amer.Zool. , 24, 139-156.

Cioffi, M., & Harvey, W. R. (1981). Comparison of K^+ transport in three structurally distinct regions of the insect midgut. J. exp. Biol., 91, 103-116.

Cioffi, M., & Wolfersberger, M. G. (1983). Isolation of separate apical, lateral and basal plasma membrane from cells of an insect epithelium. A procedure based on tissue organization and ultrastructure. Tissue & Cell, 15, 781-803.

Copenhaver, P. F., & Truman, J. W. (1982). The role of eclosion hormone in the larval ecdyses of *Manduca sexta*. J. Insect. Physiol., 28(8), 695-701.

Cross, R. L. (1981). The mechanism and regultion of ATP synthesis by the F_1 ATPases. Annu. Rev. Biochem., 50, 681-714.

Curtis, A. T., Hori, M., Green, J. M., Wolfgang, W. J., Hiruma, K., & Riddiford, L. M. (1984). Ecdysteroid regulation of the onset of cuticular melanizationin allatectomized and *black* mutant *Manduca sexta* larvae. J. Insect Physiol., 30, 597-606.

Dahlman, D. L., & Herald, F. (1971). Effects of the parasite, *Apanteles congregatus*, on respiration of tobacco hormworm, *Manduca sexta*. Comp. Biochem. Physiol., 40A, 871-880.

Darnell, J., Lodish, H., & Baltimore, D. (1986). Molecular Cell Biology. Scientific American Books, Inc.

Dawson, T. M., Bredt, D. S., Fotuhi, M., Hwang, P. M., & Snyder, S. H. (1991). Nitric oxide synthase and neuronal NADPH diaporase are identical in brain and peripheral tissues. Proc. Natl. Acad. Sci., 88, 7797-7801.

Dow, J. A. T. (1984). Extremely high pH in biological systems: a model for carbonate transport. American Journal of Physiology, 246, R633-R635.

Dow, J. A. T. (1992). pH Gradients in Lepidopteran Midgut. J.exp.Biol., 172, 355-375.

Dow, J. A. T., Boyes, B., Harvey, W. R., & Wolfersberger, M. G. (1985). An improved chamber for the short-circuiting of epithelia. J.exp.Biol., 116, 685-689.

Dow, J. A. T., Goodwin, S. F., & Kaiser, K. (1992). Analysis of the gene encoding a 16-kD proteolipid subunit of the vacuolar H^+-ATPase from *Manduca sexta* midgut and tubules. Gene, In press.

Dow, J. A. T., Gupta, B. J., Hall, T. A., & Harvey, W. R. (1984). X-ray microanalysis of elements in frozen hydrated sections of an electrogenic K+ transport system: the posterior midgut of tobacco hornworm (Manduca sexta) in vivo and in vitro. Journal of Membrane Biology, 77, 223-241.

Dow, J. A. T., & Harvey, W. R. (1988). The role of midgut electrogenic K^+ pump potential difference in regulating lumen K^+ and pH in larval lepidoptera. J. exp. Biol., 140, 455-463.

Dow, J. A. T., Maddrell, S. H. P., Görtz, A., Skaer, N. J. V., Brogan, S., & Kaiser, K. (1994). The Malpighian tubules of Drosophila melanogaster: a novel phenotype for studies of fluid secretion and its control. J. Exp. Biol., 197(In Press).

Dow, J. A. T., & O'Donnell, M. J. (1990). Reversible alkalinization by *Manduca sexta* midgut. J.exp.Biol., 150, 247-256.

Dow, J. A. T., & Peacock, J. M. (1989a). Microelectrode evidence for the electrical isolation of goblet cavities of the middle midgut of *Manduca sexta*. J.exp.Biol., 143, 101-114.

Dow, J. A. T., & Peacock, J. M. (1989b). pH 12: how might it be acheived by electrogenic K+ transport? In D. Keeling Benham, C. (Eds.), p. 300

Endo, Y., Nishiitsutsuji-Uwo, J. (1981). Gut endocrine cells in insects: the ultrastructure of the gut endocrine cells of the lepidopterous species. . Biomed.Res. , 2, 270-280.

Finbow, M. E., Eliopoulos, E. E., Jackson, P. J., Keen, J. N., Meagher, L., Thompson, P., Jones, P., & Findlay, J. B. C. (1992). Structure of a 16 kDa integral membrane protein that has identity to the putative proton channel of the vacuolar H^+-ATPase. Protein Engineering, 5(1), 7-15.

Finbow, M. E., Goodwin, S. F., Meagher, L., Lane, N. J., Keen, J., Findlay, J. B. C., & Kaiser, K. (1994). Evidence that the 16 kDa proteolipid (subunit c) of the vacuolar H+ ATPase and ductin from gap junctions are the same polypeptides in *Drosophila* and *Manduca*: molecular cloning of the Vha 16k gene from *Drosophila*. Journal Cell Science., 107, 1817-1824.

Florkin, M., Jeuniaux, C. (1974). Hemolymph: composition. vol. 5 . In M. Rockstein ed. (Eds.), Physiology of the Insecta (pp. 255-30).

Flower, N. E., & Filshie, B. K. (1976). Goblet cell membrane differentiations in the midgut of a lepidopteran larva. J.Cell Sci., 20, 357-375.

Forgac, M. (1989). Structure and function of vacuolar class of ATP-driven proton pumps. Physiol. Rev., 69, 765-796.

Gilbert, L. I., Combest, W. L., Smith, W. A., Meller, V. H., & Rowntree, D. B. (1988). Neuropeptides, second messengers, and insect moulting. Bioessayes, 8, 153-158.

Giordana, B., Parenti, P., Hanozet, G. M., & Sacchi, V. F. (1985). Electrogenic K+ -base amino acid cotransport in the midgut of lepidopteran larvae. J.Membrane Biol., 88., 45-53.

Giordana, B., Sacchi, F. V., & Hanozet, G. M. (1982). Intestinal amino acid absorption in lepidopteran larvae. Biochim.Biophys.Acta, 692., 81-88.

Gluck, S., & Nelson, N. (1992). The role of the V-ATPase in renal epithelial H^+ transport. J. Exp. Biol, 172, 205-218.

Gluck, S. L., Nelson, R. D., Lee, B. S., Wang, Z.-Q., Guo, X.-L., Fu, J.-Y., & Zhang, K. (1992). Biochemistry of the Renal V ATPase. Journal of Experimental Biology, 172, 219-229.

Gräf, R., Novak, F. J. S., Harvey, W. R., & Wieczorek, H. (1992). Cloning and sequencing of cDNA encoding the putative insect plasma membrane V-ATPase subunit A. FEBS Lett., 119-122.

Grinstein, S., Nanda, A., Lukacs, G., & Rotstein, O. (1992). V-ATPases in Phagocytic Cells. Journal of Experimental Biology, 172, 179-192.

Gullan, P. J., & Cranston, P. S. (1994). The Insects: An Outline of Entomology. London: Chapman & Hall.

Gupta, B. L., Hall, T.A. (1983). Ionic distribution in dopamine-stimulated NaCl-fluid secreting cockroach salivary glands. Am.J.Physiol. 244, R176-R186.

Gurch, R. W., & DuBose Jr, T. D. (1989). Heterogeneity of cAMP effect on endosomal proton transport. Am. j. Physiol, 257, F777-F784.

Gurich, R. W., Codina, J., & DuBose Jr, T. D. (1991). A Potential Role for Guanine Nucleotide-Binding Protein in the Regulation of Endosomal Proton Transport. Journal Clinical Investigation, 87, 1547-1552.

Hakim, R. S., Baldwin, K. M., & Bayer, P. E. (1988). Cell differentiation in the embryonic midgut of the tobacco hornworm, *Manduca sexta*. Tissue & Cell, 20, 51-62.

Hansen Bay, C. M. (1978). The secretion and action of the digestive enzymes of the blowfly, Calliphora. . J.Insect Physiol., 24, 141-149.

Harvey, W. R., Haskell, J.A., Zerahn, K. (1967). Active transport of potassium and oxygen consumption in the isolated midgut of H.c. ecropia. J.exp.Biol., 46, 235-248.

Harvey, W. R. (1980). Water and ions in the gut. In M. Locke & D. S. Smith (Eds.), VBW 80: Insect biology in the future (pp. p. 105-12). London: Academic.

Harvey, W. R., Cioffi, M., Dow, J. A. T., & Wolfersberger, M. G. (1983a). Potassium ion transport ATPase in insect epithelia. Journal of Experimental Biology, 106, 91-117.

Harvey, W. R., Cioffi, M., & Wolfersberger, M. G. (1983b). Chemiosmotic potassium ion pump of insect epithelia. American Journal of Physiology, 244, R163-R175.

Harvey, W. R., & Nedergaard, S. (1964). Sodium-independent active transport of potassium in the isolated midgut of the cecropia silkworm. PNAS, 51, 757-765.

Harvey, W. R., & Zehran, K. (1972). Active transport of potassium and other alkali metals by the isolated midgut of the silkworm. Curr. Top. Membr. Tranp., 3, 367-410.

Hewes, R. S., & Truman, J. W. (1991). The roles of central and peripheral eclosion hormone release in the control of ecdysis behavior in *Manduca sexta*. j. Comp. Physiol. A., 168, 697-707.

Hinkle, P. C., & McCarty, R. E. (1978). How cells make ATP. Sci. Am., 238(3), 104-123.

Jungreis, A. M., & Vaughn, G. L. (1977). Insensitivity of lepidopteran tissues to ouabain: absence of ouabain binding and

Na^+, K^+ ATPases in larval and adult midgut. J.Insect Physiol., 23, 503-509.

Kane, P. M., Kuehn, M. C., Howald-Stevenson, I., & Stevens, T. H. (1992). Assembly and Targeting of Peripheral and Integral Membrane Subunits of the Yeast Vacuolar H+ ATPase. Journal of Biological Chemistry, 267(1), 447-454.

Kenaga, E. E., & Morgan, R. W. (1978). Commercial and experimental organic insectisides. Ent. Soc. Am., 78-1, 1-79.

Klein, U. (1992). The Insect V-ATPase, A plasma membrane proton pump energizing secondary active transport; immunological evidence of a V-ATPase in insect ion-transporting epithelia. J.exp.Biol., 172, 345-354.

Klein, U., Löffelmann, G., & Wieczorek, H. (1991). The midgut as a model system for insect K^+-transporting epithelia: immunocytochemical localization of a vacuolar-type H^+ pump. J.exp.Biol., 161, 61-75.

Klein, U., Weerth, S., & Wieczorek, H. (1988). Proton transport and proton ATPase in K^+-transporting plasma membranes of Manduca sexta midgut epithelium. Verh. Dtsch. Zool. Ges., 81,.

Klein, U., & Zimmermann, B. (1991). The vacuolar-type ATPase from insect plasma membrane: immunocytochemical localization in insect sensilla. Cell Tissue Res., 266, 265-273.

Kopec, S. (1917). Experiments on metamorphosis of insects. Bull. Int. Acad. Cracovie., B, 57-60.

Kyte, J. (1981). Molecular considerations relevant to the mechanism of active transport. Nature, 292, 201-204.

Lincoln, T. M., & Cornwell, T. L. (1993). Intracellular cGMP-dependent receptor proteins. FASEB, 7, 328-338.

MacLennan, D. H., Brandl, C. J., Korczak, B., & Green, N. M. (1985). Ammino -acid sequence of a Ca2+, Mg2+-dependent ATPase from rabbit muscle sarcoplasmic reticulum, deduced from its complimentary DNA sequence. Nature(316), 696-700.

Maddrell, S. H. P. (1963). Excretion in the blood sucking bug, Rhodnius prolixus. The control of diuresis. J. Exp Biol., 40, 247-256.

Maddrell, S. H. P. (1971). The mechanisms of insect excretory systems. Adv.Insect Physiol., 8, 199-331.

Maddrell, S. H. P., Klunsuwan, S. (1973). Fluid secretion by in vitro preparations of the Malpighian tubules of the desert locust Schistocerca gregaria. . J.Insect Physiol. , 19, 1369-1376.

Maddrell, S. H. P. (1974). Neurosecretion. Amsterdam.: North -Holland Publishing Co.

Maddrell, S. H. P. (1991). The fastest fluid-secreting cell known: the upper Malpighian tubule cell of Rhodnius. Bio Essays, 13, 357-362.

Maddrell, S. H. P., Herman, W. S., Farndale, R. W., & Riegel, J. A. (1991a). Synergism of hormones controlling epithelial fluid transport in an insect. JEB, 174, in press.

Maddrell, S. H. P., Herman, W. S., Mooney, R. L., & Overton, J. A. (1991b). 5-hydroxytryptamine: a second diuretic hormone in *Rhodnius prolixus*. JEB, 156, 557-566.

Mandel, L. J., Riddle, T.G., Storey, J.M. (1980). Role of ATP in respiratory control and active transport in tobacco hornworm midgut. Am.J.Physiol. 238, C10-C14.

Mandel, M., Moriyama, Y., Hulmes, J. D., Pan, Y. E., Nelson, H., & Nelson, N. (1988). cDNA sequence encoding the 16kD

proteolipid of chromaffin granules implies gene duplication in the evolution of H^+ATPases. Proc. Nat. Acad. Sci., 85, 5521-5524.

Moffett, D. F., Smith, C.J., Green, J.M. (1983). Effects of caffeine, cAMP and A23187 on ion transport by the midgut of tobacco hornworm. . Comp.Biochem.Physiol. , 75C, 305-310.

Moffett, D. F., Hudson, R. L., Moffett, S. B., & Ridgeway, R. L. (1982). Intracellular K+ activities and cell membrane potentials in a K+-transporting epithelium, the midgut of the tobacco hornworm, (Manduca sexta). Journal of Membrane Biology, 70, 59-68.

Moffett, D. F., & Koch, A. (1991). Lidocane and barium distinguish separate routes of transbasal K+ uptake in The posterior midgut of the tobacco hornworm (*Manduca sexta*). Journal of Experimental Biology, 157, 243-256.

Moffett, D. F., & Koch, A. R. (1988). Electrophysiology of K^+ transport by midgut epithelium of lepidopteran insect larvae I. The transbasal electrochemical gradient. J.exp.Biol., 135:, 25-38.

Moncada, S., Palmer, J. M. R., & Higgs, E. A. (1991). Nitric oxide: physiology, pathophysiology, and pharmacology. Pharmacol. Rev., 43, 109-142.

Mordue, W. (1969). Hormonal control of Malpighian tube and rectal function in the desert locust, Schistocerca gregaria. . J.Insect Physiol. , 15, 273-285.

Morton, D. B., & Truman, J. W. (1985). Steroid regulation of the peptide- mediated increase in cyclic GMPin the nervous system of the hawkmoth, *Manduca sexta*. J. Comp. Physiol., A. 157, 423-432.

Morton, D. B., & Truman, J. W. (1988a). The eclosion hormone and cyclic GMP regulated phosphoproteins. I. Appearance and

partial charicterization in the CNS of *Manduca sexta*. J. Neurosci., 8, 1326-1337.

Morton, D. B., & Truman, J. W. (1988b). The EGPs- the eclosion hormone and cyclic GMP regulated phosphoproteins. II. regulation of appearence by the steroid hormone 20-hydroxyecdysone in *Manduca sexta*. J Neurosci., 8, 1338-1345.

Morton, D. B., & W., T. J. (1986). Substrate phosphoprotein availability regulates eclosion hormone sensitivity in an insect CNS. Nature, 323, 264-267.

Nanda, A., & Grinstein, S. (1991). Protein kinse C activates an H+ (equivalent) conductance in the plasma membrane of human neutrophils. Proc. Natl. Acad. Sci, 88, 10816-10820.

Nedergaard, S. (1977). Amino acid transport. In R. B. M. B.L. Gupta J.L. Oschman, B.J. Wall (Eds.), Transport of ions and water in animals (pp. 239-264). London: Academic.

Nelson, H., Mandiyan, S., Noumi, T., Moriyama, Y., Miedel, M. C., & Nelson, N. (1990). Molecular cloning of cDNA encoding the C-subunit of H^+-ATPase from bovine chromaffin granules. Journal Of Biological Chemistry, 265(33), 20390-20393.

Nelson, H., & Nelson, N. (1989). The progenitor of ATP synthases was closely related to the current vacuolar H^+-ATPase. FEBS Letters, 247(1), 147-153.

Nelson, H., & Nelson, N. (1990). Disruption of genes encoding subunits of yeast vacuolar H^+ ATPase causes conditional lethality. PNAS, 87(9), 3503-3507.

Nelson, H., Nelson, N., & Mandiyan, S. (1989). A Conserved Gene Encoding the 57-kDa Subunit of the Yeast Vacuolar H^+-ATPase. Journal Of Biological Chemistry, 264(3), 1775-1778.

Nelson, N. (1991). Structure and pharmacology of the proton-atpases. Trends In Pharmacological Sciences, 12(2), 71-75.

Nelson, N. (1992). The vacuolar H^+ ATPase- one of the most fundamental ion pumps in nature. J. Exp. Biol., 172, 19-27.

Nelson, N., & Taiz, L. (1989). The evolution of H^+-ATPases. Trends In Biochemical Sciences, 14(3), 113-116.

Puopolo, K., & Forgac, M. (1990). Functional Reassembly of the Coated Vesicle Proton Pump. Journal of Biological Chemistry., 265(25), 14836-14841.

Reynolds, S. E. (1977). Control of cuticle extensibilty in the wings of adult *Manduca* at the time of eclosion: effects of eclosion hormone and busicon. J. Exp. Biol., 70, 27-39.

Ribero, J., Hazzard, J., Nussezveig, R. H., Champagne, D. E., & Walker, F. A. (1991). Atrial natriuretic fctor and related peptide hormones. Science, 260, 539-541.

Riddiford, L. M. (1986). Hormonal control of sequential gene expression in insect epidermis. New York: Alan R. Liss.

Ridgway, R. L., & Moffett, D. F. (1986). Regional differences in the histochemical localization of carbonic anhydrase in the midgut of tobacco hornworm (*Manduca sexta*). J.exp.Zool., 237, 407-412.

Rouslin, W. (1987). J. Biol. Chem., 262, 3472-3476.

Russel, V. W., & Dunn, P. E. (1991). Lysosyme in the midgut of Manduca sexta during metamorphosis. Arch. Insect Biochem. Physiol., 17, 67-80.

Scherer-Singler, U., Vincent, S. R., Kimura, H., & McGeer, E. G. (1983a). Demonstration of a unique population of neurones with NADPH-Diaphorase activity. J. Neuroscience Methods, 9, 229 234.

Scherer-Singler, U., Vincent, S. R., Kimura, H., & McGeer, E. G. (1983b). Demonstration of a unique population of neurones with NADPH-diaphorase histochemistry. Journal of Neuroscience Methods, 9, 229-234.

Schwartz, L. M., & Truman, J. W. (1982). Peptide and steroid regultion of muscle degenerationin an insect. Science., 215, 1420-1421.

Schweikl, H., Klein, U., Schindlebeck, M., & Wieczorek, H. (1989). A vacuolar-type ATPase, partially purified from potassium transporting plasma membranes of tobacco hornworm midgut. J.Biol.Chem., 264,, 11136-11142.

Shull, G. E., Schwartz, A., & Lingrel, J. B. (1985). Amino acid sequence of the catalytic subunit of the (Na+- K+) ATPase deduced from a complimentary DNA. Nature, 316, 691-695.

Slama, K. (1980). Homeostatic function of ecdysteriods in ecdysis and oviposition. Acta Ent Bohemoslovaca, 77, 145.

Smith, W. A. (1993). Second messengers and the action of Prothoracicotropic hormone in *Manduca sexta*. American Zoologist, 33, 330-339.

Smith, W. A., & Wendell, L. C. (1985). Role of cyclic nucleotides in hormone action. In K. G. A. & L. I. Gilbert (Eds.), Comprehensive Insect Physiology, Biochemistry and Pharmacology (pp. 263-287). Oxford: Pergamon Press.

Steel, C. G. H., & Davey, K. G. (1985). Integration in the insect endocrine system. In G. A. Kerkut & L. I. Gilbert (Eds.), Comprehensive Insect Physiology, Biochemistry and Pharmacology. (pp. 1-35). Oxford: Pergamon Press.

Truman, J. W. (1971). Physiology of insect ecdysis. I. The eclosion behaviour of saturniid moths and its hormonal release. J. Exp. Biol., 54, 805.

Truman, J. W. (1976). Development and hormonal release of adult behavior patternsin silkmoths. J. Comp. Physiol., A 107, 39.

Truman, J. W. (1978). Hormonal release of steryotyped motor programmes from the isolated nervous tissue of the Cecropia silkmoth. J. Exp. Biol., 74, 151.

Truman, J. W., & Copenhaver, P. F. (1989). The larval eclosion neurones in Manduca sexta: Identification of the brain-proctodeal neurosecretory system. J. Exp. Biol., 147, 457-470.

Truman, J. W., Rowntree, D. B., Reiss, S. E., & Schwartz, L. M. (1983). Ecdysreriods regulate the release and action of eclosion hormone in the tobacco hornworm, *Manduca sexta*. J. Insect Physiol., 29, 895.

Truman, J. W., Taghert, P. H., Copenhaver, P. F., Tublitz, N. J., & Schwartz, L. M. (1981). Eclosion hormone may control all ecdyses in insects. Nature, 291, 70.

Truman, J. W., Taghert, P. H., & Reynolds, S. E. (1980). Physiology of the pupal ecdyses in the tobacco hornworm Manduca sexta. I. Evidence for contropl by ecloson hormone. J. Exp. Biol., 88, 327-337.

Turbeck, B. O. (1974). A study of the concentrically-laminated concretions, "spherites", in the regenerative cells of the midgut of lepidopterous larvae. . Tissue Cell , 6, 627-640.

Wang, Z.-Q., & Gluck, S. (1990). Isolation and properties of bovine kidney brush border vacuolar H^+ ATPase. J. Biol. Chem., 265, 21957-21965.

Wieczorek, H., Cioffi, M., Klein, U., Harvey, W. R., Schweikl, H., & Wolfersberger, M. G. (1990). Isolation of goblet apical membrane from tobacco hornworm midgut and purification of its vacuolar-type ATPase. Methods Enzymol., 192, 608-616.

Wieczorek, H., Putzenlechner, M., Zeiske, W., & Klein, U. (1991). A vacuolar-type proton pump energizes K+/H+ antiport in an animal plasma membrane. Journal of Biological Chemistry, 266, 15340-15347.

Wieczorek, H., Weerth, S., Schindlebeck, M., & Klein, U. (1989). A vacuolar-type proton pump in a vesicle fraction enriched with potassium transporting plasma membranes from tobacco hornworm midgut. J.Biol.Chem., 264, 11143-11148.

Wieczorek, H., Wolfersberger, M. G., Cioffi, M., & Harvey, W. R. (1986). Unique ATPase activity in purified goblet cell apical membranes from *Manduca sexta* larval midgut: a candidate for the electrogenic alkali metal ion pump. Biochim.Biophys.Acta, 857, 271.

Wigglesworth, V. B. (1984). The physiology of insect tracheoles. Adv. Insect. Physiol., 17(85-148).

Williams, C. M. (1956). The juvenile hormone of insects. Nature, 178, 212-213.

Wolfersberger, M. G., Harvey, W.R., Cioffi, M. (1982). Transepithelial potassium transport in insect midgut by an electrogenic alkali metal ion pump. . Curr.topics memb.transp. , 16, 109-133.

Wolfersberger, M. G., Giangiacomo, K.M. (1983). Active potassium transport by the isolated lepidopteran larval midgut: stimulation of net potassium flux and elimination of the slower phase decline of the short circuit current. . J.exp.Biol. , 102, 199-210.

Wolfersberger, M. G., Spaeth, D. D., & Dow, J. A. T. (1986). Permeability of the peritrophic membrane of tobacco hornworm larval midgut. American Zoologist, 26, 74A.

Wood, J. L., Farrand, P.S., Harvey, W.R. (1969). Active transport of potassium by the cecropia midgut VI. Microelectrode potential profile. J.exp.Biol., 50, 169-178.

Wood, J. L., Moreton, R.B. (1978). Refinements in the short-circuit technique and its application to active potassium transport across the cecropia midgut. . J.exp.Biol., 77, 123-140.

Yamada, E. W., & Huzel, N. J. (1988). J. Biol. Chem., 263, 11498-11503.

Yamamoto, R. T. (1969). Mass Rearing of the Tobacco Hornworm 11. larval rearing and pupation. J. Econ. Entomol., 62, 1427-1431.

Zeiske, W. (1992). Insect ion homeostasis. Journal of Experimental Biology., 172, 323-334.

Zhang, J., Myres, M., & Forgac, M. (1992a). Characterization of the V0 Domain of the Coated Vesicle (H+) ATPase. Journal of Biological Chemistry, 267(14), 9773-9778.

Zhang, K., Wang, Z.-Q., & Gluck, S. (1992b). A Cytosolic Inhibitor of Vacuolar H+-ATPases from Mammalian Kidney. The Journal of Biological Chemistry, 267(21), 14539-14542.

APPENDIX 1

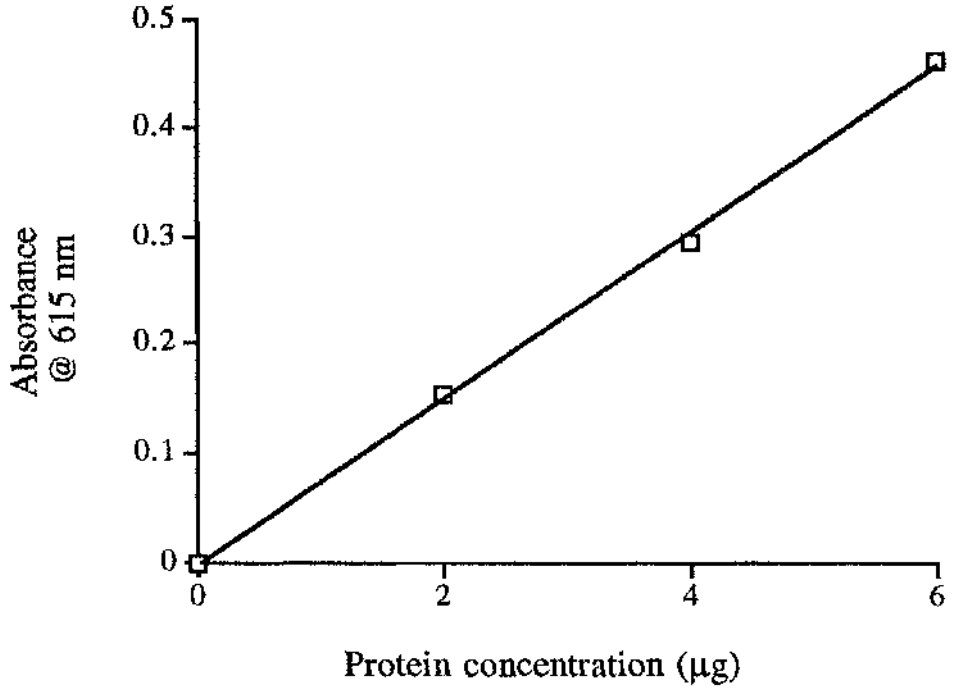

Figure A1 Representative amido black standard curve for protein concentration determination. 2, 4 or 6 μg of bovine serum albumin were used as standard concentrations. Protein was omitted from the blank and this was used as a zero control. Four micrograms of BSA produced an absorbance of approximately 0.3.

APPENDIX 2

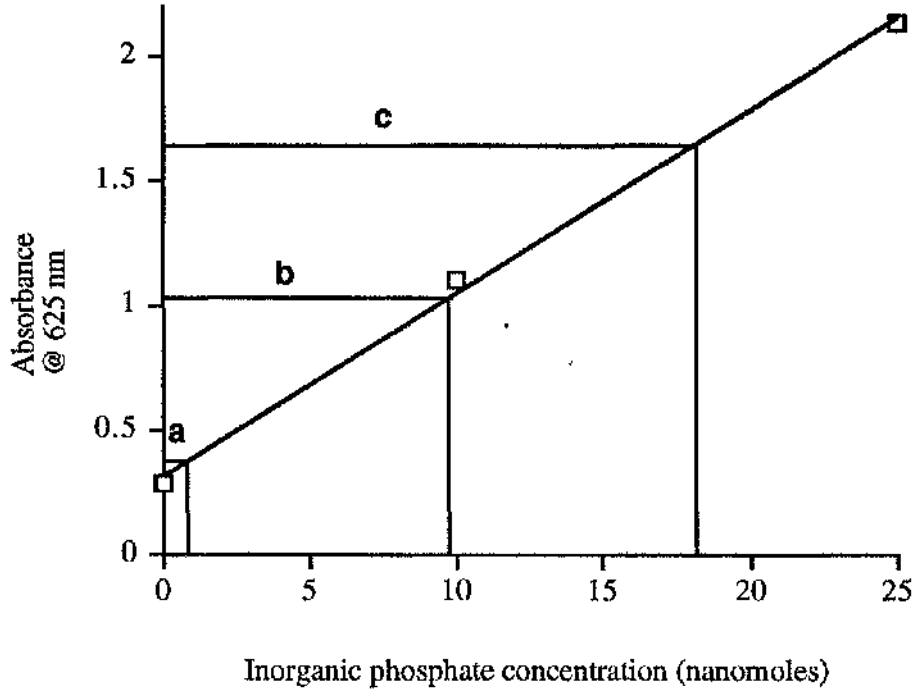

Figure A2 Representative malachite green standard curve for ATPase activity assay. Zero-time controls typically had absorbances between 0.2 and 0.3. Standard curve was generated using additions of 10 or 25 nanomoles potassium phosphate to the time zero controls. Typical experimental results are shown, all assays were conducted at 37°C for 5 min using 5 µg partially purified GCAM: **a**, V-ATPase activity isolated from moulting larvae generated 1.2 nanomoles phosphate. **b**, V-ATPase activity isolated from 5th instar feeding larvae generated 9.6 nanomoles phosphate. **c**, ATPase activity isolated from 5th instar feeding larvae in the absence of inhibitors generated 17.9 nanomoles of phosphate in 5 min.